ADAPTATION OF CANCELLOUS BONE TO HABITUAL LOADING: TRABECULAR ARCHITECTURE OF THE ARTIODACTYL CALCANEUS

by

Derinna Vivian Kopp

A dissertation submitted to the faculty of
The University of Utah
in partial fulfillment of the requirements for the degree of

Doctor of Philosophy

Department of Anthropology

The University of Utah

May 2014

The University of Utah Graduate School

STATEMENT OF DISSERTATION APPROVAL

The dissertation of **Derinna Vivian Kopp**

has been approved by the following supervisory committee members:

Dennis H. O'Rourke	, Chair	**2/13/2014** Date Approved
James F. O'Connell	, Member	**2/13/2014** Date Approved
John Martin McCullough	, Member	**2/13/2014** Date Approved
Henry C. Harpending	, Member	**2/13/2014** Date Approved
Christopher B. Ruff	, Member	**2/17/2014** Date Approved

and by **Leslie Ann Knapp** , Chair/Dean of

the Department/College/School of **Anthropology**

and by David B. Kieda, Dean of The Graduate School.

ABSTRACT

The functional adaptation model suggests that differences in biomechanical forces resulting from habitual loading will be reflected in the trabecular architecture of cancellous bone. Increasingly, trabecular architecture is used to compare habitual loading history in both extant and extinct animals. Yet, most research is limited to comparisons of differences in architectural measures between species, as it is not currently known exactly how trabecular architecture differs with varying principal loading conditions. This study analyzed the cancellous bone of the artiodactyl calcaneus (sheep and deer) to examine if and how trabecular architecture varies with respect to habitual loading in compression and tension. The artiodactyl calcaneus has been shown to be habitually loaded in bending with compression predominant in the dorsal aspect of the bone and tension predominant in the plantar aspect of the bone. Architectural measures analyzed included bone volume fraction, trabecular thickness, trabecular separation, trabecular number, connectivity density, and degree of anisotropy. Trabecular architecture was assessed across the length of the bone, between the dorsal and plantar aspects of the bone, with variation of cortical bone thickness and geometry, and between the two species to assess how cancellous bone may specifically adapt to habitual compression and tension. Across the length of the calcaneus the cancellous bone was shown to become less dense and less connected with greater trabecular separation

and fewer trabeculae for both the sheep and deer. The data from the dorsal and plantar regions of both species indicate that alteration in trabecular architecture occurs at a localized level rather than across each region as a whole. Cortical thickness and geometry were shown to have a significant effect on trabecular architecture in both species. Significant differences were found between the sheep and the deer cancellous bone specifically in the planter region and in concordance with predicted loading magnitudes for each species. While some significant differences in trabecular architectural were identified, much of the variation in the trabecular architecture across the length of the bone and between the dorsal and planar regions was not significant suggesting that loading regime alone may not be sufficient to explain trabecular architectural variation.

TABLE OF CONTENTS

ABSTRACT……. iii

LIST OF TABLES ……. vii

LIST OF FIGURES …… xii

ACKNOWLEDGEMENTS……. xiii

INTRODUCTION……... 1

Cancellous Bone Structure and Organization…….. 1
Bone Functional Adaptation and Cancellous Bone Organization...……..... 3
Project Questions and Overview…….……. 6

CONCEPTS AND LITERATURE REVIEW……...……... 12

Trabecular Architecture and Mechanical Loading…… 12
Trabecular Architecture and Material Properties…….. 13
Trabecular Bone Volume Fraction……... 15
Trabecular Thickness…… 16
Trabecular Separation……...…… 17
Trabecular Number……...…… 18
Connectivity…….. 18
Anisotropy…….…… 21
Cortical Bone……...……. 23
A Proposed Bone for Bone Adaptation to Habitual Compression and Tension …….…… 30

MATERIALS AND METHODS……..…… 37

Statistical Methods…… 42

RESULTS…….…….…… 44

Sheep Calcaneus…… 44
Question 1: Architectural Variation over Diaphyseal Length…….. 44
Question 2: Architectural Variation by Region…… 48

Question 3: Architectural Variation with Cortical Thickness Ratio….. 53
Question 4: Architectural Variation with Imax/Imin……...…….. 66
Deer Calcaneus……..…… 73
Question 1: Architectural Variation over Diaphyseal Length….…….. 73
Question 2: Architectural Variation by Region…….…… 77
Question 3: Architectural Variation with Cortical Thickness Ratio (CTR)…… 85
Question 4: Architectural Variation with Imax/Imin…….…….. 91
Both Species……..……...…… 97
Question 5: Architectural Variation by Species…….…….. 97

DISCUSSION AND CONCLUSIONS..…….. 120

Question 1: Architectural Variation over Diaphyseal Length…… 121
Question 2: Architectural Variation by Region……. 123
Question 3: Architectural Variation with Cortical Thickness Ratio (CTR).. 125
Question 4: Architectural Variation with Imax/Imin…… 127
Question 5: Architectural Variation by Species …… 129
Considerations and Conclusions…….…… 131

REFERENCES……..…….. 137

LIST OF TABLES

1 Summary statistics, mean (SD), for each trabecular architectural parameter from the sheep calcaneus…….…….. 45

2 Correlation coefficients (R) of trabecular architectural measures with percent diaphysis location by region for the sheep calcaneus.…… 46

3 Effect of location on each architectural parameter controlling for region and confounding variables for the sheep calcaneus.…….. 47

4 Effect of location on each architectural measure in the dorsal region for the sheep calcaneus…….…….……. 49

5 Effect of location on each architectural measure in the plantar region for the sheep calcaneus…….……..…… 50

6 Correlation Coefficients (R) of trabecular architectural measures with region for the sheep calcaneus…….. 51

7 Effect of region on each architectural parameter controlling for location and confounding variables for the sheep calcaneus.…….. 52

8 Effect of region on each architectural measure in the 20% diaphysis location for the sheep calcaneus…….……..…… 54

9 Effect of region on each architectural measure in the 30% diaphysis location for the sheep calcaneus..……...…….. 55

10 Effect of region on each architectural measure in the 40% diaphysis location for the sheep calcaneus.…….…….……. 56

11 Effect of region on each architectural measure in the 50% diaphysis location for the sheep calcaneus.…….……..…… 57

12 Mean and standard deviation (SD) of the cortical thickness ratio (CTR) at each percent diaphysis location for the sheep calcaneus.…….……..…… 58

13 Correlation coefficients (R) of trabecular architectural measures with CTR by region for the sheep calcaneus. ……. 61

14 Effect of CTR on each architectural parameter controlling for region and confounding variables for the sheep calcaneus……...…….. 62

15 Effect of region on each architectural parameter controlling for CTR and confounding variables for the sheep calcaneus..……. 63

16 Effect of CTR on each architectural measure in the dorsal region for the sheep calcaneus.…….…….…….……. 64

17 Effect of CTR on each architectural measure in the plantar region for the sheep calcaneus.…….……..……..…… 65

18 Mean and standard deviation (SD) of the Imax/Imin at each percent diaphysis location for the sheep calcaneus…….. 67

19 Correlation coefficient (R) of trabecular architectural measures with Imax/Imin by region for the sheep calcaneus……..…….. 68

20 Effect of Imax/Imin on each architectural parameter controlling for region and confounding variables for the sheep calcaneus.……..…… 69

21 Effect of region on each architectural parameter controlling for Imax/Imin and confounding variables for the sheep calcaneus……..……...…….. 70

22 Effect of Imax/Imin on each architectural measure in the dorsal region for the sheep calcaneus…….…….…….…… 71

23 Effect of Imax/Imin on each architectural measure in the plantar region for the sheep calcaneus……...…….……..…..… 72

24 Summary statistics, mean (SD), for each trabecular architectural parameter from the deer calcaneus……...…….……..…… 74

25 Correlation coefficients (R) of trabecular architectural measures with percent diaphysis location by region for the deer calcaneus.…….. 75

26 Effect of location on each architectural parameter controlling for region and confounding variables for the deer calcaneus…….…… 76

27 Effect of location on each architectural measure in the dorsal region for the deer calcaneus……...…….. 78

28 Effect of location on each architectural measure in the plantar region for the deer calcaneus……. 79

29 Correlation Coefficients (R) of trabecular architectural measures with region for the deer calcaneus..…..…….……..…… 80

30 Effect of region on each architectural parameter controlling for location and confounding variables for the deer calcaneus…….. 81

31 Effect of region on each architectural measure in the 20% diaphysis location for the deer calcaneus..……...…….. 82

32 Effect of region on each architectural measure in the 30% diaphysis location for the deer calcaneus……..…….……...…… 83

33 Effect of region on each architectural measure in the 40% diaphysis location for the deer calcaneus……...…….. 84

34 Effect of region on each architectural measure in the 50% diaphysis location for the deer calcaneus……...…….…….……. 86

35 Mean and standard deviation (SD) of the cortical thickness ratio (CTR) at each percent diaphysis location for the deer calcaneus…….……..…… 87

36 Correlation coefficients (R) of trabecular architectural measures with CTR by region for the deer calcaneus……...…….……..…… 89

37 Effect of CTR on each architectural parameter controlling for region and confounding variables for the deer calcaneus …...…….. 90

38 Effect of region on each architectural parameter controlling for CTR and confounding variables for the deer calcaneus……..…… 92

39 Effect of CTR on each architectural measure in the dorsal region for the deer calcaneus…….…….. 93

40 Effect of CTR on each architectural measure in the plantar region for the deer calcaneus..……..…….…….……. 94

41 Mean and standard deviation (SD) of Imax/Imin at each percent diaphysis location for the deer calcaneus ..…….……..…… 95

42 Correlation coefficient (R) of trabecular architectural measures with Imax/Imin by region for the deer calcaneus.……. 96

43 Effect of Imax/Imin on each architectural parameter controlling for region and confounding variables for the deer calcaneus..…….. 98

44 Effect of region on each architectural parameter controlling for Imax/Imin and confounding variables for the deer calcaneus……..….. 99

45 Effect of Imax/Imin on each architectural measure in the dorsal region for the deer calcaneus……...……...…….. 100

46 Effect of Imax/Imin on each architectural measure in the plantar region for the deer calcaneus……..…….…….…….. 101

47 Effect of species on each architectural parameter controlling for location and confounding variables.…….……..…… 102

48 Effect of species on each architectural parameter controlling for region and confounding variables……..…….……..…… 103

49 Effect of species on each architectural measure in the dorsal region..…….. 104

50 Effect of species on each architectural measure in the plantar region.……..… 106

51 Effect of species on each architectural measure in the 20% diaphysis location controlling for region and confounders…….……..….. 107

52 Effect of species on each architectural measure in the 30% diaphysis location controlling for region and confounders..……..…. 108

53 Effect of species on each architectural measure in the 40% diaphysis location controlling for region and confounders….…….……..…….. 109

54 Effect of species on each architectural measure in the 50% diaphysis location controlling for region and confounders …….. 110

55 Effect of species on each architectural parameter controlling for CTR and confounding variables…….……... 111

56 Effect of species on each architectural parameter controlling for region, CTR, and confounding variables ..…….……..….. 112

57 Effect of species on each architectural parameter controlling for CTR and confounding variables in the dorsal region……...……...…….. 113

58 Effect of species on each architectural parameter controlling for CTR and confounding variables in the plantar region.…..……. 114

59 Effect of species on each architectural measure controlling for Imax/Imin and confounding variables..…….……...…… 116

60 Effect of species on each architectural parameter controlling for region, Imax/Imin, and confounding variables……...…….……...…… 117

61 Effect of species on each architectural measure controlling for Imax/Imin and confounding variables in the dorsal region.…….……...…… 118

62 Effect of species on each architectural measure controlling for Imax/Imin and confounding variables in the plantar region……...…….……...……. 119

LIST OF FIGURES

1	Image of domesticated sheep housed similarly to the sheep used in this study ……..	7
2	Image of wild mule deer in natural habitat ……...	8
3	Schematic depicting a multiply connected network ……...	19
4	Micro-CT images of cross sections of A) the human femoral neck at midshaft (superior = top, inferior = bottom) and B) mule deer calcaneus at 40% shaft length (dorsal = top, plantar = bottom).……..…	25
5	Schematic representation of three different trabecular eccentricity (e) scenarios …….……	26
6	Lateral photograph of sheep calcaneus with percent length locations marked and identified ……..…...	39
7	Representative lateral view of micro-CT image of a calcaneus with percent length locations and the dorsal and plantar regions of interest (ROIs) noted …	41
8	Micro-CT images of cross sections of a sheep calcaneus for each of the percent diaphyseal length location ……..	59
9	Micro-CT images of cross sections of a deer calcaneus for each of the percent diaphyseal length location ……..…	88

ACKNOWLEDGEMENTS

I would like to first thank my committee members, Dennis O'Rourke, Christopher Ruff, Jim O'Connell, John McCullough, and Henry Harpending for their support, guidance, understanding, and patience throughout this process. Special thanks to Christopher Ruff, whose comments, criticism and guidance were essential to the completion of this dissertation.

I would also like to thank Roy Bloebaum, John Skedros, and the VA Medical Center for preliminary mentoring and material support. This work benefited from the decades long research of Bloebaum and Skedros on skeletal adaptation and without them would not have been possible.

I would like to thank my many friends, colleagues, and mentors I have had the benefit of knowing and learning from throughout my graduate career. Finally, I am forever and deeply indebted to Nora Lundin and our families for their continued love and support throughout my graduate studies.

INTRODUCTION

Cancellous Bone Structure and Organization

The primary role of the mammalian skeleton is to bear mechanical loads with a limited amount of deformation (Martin et al., 1998). These loads originate from activities related to locomotion and movement, as well as muscle and ligament forces that act on the bones. It has long been believed that the structure of bone (cortical and cancellous) is determined by the magnitude and orientation of the loads applied to the bone. The interaction between musculoskeletal loading and bone remodeling is believed to determine the ultimate structural organization of bone.

Cancellous bone is composed of an interconnected series of rods and plates made up of individual trabeculae that form a honeycomb-like structure. This structure varies in density, thickness, number, and separation of trabeculae both between skeletal elements and within regions of individual bones. Some regions of cancellous bone tend to be very dense while others have only sparse amounts of trabeculae. Some regions have very thin trabeculae while others have more coarse thick trabeculae (Odgaard, 2001).

Additionally, the organization of cancellous bone has been shown to vary with location within the skeleton, at times appearing to be organized in orthogonal arrays, and at others appearing more randomly arranged (Singh, 1978). It is the arrangement of the trabeculae in cancellous bone along with the material properties of the bone that are considered to determine the mechanical strength and integrity of cancellous bone.

The structural organization of cancellous bone is generally believed to be determined by the interaction between morphological and functional limitations of a particular bone (size and shape), biochemical processes (hormonal and nutritional, or as influenced by hormones, nutrition, and disease), and applied loads from locomotion (Lanyon, 1990). It is theorized that bone has the ability to transpose habitual loading conditions experienced into definite changes in structure that accommodate the loads (Roesler, 1981). Thus the ultimate structure of bone is determined by the magnitude and orientation of loads applied though habitual loading. This has led to the belief that the structure of cancellous bone can be used to distinguish, identify, and/or reconstruct the loading conditions to which the structure is adapted (Currey, 2002; Lovejoy et al., 2003). It has also been suggested, however, that there may be significant differences in the gene expression, biophysical stimuli, and the developmental fields that mediate the creation of trabecular architecture in different bones and that these aspects may have a greater influence on trabecular architecture than habitual loading alone (Kriz, 2002; Kriz et al., 2002; Lovejoy et al., 2003). Lovejoy and colleagues suggest that the distributions and structure of bone (both cancellous and cortical) can be better understood if they are assumed to "reflect the expression of positional information in its anabolic growth zones" (2003; p. 101). They propose that the position of the epiphyseal plate plays a significant role in the final structure of cancellous bone. However, they also include that the "material properties and maintenance are also affected by local strain threshold(s) (which may be small and/or at least broadly tissue-specific)" (2003; p. 101).

While the mechanisms that mediate trabecular architectural anisotropy are still debated (Huiskes, 2000; Carter D.R., 2001; Cowin, 2001a; Kriz, 2002; Kriz et al., 2002; Lovejoy et al., 2003), trabecular structure is likely to be governed by complex

interactions between genetic and epigenetic actions, morphological and functional constraints, applied loads, and biochemical processes.

Bone Functional Adaptation and Cancellous Bone Organization

The paradigm commonly known as Wolff's Law has dominated skeletal research since its origination (Meyer, 1867; Wolff, 1879; Biewener and Bertram, 1993; Fyhrie and Kimura, 1999; Keaveny et al., 2001). In the mid-nineteenth century it was theorized by Wolff and others that cancellous bone was organized following principal loads placed on the bone. Wolff hypothesized a mathematical relationship between the organization of the bone and the biomechanical loads. This trajectorial theory of bone architecture was ultimately combined with Roux's theory of functional adaptation into what is commonly known today as "Wolff's law of bone transformation" (Roesler, 1981). Wolff's law says that "every change in the form and function of the bones, or of their function alone, is followed by certain definite changes (or transformations) in their internal architecture, and equally definite secondary alterations of their external conformation, in accordance with mathematical laws" (Freiberg, 1902). Most researchers, however, use a generalized concept of Wolff's law that states that mechanical loads applied to bone during life influence the structure of the bone tissue and do not include the mathematical element (Cowin, 2001). Due to the differences between the commonly used definition of Wolff's law and the actual definition as written by Wolff, several researchers have suggested that the term "bone functional adaptation" be used for the more commonly used definition and "Wolff's law" for the actual definition with the mathematical inferences (Ruff et al., 2006).

The theory that bone dynamically responds to loading through growth has been

the predominant paradigm for the study of bone since it was first proposed. It is generally believed that there is a direct relationship between the organization of cancellous bone and the direction and magnitude of the principal stresses placed on the bone during habitual loading (Roesler, 1981; Currey, 2002). This has led to the belief that differences in biomechanical forces, resulting from different habitual loading conditions (i.e., locomotor behaviors), will be reflected in the trabecular architecture of cancellous bone (Currey, 2002). Accordingly, anisotropic patterns in trabecular architecture are increasingly used to compare habitual loading history in both extant and extinct animals (i.e., Macchiarelli et al., 1999; Zylstra, 2000; Fajardo and Müller, 2001; Martinón-Torres, 2003; Black, 2004; Ryan and Ketcham, 2005a).

More recently trabecular architectural measures (obtained from both two-dimensional (2D) and three-dimensional (3D) imaging analyses) have been used to attempt to distinguish loading conditions related to habitual loading (i.e., Fajardo et al., 1999, 2000, 2002; Ryan, 2000; Fajardo, 2004; Fajardo and Muller, 2001; Ryan, 2001; MacLatchy and Muller, 2002; Ryan and Ketcham, 2002a, 2002b, 2005b; Maga et al., 2006). These studies have attempted to correlate variation in trabecular architecture with different habitual loading conditions, and have identified some variation among trabecular architectural measures based on mode of locomotion. However, it has been noted that these studies and others are limited to simple comparisons of differences in structural measures, as it is not currently known exactly how trabecular architecture differs with varying principal loading conditions (Skedros and Baucom, 2007).

Additionally, studies on cancellous bone have correlated trabecular architectural measures with mechanical properties of cancellous bone specimens (i.e., Goldstein, 1987; Hodgskinson and Currey, 1990a; Hodgskinson and Currey, 1990b; Keaveny and Hayes,

1993b; Goulet et al., 1994; Odgaard et al., 1997; Kabel et al., 1999b, 1999c; Keaveny et al., 1999, 2001; Ulrich et al., 1999; Keaveny, 2001; Follet et al., 2005; Mittra et al., 2005, 2008; Perilli et al., 2008). These studies have shown that cancellous bone is stronger when loaded in its physiological main axis and that trabecular architecture measures often correlate significantly with various mechanical properties including strength and modulus. These data have been used to further substantiate the hypothesis that trabecular architecture is adapted to best accommodate the habitual loads to which it is subjected.

The utility of trabecular architectural measures to assess differential habitual loading conditions is prevalent in the literature. However, it appears that trabecular architectural measures specifically from cancellous bone under compression and tension have not been fully assessed to determine to what extent, if any, cancellous bone organizes along the principle loading trajectories, or if trabecular architectural measures can be utilized to identify differential loading conditions. In this context a bone with known loading conditions at known locations that could serve as a quantitative reference for correlating architectural parameters and loading conditions is needed.

The artiodactyl (e.g., sheep, deer, and goat) calcaneus has been introduced as a model for interpreting functional adaptation of bone because it has been shown to be loaded in relatively simple dorsal/plantar bending (Lanyon, 1974; Su, 1998; Su et al., 1999). This loading produces predominant compression strains in dorsal cortex and tension in the plantar cortex, with the highest strain magnitudes in dorsal (compression) cortex. Skedros and colleagues have shown significant regional differences between the cortical bone of the compression and tension cortices of artiodactyl calcaneus. They have shown the compression cortex to have significantly greater cortical thickness and mineralization when compared to the tension cortex (Skedros, 1994; Skedros et al., 2004;

Skedros et al., 2007). Additionally, the arched trabecular patterns seen in lateral radiographs of this bone also have been shown to follow the lines of dorsal/compression and plantar/tension stress trajectories (Skedros and Baucom, 2007). The artiodactyl calcaneus would appear to be an appropriate bone to use to examine trabecular architecture under compression and tension.

Project Questions and Overview

Following the work of Lanyon, Skedros, and Su the artiodactyl calcaneus will be examined as a possible control bone for trabecular architecture in this study. The primary goal of this research is to examine the trabecular architecture of the artiodactyl calcaneus in the dorsal and plantar regions over several diaphyseal length locations and with regard cortical thickness (as measured by cortical thickness ratio) to investigate how the architecture of cancellous bone may adapt to habitual loading in the artiodactyl calcaneus.

The research will first examine the domesticated sheep (*Ovis aries*) calcaneus to examine trabecular bone architecture in cancellous bone habitually loaded in compression and tension. As habitually penned animals, the sheep from which the study specimens were obtained are likely to have experienced little habitual extreme locomotor behavior such as running or jumping which could cause differences in the habitual directional loading of the calcaneus (Figure 1). The research will then analyze the mule deer calcaneus (*Odocoileus hemionus hemionus*). The wild mule deer live in a much more rugged habitat with the possibility of habitual extreme loading likely (Figure 2). It has

Figure 1. Image of domesticated sheep housed similarly to the sheep used in this study. Photo used by permission, Ray Olsen.

Figure 2. Image of wild mule deer in natural habitat. Photo by author.

been shown with in vitro data (Su, 1998; Su et al., 1999) that even under simulated extreme loading (as would be expected during running, jumping and scattering) the mule deer calcaneus remains predominantly habitually loaded in bending. The mule deer calcaneus may therefore be a robust test of trabecular architectural differences for bone under compression and tension. Finally, the trabecular architecture of the two species will be compared to examine the possible effects of more extreme loading on trabecular architecture.

There are four primary questions posed by this research:

1) Does trabecular architecture differ across the length of the calcaneal diaphysis? Beam theory indicates that bending moments should increase toward the middle region of a cantilevered beam such as the artiodactyl calcaneus. It is known that bending is more effectively countered by compact bone than cancellous bone (Guo and Goldstein, 2001; Keaveny, 2001). Thus one would expect that toward the middle of the calcaneus diaphysis there would be an increase in cortical bone thickness (as has been elucidated by Skedros and colleagues 1994, 1997, 2004) and decrease in cancellous bone with associated changes in trabecular architecture. The more posterior region of the bone, however, is likely subject to more complex loading, including shear (due to the insertion of the Achilles tendon) and would likely result in increased cancellous bone and associated changes in trabecular architecture (Keaveny, 2001; Odgaard, 2001). The null hypothesis for this question will be that there will be no statistically significant difference in the trabecular architectural measures across the length of the bone.

2) Does trabecular architecture vary between cancellous bone believed to be under habitual compression (dorsal region) and that under habitual tension

(plantar region)? Studies have shown that cancellous bone is generally weaker in tension than in compression for biomechanical measures (Keaveny, 2001). Additionally, studies have shown that trabecular architectural measures are correlated with biomechanical strength properties (see discussion in Concepts and Literature Review). Thus it can be expected that the regions of the artiodactyl calcaneus that are habitually under compression and tension would exhibit differential trabecular architecture. The null hypothesis for this question will be that there will be no statistically significant difference between the trabecular architectural measures from the bone in the dorsal (compression) and plantar (tension) regions.

3) Does trabecular architecture vary with cortical thickness as measured by cortical thickness ratio? It is known that cortical bone has greater compressive and tensile strength than cancellous bone (Keaveny, 2001) and accordingly bending is more effectively countered by cortical bone than cancellous bone. Additionally, the middle region of a beam/bone under habitual bending should experience greater bending strains than the distal/free end. As more of the load is effectively countered by cortical bone one would expect alterations in the trabecular bone architecture. The null hypothesis for this question will be that trabecular architectural measures will not vary significantly with cortical thickness ratio.

4) Does trabecular architecture vary with Imax/Imin ratio? Imax/Imin is an estimation of cross-sectional shape and bending rigidity. The greater the deviation from 1 of the Imax/Imin ratio of a cross section, the greater departure from true circularity and the direction of greatest bending rigidity is more strongly

defined. The shape of the cross section changes over the length of both the sheep and deer calcaneus, becoming more oval and less round suggesting that the Imax/Imin ratio will be greater, and further away from 1, towards the middle of the bones. It can be expected that greater Imax/Imin ratios will be associated with greater directional bending rigidity that will result in alterations in the trabecular bone architecture. The null hypothesis for this question will be that trabecular architecture will not vary significantly with Imax/Imin ratio.

5) Does trabecular architecture vary between the two species? The sheep and deer are species that share a similar body design and similar evolutionary history; yet, the deer is considered to have increased loading due to the natural habitat and habitual activity levels. This would subject the deer calcaneus to more extreme loading and thus higher bending loads. This differential loading would be expected to produce trabecular architecture more suited to higher stresses, greater strains and bending loads produced from their habitual activity when compared to the sheep with a less extreme habitual loads and activity levels. The null hypothesis for this question will be that trabecular architectural measures will not vary significantly between the two species.

Each aspect of the study will utilize microcomputed tomography (micro-CT) to image the trabecular bone within the specimens. Micro-CT imaging allows for the internal structure of the specimens to be analyzed without destruction of the specimens. The trabecular architecture of each specimen will then be quantified using computer based analyses designed to assess trabecular architecture from the micro-CT scans. The trabecular architecture measures will then be statistically analyzed to identify similarities and differences in trabecular organization to answer the four research questions.

CONCEPTS AND LITERATURE REVIEW

Trabecular Architecture and Mechanical Loading

"The geometric and spatial properties of trabeculae in cancellous bone are collectively known as the cancellous bone architecture" or trabecular architecture (Odgaard, 2001 p 14-1). Research to identify the relationship between trabecular architecture/structure and habitual musculoskeletal stresses has mainly focused on identifying the influence of loads on the remodeling processes and the influence of trabecular architecture on mechanical properties of cancellous bones. Following Wolff, Meyer, and Roux the earliest quantitative work attempted to elaborate the relationship between mechanical loading and the structure of cancellous bone.

Pauwels (1980) found a correspondence between the pattern of stresses experienced and the distribution of cancellous bone in the human femoral head. It was concluded that the density, thickness, and number of trabeculae corresponded to the magnitude and direction of load to minimize bending stresses. Lanyon (1974) used stress gauges attached to the calcaneus of sheep to record the principle strain directions during normal locomotion in vivo. He noted a correspondence between the orientation of the calcaneal trabeculae and the strain directions of the maximum deformation. Similarly, Biewieener et al. (1996) recorded in vivo principle strains in the potoroo calcaneus during treadmill walking and in situ during experimental loading followed by thin sectioning and stereological analysis of the orientation of the cancellous bone under the Achilles tendon.

They showed that there were two main trabecular tracks, one aligned closely with the direction of the principle compressive strain and the other aligned closely with the principle tensile strain direction. Biewieener and colleagues also showed that in the experimental group of tenotomized potoroos trabecular bone volume fraction, thickness, and number were reduced compared to the control group, thus showing a relationship between trabecular architecture, loading, and disuse. In a study of different substrates Radin et al. (1982) reported that hard surfaces produced stiffer more isotropic cancellous bone in the femora of sheep compared to softer surfaces.

It has also been shown that trabecular orientation is correlated with principle stress directions with finite element analysis (FEA) models. Early work with FEA showed significant correlations between trabecular architecture and principle strains in a human patella model (Hayes and Snyder, 1981). This work and later work also indicated that maximum shear stresses and high bending loads are additionally important factors for the arrangement of cancellous bone. Shear coupling caused by multidirectional loading was shown to be reduced when trabeculae were aligned nonorthogonally, suggesting that nonorthogonal structure maybe be optimal for cancellous bone under multidirectional loads (Piaparti and Turner, 1997). It has also been shown that multidirectional loading produced less extreme stress gradients than unidirectional loading and can have an effect on the density and distribution of cancellous bone (Carter et al., 1989).

Trabecular Architecture and Material Properties

The architecture of cancellous bone is oriented in such a way that a “grain” can usually be recognized in radiographs and/or cross sections of bone. The direction of the

grain generally follows the direction of the perceived main physiological habitual loading axis (Wolff, 1879; Goldstein, 1987; Turner, 1992; Keaveny and Hayes, 1993a; Cowin, 2001b; Keaveny, 2001; Skedros and Baucom, 2007; Perilli et al., 2008), and the greatest mechanical stiffness and strength are considered to be in the direction of the grain (Fox and Keaveny, 2001, 2003; Keaveny et al., 2001). Supporting this, cancellous bone has been shown to be stronger for both static and cyclic loading in the physiological main loading axis than in off-axis loading (Turner et al., 1990; Ford and Keaveny, 1996; Bayraktar and Keaveny, 2004; Dendorfer et al., 2008). Consequently, trabecular architecture is generally considered one of the primary determinants for the strength of cancellous bone (McCalden et al., 1997; Kabel et al., 1999b; van Rietbergen et al., 1999; van Rietbergen and Huiskes, 2001), and therefore is often a central feature in describing cancellous bone properties.

The initial work to establish morphological terms to describe and categorize cancellous bone structure was qualitative description with little to no quantitative analyses (Singh, 1978). Whitehouse and colleagues were among the earliest to conduct quantitative analyses on cancellous bone structure (Whitehouse, 1974; Whitehouse and Dyson, 1974; Whitehouse, 1975). Using stereological techniques and scanning electron microscope imaging to quantify histomorphometric parameters they demonstrated significant variation in trabecular architecture (size, shape, connectivity, and structural anisotropy) dependent on anatomic location (Whitehouse, 1974; Whitehouse and Dyson, 1974; Whitehouse, 1975;). This early work was limited because the methods were not only very time consuming but required destruction of the specimen prohibiting further analysis.

Today there are several nondestructive techniques available to assess and quantify

trabecular architecture measures; the most prominent and widely used are either obtained from histological sections (2D) or from 3D reconstructions of cancellous bone using adapted stereological methods. The following is a review of the most commonly used measures used to quantify and characterize trabecular architecture in cancellous bone studies.

Trabecular Bone Volume Fraction

Trabecular bone volume fraction (BV/TV) is one of the fundamental properties of cancellous bone. It is defined as trabecular bone volume per total reference volume. For a region or volume of interest,

$$BV/TV = \frac{\text{trabecular bone volume}}{\text{trabecular bone volume} + \text{marrow space volume}} \qquad [1]$$

Bone volume fraction can be considered the histomorphometric counterpart of apparent density, or the total mass per unit volume of bone and a measure of the degree of mineralization (Keaveny et al., 2001; Odgaard, 2001). Apparent density has been shown to be highly correlated with cancellous bone mechanical properties including compressive and tensile yield stress, Young's modulus, and ultimate stress (Hodgskinson and Currey, 1990; Keaveny and Hayes, 1993b; Keaveny et al., 1999; Keaveny, 2001; Keaveny et al., 2001;). BV/TV has been shown to be directly correlated with apparent density and is considered an appropriate alternate measure of bone density in analyses of cancellous bone (Goulet et al., 1994; Keaveny et al., 2001; Ding et al., 2002; Perilli et al., 2008).

Bone volume fraction has been shown to be highly correlated with several mechanical properties of cancellous bone including trabecular bone stiffness, ultimate

stress, yield stress, maximum compressive stress, and Young's modulus (Feldkamp et al., 1989; Fyhrie et al., 1993; Goldstein et al., 1993; Goulet et al., 1994; Odgaard et al., 1997; Kabel et al., 1999b, 1999c; Ulrich et al., 1999; Follet et al., 2005; Mittra et al., 2005, 2008; Diederich et al., 2009; Liu et al., 2010). An increase in BV/TV is associated with increasing strength and stiffness of cancellous bone, while a reduction in bone volume fraction has been shown to lead to a decrease in modulus and strength values (Goulet et al., 1994; Silva and Gibson, 1997; Diederich et al., 2009; Keaveny, 2001; Keaveny et al., 2001; Follet et al., 2005; Mittra et al., 2008; Perilli et al., 2008; Liu et al., 2010).

Bone volume fraction, while an important measure of cancellous bone, does not provide any information about the actual organization or structure of cancellous bone. It is believed that a full understanding of modulus-density relationship requires an equal understanding of the role trabecular architecture plays (Keaveny et al., 2001). Parameters that quantify trabecular geometry include mean trabecular number (TbN), thickness (TbTh), separation (TbSp), connectivity, and degree of anisotropy.

Trabecular Thickness

Trabecular thickness (TbTh) is a calculation of the average thickness of individual trabeculae within a region of interest. The measure is directly calculated from 3D reconstructions by measuring the mean diameter of maximally sized spheres filling the trabecular structure (Odgaard, 2001; Patel et al., 2003). Higher values of TbTh have been found in regions of cancellous bone believed to be the principal compressive regions of the femoral head (Fazzalari et al., 1983). Trabecular thickness has been shown to be highly correlated with maximum compressive stress, ultimate stress, and Young's

modulus (Follet et al., 2005; Perilli et al., 2008). High TbTh values have been shown to be associated with higher trabecular bone stiffness, ultimate compressive strength, Young's modulus, and shear modulus while lower TbTh values have been associated with lower Young's and shear moduli (Ulrich et al., 1999; Mittra et al., 2005; Diederich et al., 2009; Liu et al., 2010). Additionally, the failure regions of mechanically tested cancellous bone have been shown to have lower TbTh values (Perilli et al., 2008).

Trabecular Separation

Trabecular separation (TbSp) is an average measure of the distance between trabeculae within a region of interest, or a measure of the average diameter of the marrow spaces in the cancellous bone in a region of interest. The measure is directly calculated by taking the mean diameter of spheres filling the marrow spaces within a region of interest (Odgaard, 2001; Patel et al., 2003). TbSp has been shown to be significantly negatively correlated with maximum compressive stress, ultimate stress, yield stress and Young's modulus (Follet et al., 2005; Mittra et al., 2008). Cancellous bone with larger TbSp values has been shown to have lower trabecular bone stiffness, Young's modulus and shear modulus (Ulrich et al., 1999; Follet et al., 2005; Mittra et al., 2008; Diederich et al., 2009; Liu et al., 2010). Additionally, Perilli et al. (2008) showed that higher TbSp values were found in the failure regions of mechanically tested cancellous bone. TbSp was also found to be lower in the regions of cancellous bone believed to be the principal compressive regions of the femoral head (Fazzalari et al., 1983).

Trabecular Number

Trabecular number (TbN) is a calculation of the number of individual trabeculae within a region of interest. Most often the TbN is calculated as the inverse of the mean diameter of spheres filling the skeletonized structure (Odgaard, 2001; Patel et al., 2003). The TbN parameter has been shown to be highly correlated with maximum compressive stress, ultimate stress, yield stress, and Young's modulus (Follet et al., 2005; Mittra et al., 2008). Cancellous bone with low TbN values has been shown to have low Young's modulus and low shear modulus while cancellous bone with higher TbN values has been shown to have higher Young's, and shear moduli (Ulrich et al., 1999). Additionally, Perilli et al. (2008) found that TbN values were lowest in the failure regions of mechanically tested cancellous bone. Using 2D finite element analysis, Silva and Gibson (1997) presented that a reduction in the number of trabeculae had a greater effect on the strength of cancellous bone than did a reduction in trabecular thickness.

In addition to these basic geometric measures, parameters to account for the connectivity and architectural anisotropy of cancellous bone have also been developed.

Connectivity

Connectivity of a structure is defined as a measure of the degree to which a structure is multiply connected and reports the maximum number of branches that can be severed before the structure is broken into separate parts (Odgaard and Gundersen, 1993). If a structure consisting of nodes and branches has more than one possible pathway between nodes it is defined as multiply connected (Figure 3). Connectivity is most often estimated, in both 2D and 3D analyses, using the Euler number. The Euler number is a topological property based on the number of holes and connected components within an

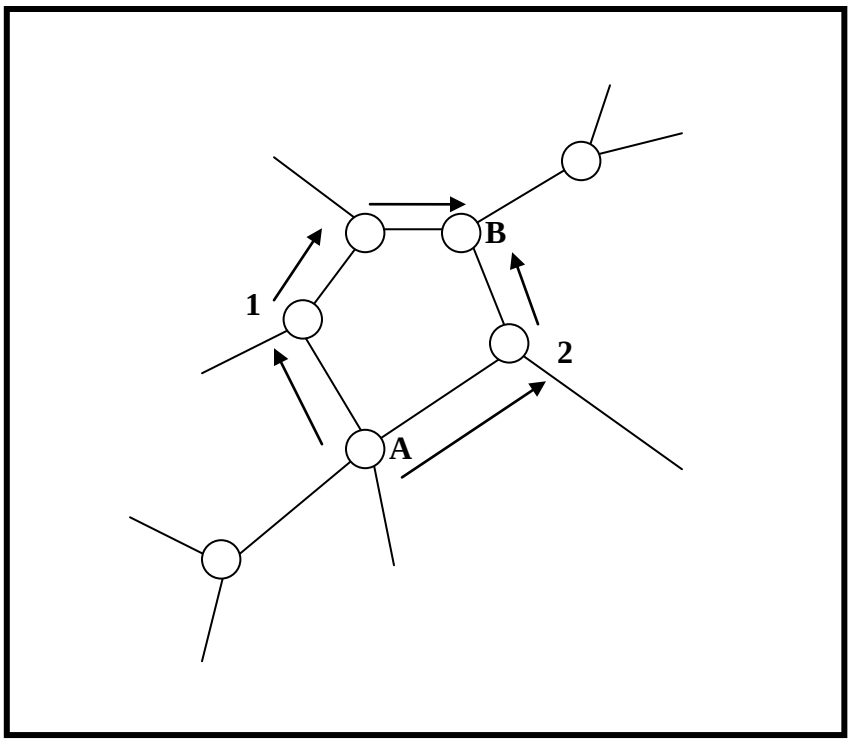

Figure 3. Schematic depicting a multiply connected network. There are two pathways (1 & 2) between node A to node B.

object (Compston, 1994). In a 3D structure, the Euler number is defined as the number of cuts that can be made before separating the structure and thus provides a direct measure of connectivity (Odgaard and Gundersen, 1993; Compston, 1994). The final Euler number calculation provides a negative number, structures that have a high degree of connectivity have a high negative number while those with less connectivity will have a lower, but still negative, Euler number (Compston, 1994). For 3D analyses of cancellous bone, connectivity is often represented as connectivity density (ConnD), which is simply the Euler number divided by the volume of the region of interest (ROI) from which it was calculated. Because the Euler number is negative, ConnD is also a negative metric with higher negative numbers representing higher values of connectivity. Due to the possible confusion that may arise from the negative values of the Euler number and connectivity density, the absolute values of the metrics are sometimes presented, especially in recent bone analysis software packages developed to work with micro-CT data (i.e., Scanco Corp and GE HealthCare MicroView).

Connectivity is considered to be independent of trabecular shape, size, or orientation, and may therefore not be directly related to mechanical properties of cancellous bone (Compston, 1994). Not surprisingly, the published data on connectivity and connectivity density of cancellous bone is often conflicting and there has yet to be a consensus on the exact relationship between the connectivity and mechanical properties of cancellous bone. Follet and colleagues (2005) showed a nonsignificant correlation between connectivity density and both Young's modulus and maximum compressive stress. Their data showed that as maximum compressive stress and Young's modulus increased cancellous bone structure tended to be more highly connected (Follet et al., 2005). More recently, Mittra and colleagues (2008) presented data that showed a

statistically significant moderate correlation between ConnD and yield stress and ultimate stress. Their data showed that more highly connected cancellous bone was associated with higher yield stress and ultimate stress, and that ConnD was better at predicting these mechanical measures than was bone mineral density from DEXA scans (Mittra et al., 2008). Finally, Perilli et al. (2008) using trabecular bone patter factor (TbPf), an alternate measure of connectivity density that has been shown to be sensitive to imaging parameters and therefore not commonly used, showed that the higher ultimate stress values were significantly correlated with more highly connected structures.

Anisotropy

Trabecular architectural anisotropy, or the differential orientation of trabeculae, has been noted and considered mechanically important since the work of Wolff and von Meyer. Trabecular anisotropy is most often quantified using a fabric tensor (Odgaard, 1997). Introduced by Cowin (Cowin, 1985), a fabric tensor is defined as a second-rank tensor that gives a local description of the architectural anisotropy. There have been several methods developed to capture architectural anisotropy. The most widely used one is Mean Intercept Length (MIL) (Odgaard, 1997; Odgaard, 2001).

Mean Intercept Length (MIL) was developed by Whitehouse (1974). In this technique the number of intersections between a linear grid of parallel lines and the bone/marrow interface are counted as a function of the grid's 3D orientation (Whitehouse, 1974). The MIL is the total line length divided by the number of intersections. MIL data are often fit to an ellipse (2D) or ellipsoid (3D) with the primary axis representing the primary direction of the trabecular structure, to graphically represent the structural anisotropy.

There are a few caveats associated with MIL. The results of MIL analyses are dependent on the interface between the bone/marrow phases, not the actual structure, and therefore may not necessarily fully characterize all types of structures (Odgaard, 1997; Odgaard et al., 1997). Additionally, MIL is dependent on the length and orientation of the intercepts and not the position of the components of the structure. This can result in some anisotropic structures appearing isotropic (Odgaard, 1997; Odgaard et al., 1997). This does not have a significant effect on the determination of anisotropy for most structures and appears to be negligible for most cancellous bone structures (Kuo and Carter, 1991; Odgaard, 1997; Odgaard et al., 1997). While it has been shown that MIL can underestimate the complexity of some cancellous bone specimens (Geraets, 1998), MIL has never the less been shown to be an effective method to characterize the anisotropy of cancellous bone structures (Odgaard et al., 1997; Odgaard, 2001; Ketcham and Ryan, 2004).

Using the MIL method, trabecular architectural anisotropy is "…described by main directions perpendicular to symmetry planes of the structure and by numbers describing the concentration of directions around the main directions." (Odgaard, 2001:14-7). Fabric tensors provide the descriptions of trabecular architecture where the eigenvectors of a 3x3 orientation matrix give the main directions and the eigenvalues give the degree of concentration around the main directions (Cowin, 1985). The degree of anisotropy (DA) is a commonly used index of anisotropy and is calculated as the primary eigenvalue divided by the tertiary eigenvalue (t1/t3). DA ratios near 1 indicate the structure is more isotropic and less anisotropic. As the DA values increase from 1 the structure becomes increasingly anisotropic.

The degree of anisotropy (DA) has not been shown to have a statistically significant relationship with the mechanical properties of cancellous bone, but several researchers have assessed the relationship between DA and mechanical properties. Ulrich et al. (1999) showed that the lowest DA was found in cancellous bone with the lowest Young's and Shear moduli, and the highest DA values were associated with the cancellous bone with the highest Young's and shear moduli. Follet et al. (2005) and Mittra et al. (2008) have shown that DA does not have a statistically significant correlation to maximum compressive stress, ultimate stress, or Young's modulus. In general, however, they showed that increasing DA values are associated with increasing values of the mechanical properties (i.e., elastic modulus, yield strength, and ultimate stress) when cancellous bone samples were loaded in the principal direction of trabecular structure (Follet et al., 2005; Mittra et al., 2008).

Cortical Bone

The role that the surrounding cortical bone plays in the architecture of trabecular bone cannot be over looked. Cortical bone is known to carry the majority of the mechanical loads experienced by bones. The thickness and the relative orientation/arrangement of cortical bone surrounding cancellous bone should be accounted for in any analysis of trabecular architecture. The two types of bone, while morphologically distinct are in reality a continuum of bone that work as one to withstand applied mechanical loads.

Differential thickening of opposing cortical bone aspects have been studied to examine the effect cortical thickness on bone load adaptation. Trabecular eccentricity, or the noncentral placement of cancellous bone within a cortical envelope, has been

proposed as a mechanism of bone adaptation to habitual loads (Fox and Keaveny, 2001, 2003). In tubular bones or bone sections where the cancellous bone is surrounded by a cortical envelope, trabecular eccentricity results in thicker cortical bone on one aspect compared to the opposing aspect. Essentially, trabecular eccentricity is a measure of cortical bone thickness on opposing aspects of a bone. For example in the human femoral neck, trabecular eccentricity results in thicker cortical bone on the inferior aspect than on the superior aspect, and in the midshaft of the artiodactyl calcaneus trabecular eccentricity results in thicker cortical bone on the dorsal aspect than on the plantar aspect (Figure 4).

Fox and Keaveny (2001, 2003) used the human femoral neck to test the biomechanical significance of, and provide a mechanistic explanation for, the relationship between trabecular eccentricity/differential cortical bone thickness and stresses in the femoral neck. They used composite beam theory and modeled the femoral neck with axial compressive as well as tensile and compressive bending stresses to estimate the effect of varying trabecular eccentricity on periosteal stresses in the superior "tension" and inferior "compression" aspects of the neck. Trabecular eccentricity (e) was defined as the superior position of cancellous bone with respect to the midplane of the neck, resulting from thicker cortical bone in the inferior aspect and thinner cortical bone in the superior aspect (Figure 5). Therefore, higher values of trabecular eccentricity in their study meant the trabecular bone was more superiorly placed, toward the "tension" aspect of the human femoral neck.

The study showed that compared to the concentric cases (e=0) with equal thickness of cortical bone on both aspects, stresses at the periosteal surface changed (± 20%) when eccentricity was varied from e=0 to e=1.5. In the superior "tension" aspect

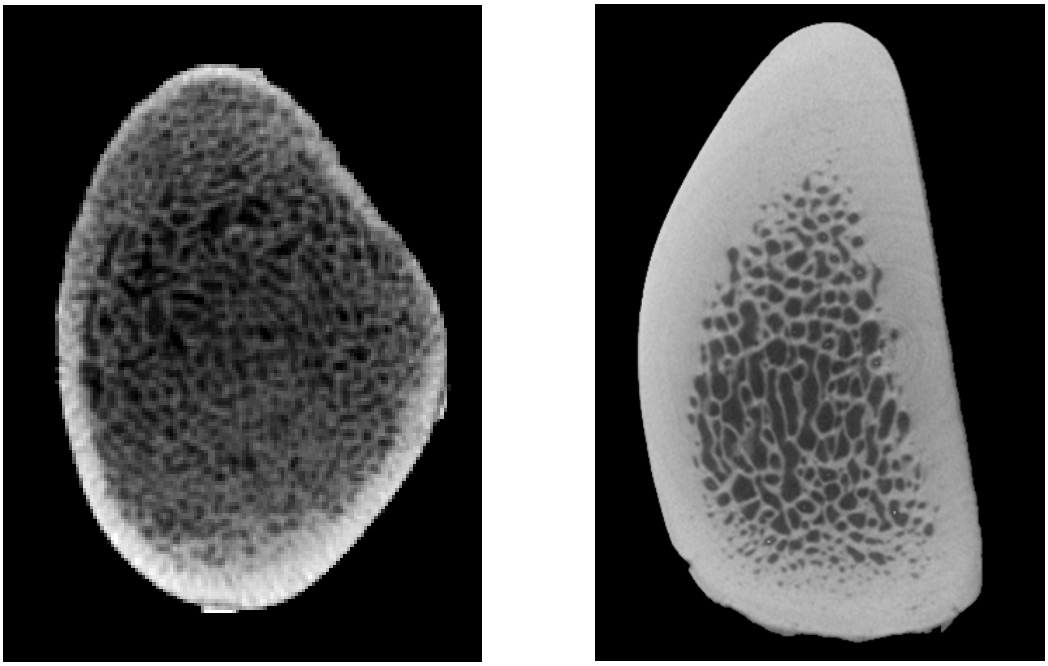

A **B**

Figure 4. Micro-CT images of cross sections of A) the human femoral neck at midshaft (superior = top, inferior = bottom) and B) mule deer calcaneus at 40% shaft length (dorsal = top, plantar = bottom). Both showing trabecular eccentricity (noncentral placement) of each cross section. Images not to scale and enlarged to show detail.

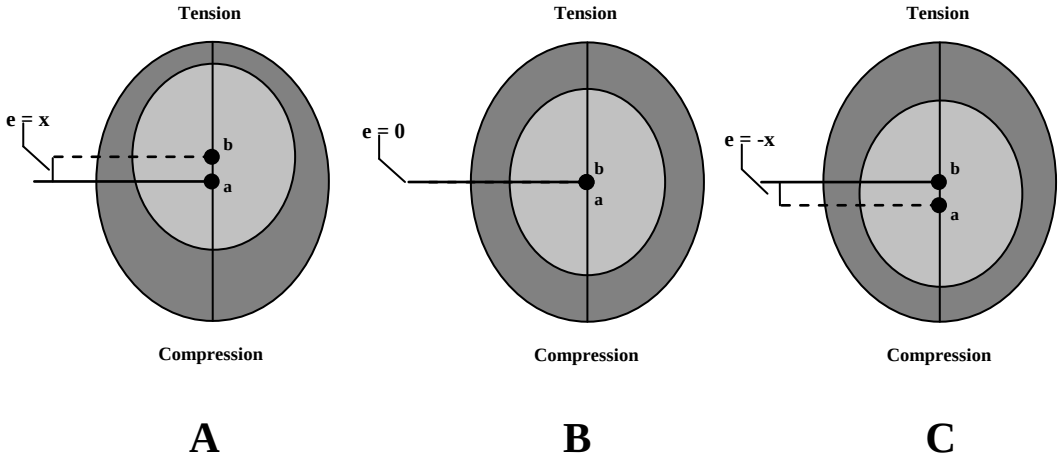

Figure 5. Schematic representation of three different trabecular eccentricity (e) scenarios. Following the definition from Fox and Keaveny (2001). Dark gray represents the cortical envelope with center = a, and lighter gray represents cancellous bone with center = b. A) Trabecular eccentricity toward the tension aspect (e = x). B) No trabecular eccentricity (e = 0). C) Trabecular eccentricity toward the compression aspect (e = -x). Fox and Keaveny did not include negative trabecular eccentricity in their study, but it is included here for clarification of the measure and future discussion.

(with thinner cortical bone) of the femoral neck, stress increased with increasing trabecular eccentricity. Conversely, in the inferior "compression" aspect (thicker cortical bone), the magnitude of stress decreased with increasing eccentricity.

Trabecular eccentricity was suggested to have an overall protective effect by decreasing the magnitude of the effective bending moment at the cross section of the bone. Increasing trabecular eccentricity was shown to have an effect equivalent to increasing overall cortical thickness or increasing trabecular modulus. The harmful effect of increasing trabecular eccentricity at the tension aspect was shown to be outweighed by the greater beneficial effect in the compression aspect.

Trabecular eccentricity alters the amount of cortical bone on opposing aspects of the cortical envelope of a bone. This results in thinner cortical bone in the tension aspect and thus the cancellous bone on the tension aspect bears more of the load experienced in that aspect. It is known that generally cancellous bone is substantially weaker in tension than it is in compression (Keaveny, 2001). However, it was shown that the tension aspect was less sensitive to increased stresses caused by the increased trabecular eccentricity. It is possible that trabecular architecture is optimized in this region to accommodate the increased load. Conversely, the trabecular architecture of the cancellous bone on the compression side would be organized to reflect the lessening of load experienced with increasing trabecular eccentricity/cortical bone thickness.

Limb/Tubular bones are often examined using a beam model to predict stress, strength, and rigidity through the use of cross-sectional geometric properties. In most analyses, limb bones are modeled as either solid or hollow cylindrical beams subjected to two-point bending forces applied to their ends. Beams/Bones loaded in pure bending will have a neutral axis that runs through the area centroid of the cross section (the center of

the area of the section). Because of bone curvature, muscle action and other factors bones are subjected to bending as well as pure axial loads in vivo. If the beams/bones are loaded with a combination of bending moments and axial forces, then the neutral axis will be shifted away from the centroid and toward the cortex under tension (Leiberman et al., 2004; Ruff and Hayes, 1983).

Cross-sectional geometric properties have been used to test hypotheses and make inferences about mechanical adaptation of bones for several decades. The earliest studies utilized cortical bone cross-sectional area to infer a bone's resistance to axial compression and tension. Cross-sectional area or measures of cortical thickness can provide poor or skewed results because resistance to bending is dependent on the distribution of material in a cross section. Second moments of area or moments of inertia measure how material is distributed about a defined axis and thus became the primary measures used because they better characterize the resistance of a tubular bone to bending around a particular axis.

The second moment of area (I) is generally calculated with respect to orthogonal axes determined either by anatomical or arbitrary planes (Ix, Iy) or with respect to orthogonal principal axes (Imax, Imin). The principal axes of a section define the directions of greatest and least bending rigidity. Imax and Imin indicate the relative magnitudes of greatest and least bending rigidity of a section. Ratios of the orthogonal measures of I (Ix/Iy or Imax/Imin) have been used to quantify cross-sectional shape. The Imax/Imin ratio indicates the degree to which the cross section deviates from circularity. An Imax/Imin ratio close to 1.0 indicates near circularity in shape while a ratio much greater than 1.0 indicates a departure from circularity and a strongly defined direction of greatest bending rigidity (Ruff and Hayes, 1983).

Numerous studies have examined bone functional adaptation of limb bones using cross-sectional geometric properties of cortical bone for both human and nonhuman species and have shown varying degrees of correlation between cross-sectional geometric properties and habitual loading strains (i.e., Ruff, 1981; Woo et al., 1981; Ruff and Hayes; 1983; Ruff, 1989; Swartz, 1993; Heinrich et al., 1999; Robling et al., 2002). A series of studies (Demes et al., 1998, 2001; Lieberman et al., 2004) showed that in vivo strain patterns obtained using strain-gauges during locomotion in laboratory animals were not well correlated with cross-sectional geometry of bones. These studies found that the predicted bending axes generally did not match well with the experimentally determined neutral axes or that the cross sections were not geometrically reinforced in regions of maximum strain. These data prompted the authors to advise against making "broad behavioral conclusions" from cross-sectional geometry alone (Demes et al., 2001). However, cross-sectional properties calculated relative to the centriod can still be considered as valid approximations of true bending rigidity and strength (Ruff et al., 2006). Deviations of the estimated values from actual values are also of less concern when individuals being compared are from the same species or closely related species that share an evolutionary history and basic body design (Ruff et al., 2006); research continues to provide support for cross-sectional morphology and mechanical loading under such circumstances (Ruff, 1989; Nunamker et al., 1990; McCarthy and Jeffcoat, 1992; Stock and Pfeiffer, 2001; Robling et al., 2002). Most researchers calculate cross-sectional properties using the area centroid due to the lack of experimental data on the neutral axis position. Because of this, most analyses of cross-sectional geometric properties do not assume the absolute values are correct but rather that the relative values or patterns are assumed to be useful for making comparisons (Ruff et al., 2006;

Lieberman et al., 2004).

A Proposed Bone for Bone Adaptation to Habitual Compression and Tension

The artiodactyl (sheep, deer, goats) calcaneus has been introduced as a model for interpreting bone adaptation to habitual loads due to its identification as a short-cantilevered beam with longitudinal compression and tension strains predominating in the opposing dorsal and plantar aspects of the bone (Lanyon, 1973,1974,1981,1992; Skedros, 1994; Skedros et al., 1993b, 1994a, 1995, 1996, 1997, 2001d, 2003b, 2004, 2012; Su, 1998; Su et al., 1999; Skedros and Baucom, 2007; Sinclair et al., 2013).

Lanyon (1973; 1974) first described the sheep calcaneus as being under a habitual simple bending regime. Using in vivo strain gauges placed on the cortical bone of the calcanei of a total of 15 live active adult domesticated sheep (*Ovis aries*), Lanyon showed a close correspondence between arched trabecular patterns and orientations of principal strains experienced by the bones. He described the calcaneus as a cantilevered beam-like structure that typically experiences relatively simple compression-tension (bending) loading. Lanyon determined that during locomotion the "…principal compressive strain coincided with the trabeculae in the dorsal tract and the principal tensile strain with those in the plantar tract" (1974).

Following the work of Lanyon, Su and colleagues (1998; 1999) conducted an in-vitro study using simulated loading of the mule deer (*Odocoileus hemionus hemionus*) calcaneus to further characterize the artiodactyl calcaneus. Su et al. used strain gauges to record principal strains, maximum shear strains, and principal strain angles from several locations on ten adult mule deer calcanei in fully articulated hind limbs throughout a

range of simulated habitual and extreme loading conditions. The results showed that the dorsal cortex of the mule deer calcaneus experienced longitudinal compressive strains while the plantar cortex received longitudinal tensile strains, indicating that the deer calcaneus is in simple bending during habitual loading condition similar to the sheep calcaneus (Su, 1998; Su et al., 1999). This same study showed that during off axis loading, to simulate extremes of twisting, turning, running and jumping, the dorsal/compression- plantar /tension strain dichotomy was highly consistent. Additionally, as noted in other skeletal elements and hypothesized for the artiodactyl calcaneus, the plantar ligament and tendon of the superficial digital flexor muscle were shown to play a key role in load sharing on the plantar surface. The study demonstrated that the functionally loaded (both habitual and extreme) mule deer calcaneus generally behaves like a short cantilevered beam with compression and tension strains predominating the dorsal and plantar cortices, respectively (Su, 1998; Su et al., 1999).

Based on the identification of the artiodactyl calcaneus as a cantilevered beam in simple bending, Skedros and colleagues have introduced the artiodactyl calcaneus as a control bone for bone adaptation to habitual loading and characterized the material property differences between cortical bone under habitual compression and tension (Skedros and Bloebaum, 1991; Skedros, 1994; Skedros and Dirksmeier, 1995; Skedros et al., 1993a, b, 1994c, 1995, 1996, 1997, 2001a, b, c, d, 2003a, b, c, 2004, 2006, 2007). The work of Skedros and colleagues has been extensive and has attempted to characterize material properties of the artiodactyl calcaneus as fully as possible. This characterization has primarily been concerned with identifying and characterizing differences between cortical bone under compression and tension. The group has identified numerous statistically significant structural properties that differ between the dorsal “compression”

and plantar “tension” cortices including greater cortical thickness, increased mineral content, increased secondary osteon population density, more cross-linked collagen fibers, and lower porosity in the dorsal cortex compared to the plantar cortex.

Skedros and Baucom (2007) showed that the trabecular tracts of the artiodactyl calcaneus from the compression and tension loaded aspects of the bone follow the trajectories of compression/tension stress, form orthogonal (90°) intersections, and are described by the same nonlinear equations that can be superimposed on the those of cantilevered beams. They present their data as further evidence that the artiodactyl calcaneus can be accurately modeled as a short cantilevered beam and that the cancellous bone of the artiodactyl calcaneus, similar to the cortices, is under habitual compression in the dorsal aspect and tension in the plantar aspect.

Recently, Skedros and colleagues (2012) examined if trabecular tracts from the compression and tension regions of the artiodactyl calcaneus exhibit similar differences in mineral content and microscopic mineralization heterogeneity as the cortical bone from the same regions. They included both skeletally immature and mature deer in the analysis. They found that mineral content, as determined by backscatter electron (BSE) images, was significantly greater in the compression tracts for both the immature and mature groups. Similarly, they also showed that bulk mineral ash content tended to be greater in the compression tracts for both groups. Mineralization heterogeneity was found to only differ between the tracts in the immature group. The differences in mineral content and bulk ash in the trabecular tracts were much less than those seen in the cortices and published data. However, the data suggest that the small differences may not be mechanically important. The authors suggest that the study supports the probability

that architectural modifications primarily adapt the trabecular tracts to local load demands.

Sinclair et al. (2013) sought to quantify regional variation in trabecular architecture of the sheep and deer calcaneus toward further establishing the bone as a possible control bone for studies examining relationships between trabecular architecture and stress transfer in the anthropoid femoral neck. They hypothesized that differences in specific trabecular architectural characteristics would be seen between the dorsal/compression and plantar/tension trabecular tracts in the calcaneus. The authors based their hypotheses on studies of ovine and human trabecular bone that showed that 1) energy absorption to yield, ultimate stress, and yield strength are nearly 30% lower in tension versus compression (Keaveny et al. 1994 a, b,; Bayraktar et al., 2004); 2) trabecular bone is weakest in shear when compared to compression and tension (Mitton et al., 1997; Keaveny et al., 2001; Sanyal et al., 2012); 3) compressive yield strains are higher in tension (Keaveny et al., 1994; Kopperdahl and Keaveny, 1998; Rincon-Kohli and Zysser, 2009; Wolfram et al., 2011); 4) microdamage initiation and propagation occur differently and asymmetrical in tension, compression, and shear (Nyman et al., 2009; Wu and Neiber, 2012); 5) trabecular architecture is highly sensitive to change in prevalent/predominant loading direction and magnitude (Pontzer et al., 2006; van der Meulen et al., 2006, 2009; Barak et al., 2011). Following methods established by Skedros et al. (1997), they divided the diaphysis of the calcaneus up into the midshaft (40% and 50% of diaphysis length) and distal shaft (20% and 30% of diaphysis length).

They made four predictions/hypotheses. 1) That the midshaft would show dorsal-plantar trabecular architecture differences with enhancements occurring in the plantar/tension trabecular tracts because of its “comparatively deficient mechanical

properties." Predicted enhancements include BV/TV, TbTh, TbN, ConnD, and DA being higher in the plantar region compared to the dorsal, and TbSp being higher in the dorsal compared to plantar. 2) That the distal shaft would show fewer dorsal-plantar differences in trabecular architecture due to the extensive interconnections and increased load complexity of the region that would be expected to reduce differences in ambient strain magnitudes between the dorsal and plantar trabecular tracts. 3) That the midshaft would show dorsal-middle-plantar differences that reflect low strains/stresses and/or increased prevalence of shear stresses in the neural axis (middle). The hypothesized differences included the middle region having lower BV/TV, TbTh, TbN, ConnD, and DA and higher TbSp than the dorsal or plantar regions. 4) That the distal shaft would show fewer and less distinct/consistent dorsal-middle-plantar differences in trabecular architecture compared to the midshaft.

To test the hypotheses, volumes of interest (VOI) were obtained from micro-CT scans of the bones and the trabecular architecture measures were obtained using the MicroView software (GE Health Care). The VOIs obtained from each specimen at each location were of varying sizes. Mean VOI sizes for the deer ranged from 105 ± 40 mm^3 to 297 ± 66 mm^3 and for the sheep from 202 ± 65 mm^3 to 340 ± 79 mm^3. The analyses utilized three-way ANOVA to assess effects and interactions between region (dorsal, middle, plantar), section (midshaft, distal shaft), and species. Then paired T-tests were utilized to compare differences in each region at each section for each species. Pearson's correlation coefficients were calculated to identify association between pairs of trabecular architectural characteristic and between cortical bone thickness and each trabecular architecture characteristics within each species. The authors do not indicate if specific statistics for multiple/repeated measures were completed for this data set, or if each

measure was considered independent in the analysis as the described statistics would indicate.

The results showed that for the deer calcaneus midshaft only TbN differed in the hypothesized manner between the dorsal and plantar regions. The deer midshaft showed no other statistically significant differences between the dorsal and plantar regions. Statistical "trends" were seen in ConnD and TbSp, but they were not consistent with the hypothesized relationships. When only similar sized volumes of interest were compared, the differences in ConnD became statistically significant. In the sheep midshaft significant differences were found between the dorsal and plantar regions for TbSp, TbN and ConnD, but the differences were not consistent with the hypothesized relationships. In the distal shaft of the deer calcaneus, only ConnD had statistically significant differences between dorsal and plantar regions. In the sheep calcaneus distal shaft significant differences were seen between dorsal and plantar regions in BV/TV, TbTh, TbN, ConnD, and DA, rejecting the hypothesis that fewer differences would be seen in the distal shaft versus the midshaft. Finally, the data showed that in the midshaft the middle region of both the deer and sheep generally differed from the dorsal and plantar regions. The distal shaft of the deer had five of eight characteristics differing in a similar manner to the midshaft, which was not consistent with the hypotheses. The sheep distal shaft, however, showed only one of eight characteristics differing as predicted between dorsal-middle-plantar regions compared to five of eight at the midshaft, thus supporting the hypothesis that the distal shaft would have fewer differences than the midshaft.

The results of the study showed that none of the hypotheses were fully supported and that the trabecular architecture characteristics that have been shown to be most important in trabecular strength and stiffness (BV/TV, DA, and SMI) did not

significantly differ between the dorsal and plantar tracts in either species. This suggests that trabecular architecture characteristics, when considered in isolation, do not relate to the nonuniform strain mode/magnitude distribution in predicted or obvious ways. The authors indicate that differences seen between the species could be a result of differences in 1) body size, 2) activity levels, 3) sex ratio of samples, or 4) VOI size.

The correlation analyses between adjacent cortical thickness and each measure for the deer showed that only one trabecular architectural characteristic moderately correlated at each of the shaft locations (DA at the midshaft and ConnD at the distal shaft). In the sheep there were several significant moderate correlations (BV/TV, BS/BV, TbTh, TbSp, TbN, ConnD, and SMI). The authors indicate that the data and observations suggest that the cortices of the artiodactyl calcaneus "…do not have an important role in influencing their trabecular architecture as might have been anticipated." They further suggest that additional analyses that consider the cortical bone distribution across and along the entire shaft are needed to examine these issues.

The works to date provide considerable evidence for the use of the artiodactyl calcaneus to examine trabecular architecture from cancellous bone under habitual compression and tension. Cancellous bone of the artiodactyl calcaneus has yet to be fully studied and characterized to examine the distribution and alterations of trabecular architecture across the length of the diaphysis and between dorsal and plantar regions with appropriate statistical analyses for repeated/multiple measures. The present study will examine the variation in trabecular architecture within and across the length of the artiodactyl calcaneus and with regard to cortical bone thickness and distribution to investigate how the architecture of cancellous bone may adapt to habitual loading.

MATERIALS AND METHODS

To assess the study questions sheep and deer calcanei were analyzed. For the sheep study specimens, one calcaneus was randomly selected from eleven skeletally mature domesticated sheep carcasses (*Ovis aries*) (N=6 left and 5 right), (n=4 male and 7 female). For the deer, one calcaneus was randomly selected from nine skeletally mature wild mule deer (*Odocoileus hemionus hemionus*) (N=5 left and 4 right), (n=4 male and 5 female). All study specimens were obtained from animals that did not display any signs of skeletal disease, lameness, or advanced age. No animals were specifically sacrificed for this study and all specimens were collected as part of a multiyear/multicomponent study of artiodactyl calcanei lead by J. Skedros and colleagues. Skeletal maturation was confirmed using medial to lateral radiographs and the presence of a completely fused distal epiphysis. Based on the data presented by Lanyon (1973, 1974) and Skedros and colleagues (1994, 2004, 2007) the dorsal region of calcaneus was considered the compression region and the plantar region the tension region for the analysis.

To allow for standardized comparison between calcanei of varying size, diaphyseal length was used following Skedros and colleagues (1994a). The diaphyseal length was measured as the distance from the inflection of the midarticular surface, 100% of length to the point where the dorsal tubercle merges with the distal portion of the shaft, 0% length (Skedros et al., 1994a:398). The diaphyseal length of each bone was measured using a digital vernier caliper (MitutoyoTM, Japan), the 20, 30, 40, and 50% diaphyseal

length locations were located and marked (Figure 6), and the distance of each from the 0% location was recorded. A longitudinal axis was also defined, following Skedros et al. (1994a), to allow for standardized orientation of the calcanei for analysis. The longitudinal axis was defined by two points that were marked at one-half the dorsal-plantar thickness of the cancellous bone, or the medullary cavity, at the 30% and 60% locations.

The bones were then scanned in a General Electric Medical Systems EVS-RS9 Micro-CT scanner at a 46-micron resolution (80 kVp, 450 µA and exposure time of 500 ms) at the University of Utah Small Animal Imaging Facility. The resulting voxel size for all scans was 0.0464 x 0.0464 mm. Care was taken to scan the entire calcaneal diaphyseal length (0-100%), and when that was not possible due to larger sized calcanei, the scans minimally included the dorsal tubercle (0% location) to at least 60% of diaphyseal length to ensure each of the study locations was scanned. Imaging data were exported as 16-bit files for 3D reconstructions. Three-dimensional reconstructions of each bone were then produced from the high-resolution scan slices using software provided by GE Health Care for use with the EVS-RS9 scanner (eXplore Series MicroCT Software, GE Health Care). The 3D reconstructions were then analyzed using the MicroView program (GE Health Care). While the bones were scanned in a standardized orientation ensuring the dorsal-plantar, medial-lateral, and anterior-posterior axes were maintained, the orientation of each 3D reconstruction was checked using the linear measurement tool within MicroView and when necessary adjustments were made using the MicroView plane rotation mode to ensure proper anatomical cancellous orientation. The 20, 30, 40, and 50% locations were then located in the 3D reconstructions by measuring the prerecorded distance from the dorsal tubercle to each percent location

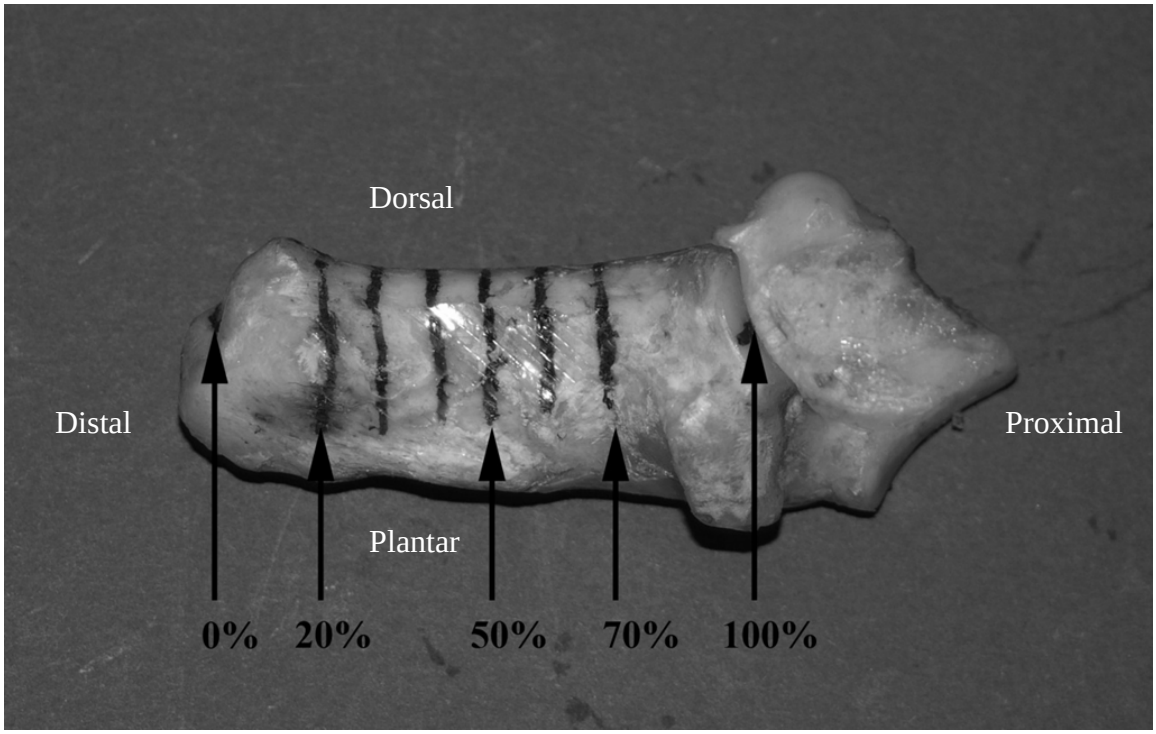

Figure 6. Lateral photograph of sheep calcaneus with percent length locations marked and identified.

with the linear measurement tool.

The Advanced Bone Application (ABA) module of MicroView was used to obtain the architectural parameters from 3 mm cubic regions of interest (ROI) located within the cancellous bone of the dorsal (compression) and plantar (tension) regions at 20, 30, 40, and 50% locations. The size of the ROI was dictated by the smaller dimensions of the sheep and deer calcaneus, especially the medial-lateral width of the cancellous bone mass. Care was taken to place each ROI as dorsal or plantar as possible, while making sure each ROI was entirely within the cancellous bone in all three dimensions and did not include any cortical bone or cancellous-cortical transition bone of lower porosity that could not be easily identified to bone type. Prior to running each ROI through the ABA analyses, the auto threshold tool was used following MicroView standard operating protocols to compute the gray-level threshold for each ROI that best distinguished bone from nonbone within the ROI. The analysis yielded two ROIs within each of the four locations (Figure 7).

The ABA module of MicroView provides quantification of each of the study parameters following standard published methods. For the analyses basic stereological measures of BV/TV and TbN, as well as direct, model free measures of TbTh and TbSp were obtained (Hildebrand and Ruegsegger, 1997a; Hildebrand and Ruegsegger, 1997b). Connectivity density (ConnD) was estimated by dividing the Euler number by the ROI volume and reporting the absolute value of the result (Hildebrand and Ruegsegger, 1997b). Degree of anisotropy was estimated using the mean intercept length (MIL) method (Whitehouse, 1974; Harrigan and Mann, 1984). In the MIL method, fabric tensors provide the descriptions of trabecular architecture with the eigenvectors of a 3x3

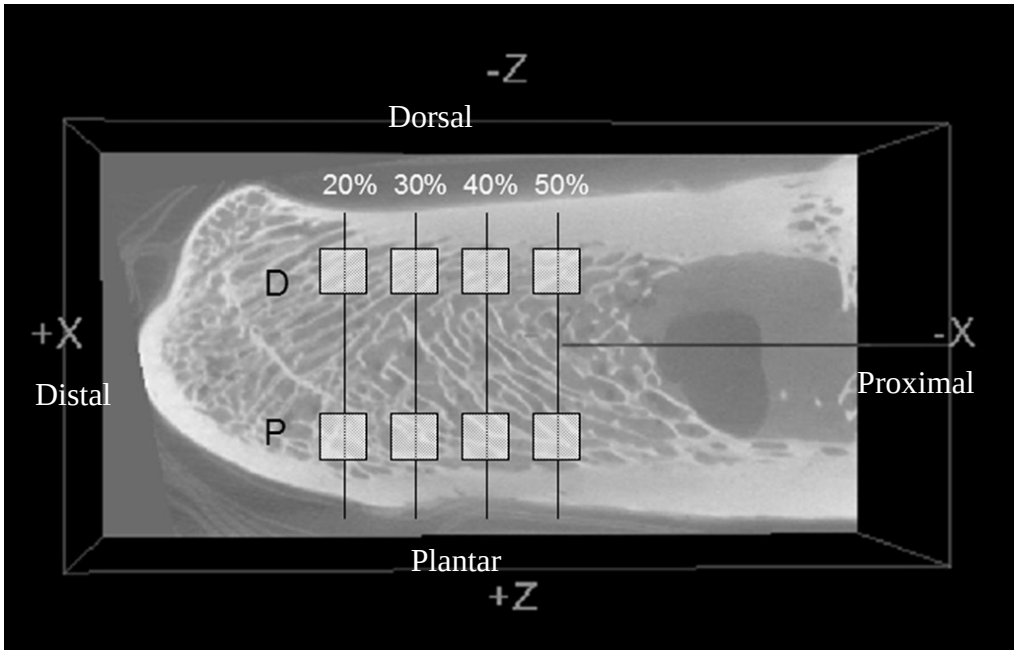

Figure 7. Representative lateral view of micro-CT image of a calcaneus with percent length locations and the dorsal and plantar regions of interest (ROIs) noted. Image not to scale.

orientation matrix giving the main directions and the eigenvalues giving the degree of concentration around the main directions (Cowin, 1985; Cowin, 1986). The degree of anisotropy (DA) is defined as the ratio of the primary eigenvalue divided by the tertiary eigenvalue (t1/t3) (Cowin, 1985; Odgaard, 2001).

Using the line measurement tool within MicroView the dorsal and plantar cortical bone thicknesses were obtained from the middle of each percent diaphysis location and recorded in millimeters. The cortical thickness ratio (CTR) was calculated as the dorsal cortical thickness/the plantar cortical thickness for each location.

To obtain cortical bone cross-sectional geometry measures, the single micro-CT slice at the prerecorded distance for each percent diaphysis location was exported as an 8-bit TIFF image. The cancellous bone was removed using Adobe Photoshop CS6 (Adobe Systems Incorporated, 2012). The cross-sectional geometric data was then obtained using image-J 1.47v (National Institutes of Health, 2012) and the macro MomentMacroJ v1.4 (http://www.hopkinsmedicine.org/fae/MMacro.htm, Sylvester, 2012). The Imax/Imin ratios for each section were then calculated.

Statistical Methods

Statistical analyses specifically for repeated measures were required for the data in this study since multiple measurements were obtained from each study specimen. When multiple measurements are taken from the same subject/specimen, the correct statistical analysis is more complex than if only one measurement was taken from each subject/specimen. This is because the variability of measurements from different subjects/specimens is usually much greater than the variability of measurements from the same subject/specimen. Data sets consisting of multiple/repeated measurements violate

the assumption of independence inherent in many statistical analyses such as T-tests, correlation, and regression (Bland and Altman, 1994). Analyses for repeated measures specifically account for the lack of independence among the measurements analyzed.

To test for correlation between the trabecular architectural measurements and percent diaphysis location, region, CTR, and Imax/Imin, a "within-subjects" correlation coefficient was calculated. This correlation coefficient accounts for the lack of independence among the repeated measurements by removing the variation between subjects (Bland and Altman, 1995). A within-subjects correlation coefficient examines whether an increase in a variable is associated with an increase in another variable within the same individual (Bland and Altman, 1995).

Multiple regression models for repeated measurements were used to test for differences in the architectural parameters between the dorsal and plantar regions (region), over the length of the diaphysis (location), with CTR, with Imax/Imin, and by species. For these analyses, each architectural parameter was used as the outcome measure while region, location, CTR, Imax/Imin, and species were the predictor variables. Each analysis was adjusted for potential confounders. Potential confounders included other architectural parameters due to possible high intercorrelation of the measures. Confounders were retained in the final model if they were significant at the 0.05 level or if they altered the coefficient of the primary exposure (region) by at least 10% (Greenland, 1989). These statistical methods, while more complicated, provide the most accurate analysis of the variation and difference in the data.

The statistical package STATA 10.1 (StataCorp, College Station, TX) was used for all statistical analyses and a p value of 0.05 or less was considered to indicate statistical significance.

RESULTS

Sheep Calcaneus

The mean and standard deviation of each trabecular architectural measure by region and diaphysis location are presented in Table 1.

Question 1: Architectural Variation over Diaphyseal Length

For the sheep data, correlation analyses show that all the trabecular architecture measures are moderately to strongly and statistically significantly correlated with the percent diaphysis location, except for ConnD in the dorsal region (Table 2).

To assess if the trabecular architecture measures differ over the length of the sheep calcaneal diaphysis, multiple regression analyses for repeated measures were employed. First the analyses examined all the sheep data together using location and region as predictor variables. The results examining the effect of percent diaphysis location (as predictor variable) on each measure, when controlling for region (dorsal/plantar) and confounding variables, are presented in Table 3. Percent diaphysis location is shown to have a statistically significant effect on BV/TV, TbTh, TbN, ConnD and DA. Bone volume fraction (BV/TV), TbN and ConnD are shown to significantly decrease as percent diaphysis location increased (moving from 20% to 50% diaphysis location). Trabecular thickness (TbTh) and DA significantly increase with percent diaphysis location. Trabecular separation (TbSp) was the only trabecular architectural

Table 1. Summary statistics, mean (SD), for each trabecular architectural parameter from the sheep calcaneus.

		20%	30%	40%	50%
Dorsal	BV/TV	0.491 (0.046)	0.455 (0.044)	0.398 (0.035)	0.311 (0.063)
	TbTh	0.227 (0.037)	0.192 (0.025)	0.165 (0.019)	0.183 (0.040)
	TbSp	0.342 (0.057)	0.352 (0.065)	0.372 (0.053)	0.538 (0.138)
	TbN	1.964 (0.197)	2.102 (0.175)	2.096 (0.158)	1.618 (0.366)
	ConnD	4.41 (2.322)	6.00 (2.143)	6.517 (2.012)	3.552 (1.350)
	DA	2.08 (0.303)	1.779 (0.249)	1.755 (0.219)	1.769 (0.205)
Plantar	BV/TV	0.437 (0.028)	0.432 (0.056)	0.396 (0.048)	0.386 (0.044)
	TbTh	0.194 (0.017)	0.195 (0.032)	0.221 (0.039)	0.226 (0.045)
	TbSp	0.375 (0.048)	0.381 (0.063)	0.479 (0.091)	0.533 (0.113)
	TbN	2.045 (0.167)	1.997 (0.191)	1.737 (0.166)	1.654 (0.187)
	ConnD	6.872 (2.064)	5.617 (2.387)	3.794 (1.187)	3.104 (1.206)
	DA	1.479 (0.190)	1.802 (0.343)	1.924 (0.199)	1.930 (0.291)

BV/TV: bone volume fraction; TbTh: trabecular thickness (mm); TbSp: trabecular separation (mm); TbN: trabecular number (mm^{-1}); ConnD: connectivity density (number per mm^3); DA: degree of anisotropy.

Table 2. Correlation coefficients (R) of trabecular architectural measures with percent diaphysis location by region for the sheep calcaneus.

	Dorsal		Plantar	
	R	p value	R	p value
BV/TV	-0.86	<0.001	-0.70	<0.001
TbTh	-0.62	<0.001	0.55	<0.001
TbSp	0.66	<0.001	0.78	<0.001
TbN	-0.48	0.004	-0.87	<0.001
ConnD	-0.15	0.394	-0.86	<0.001
DA	-0.61	<0.001	0.71	<0.001

Table 3. Effect of location on each architectural parameter controlling for region and confounding variables for the sheep calcaneus. Coefficient represents the amount of change in outcome variable (architectural parameter) for a unit of change in the predictor variable (location).

BV/TV	Coefficient (95%CI)	p value	Controlling for (confounding variables):
Location	-0.022 (-0.031 to -0.013)	<0.001	Region, TbSp, ConnD
TbTh	Coefficient (95%CI)	p value	Controlling for (confounding variables):
Location	0.004 (0.002 to 0.007)	0.002	Region, BV/TV, TbN, ConnD, DA
TbSp	Coefficient (95%CI)	p value	Controlling for (confounding variables):
Location	0.009 (-0.003 to 0.020)	0.135	Region, BV/TV, TbN, ConnD, DA
TbN	Coefficient (95%CI)	p value	Controlling for (confounding variables):
Location	-0.022 (-0.011 to- 0.034)	<0.001	Region, BV/TV, TbTh, TbSp, ConnD, DA
ConnD	Coefficient (95%CI)	p value	Controlling for (confounding variables):
Location	-0.378 (-0.57 to -0.18)	<0.001	Region, BV/TV, TbTh, TbSp, TbN, DA
DA	Coefficient (95%CI)	p value	Controlling for (confounding variables):
Location	0.045 (-0.030 to 0.119)	0.024	Region, BV/TV, TbTh, TbSp

measure for the sheep calcaneus that did not significantly change with percent diaphysis location

The results of the analyses for the separate dorsal and plantar data examining the effect of location (as predictor variable) while controlling for confounding variables are presented in Tables 4 and 5. In the dorsal region, BV/TV was the only architectural measure to significantly change over the length of the diaphysis. It was shown to decrease with percent location (from 20% to 50%) (Table 4). In the plantar region BV/TV, TbN, and ConnD were all shown to significantly decrease and TbTh and DA were shown to significantly increase with percent location (Table 5). These analyses indicate that trabecular architectural measures in the plantar region change more significantly over the length of the diaphysis than do the measures in the dorsal region.

Question 2: Architectural Variation by Region

All architectural measures were shown to be weakly and not significantly correlated with region, except for TbTh which was weakly, but significantly, correlated with region (Table 6).

To assess if the trabecular architectural measures significantly differ by region (dorsal vs. plantar) multiple regression analyses were conducted with region as the predictor variable and controlling for location and confounding variables. Table 7 presents the results of the analyses. None of the trabecular architectural measures were found to significantly differ between the dorsal and plantar regions.

The sheep data were next examined by each percent location (20%, 30%, 40%, 50%) with region (dorsal/plantar) as the predictor variable. In the 20% location only DA was shown to significantly differ between the dorsal and plantar regions, it was shown to

Table 4. Effect of location on each architectural measure in the dorsal region for the sheep calcaneus.

BV/TV	Coefficient (95%CI)	p value	Controlling for (confounding variables):
Location	-0.033 (-0.044 to -0.022)	< 0.001	TbSp, ConnD
TbTh	Coefficient (95%CI)	p value	Controlling for (confounding variables):
Location	-0.003 (-0.008 to 0.001)	0.153	BV/TV, TbN, ConnD, DA
TbSp	Coefficient (95%CI)	p value	Controlling for (confounding variables):
Location	0.003 (-0.019 to 0.025)	0.805	BV/TV, TbN, ConnD, DA
TbN	Coefficient (95%CI)	p value	Controlling for (confounding variables):
Location	-0.009 (-0.043 to 0.026)	0.620	BV/TV, TbTh, TbSp
ConnD	Coefficient (95%CI)	p value	Controlling for (confounding variables):
Location	-0.303 (-0.781 to 0.175)	0.215	BV/TV, TbTh, TbSp, TbN, DA
DA	Coefficient (95%CI)	p value	Controlling for (confounding variables):
Location	-0.047 (-0.142 to 0.048)	0.336	BV/TV, TbTh, TbSp

Table 5. Effect of location on each architectural measure in the plantar region for the sheep calcaneus.

BV/TV	Coefficient (95%CI)	p value	Controlling for (confounding variables):
Location	-0.011 (-0.019 to -0.003)	0.006	TbTh, TbSp, ConnD
TbTh	Coefficient (95%CI)	p value	Controlling for (confounding variables):
Location	0.007 (0.003 to 0.011)	0.001	BV/TV, TbN, ConnD, DA
TbSp	Coefficient (95%CI)	p value	Controlling for (confounding variables):
Location	0.005 (-0.011 to 0.020)	0.577	BV/TV, TbN, ConnD, DA
TbN	Coefficient (95%CI)	p value	Controlling for (confounding variables):
Location	-0.025 (-0.051 to 0.002)	0.020	BV/TV, TbTh, TbSp, ConnD
ConnD	Coefficient (95%CI)	p value	Controlling for (confounding variables):
Location	-0.299 (-0.536 to -0.063)	0.013	BV/TV, TbTh, TbSp, TbN, DA
DA	Coefficient (95%CI)	p value	Controlling for (confounding variables):
Location	0.170 (0.090 to 0.251)	< 0.001	BV/TV, TbTh, TbSp

Table 6 Correlation Coefficients (R) of trabecular architectural measures with region for the sheep calcaneus.

	R	p value
BV/TV	-0.01	0.925
TbTh	0.30	0.007
TbSp	0.21	0.064
TbN	-0.19	0.095
ConnD	-0.08	0.483
DA	-0.12	0.300

Table 7. Effect of region on each architectural parameter controlling for location and confounding variables for the sheep calcaneus.

BV/TV	Coefficient (95%CI)	p value	Controlling for (confounding variables):
Region	-0.001 (-0.007 to 0.006)	0.869	Location, TbTh, TbSp, TbN, ConnD, DA
TbTh	Coefficient (95%CI)	p value	Controlling for (confounding variables):
Region	0.002 (-0.002 to 0.006)	0.269	Location, TbSp, BV/TV, TbN, ConnD
TbSp	Coefficient (95%CI)	p value	Controlling for (confounding variables):
Region	0.013 (-0.006 to 0.032)	0.168	Location, TbTh, BV/TV, TbN, DA
TbN	Coefficient (95%CI)	p value	Controlling for (confounding variables):
Region	-0.005 (-0.030 to 0.04)	0.766	Location, TbTh, TbSp, ConnD
ConnD	Coefficient (95%CI)	p value	Controlling for (confounding variables):
Region	0.193 (-.248 to 0.634)	0.392	Location, TbTh, TbSp, TbN, DA
DA	Coefficient (95%CI)	p value	Controlling for (confounding variables):
Region	-0.058 (-0.164 to 0.048)	0.282	Location, TbTh, ConnD

be greater in the dorsal region (Table 8). None of the trabecular architecture measures were shown to be significantly different between the dorsal and plantar regions at the 30% diaphysis location (Table 9). In the 40% diaphysis location, only TbSp was significantly different between dorsal and plantar, it was higher in the plantar region (Table 10). None of the trabecular architectural measures were found to significantly differ between the dorsal and plantar regions at the 50% location (Table 11). The results of the separate region and location data analyses again indicate that the trabecular architectural measures of the sheep calcaneus differ more significantly across the length of the diaphysis than they do between the dorsal and plantar regions.

The results of this primary analysis indicate that there is more significant change in trabecular architectural measures over the length of the sheep calcaneus diaphysis than between the dorsal and plantar regions. To further examine the variation of trabecular architecture of the sheep calcaneus the data from the dorsal and plantar regions and each percent location were then examined separately.

Question 3: Architectural Variation with Cortical Thickness Ratio

Across the length of the diaphysis, the cortical bone thickness changes in both the dorsal and plantar regions. Since the role of cortical bone in carrying and absorbing loads is much greater than that of trabecular bone, the effect of the cortical bone thickness on the architectural measures was examined via a cortical thickness ratio (CTR), dorsal thickness/plantar thickness. The CTR mean and standard deviation for each percent diaphysis location is presented in Table 12. Cortical thickness ratio increases with percent diaphysis location (also see Figure 8). A within-subjects variation correlation analysis for repeated measures indicates that CTR is significantly and strongly correlated

Table 8. Effect of region on each architectural measure in the 20% diaphysis location for the sheep calcaneus.

BV/TV	Coefficient (95%CI)	p value	Controlling for (confounding variables):
Region	-0.013 (-0.031 to 0.004)	0.136	TbTh, TbSp, TbN, DA
TbTh	Coefficient (95%CI)	p value	Controlling for (confounding variables):
Region	-0.003 (-0.018 to 0.012)	0.714	TbSp, BV/TV, TbN, ConnD, DA
TbSp	Coefficient (95%CI)	p value	Controlling for (confounding variables):
Region	0.004 (-0.010 to 0.019)	0.556	BV/TV, TbTh, TbN
TbN	Coefficient (95%CI)	p value	Controlling for (confounding variables):
Region	0.031 (-0.020 to 0.081)	0.232	BV/TV, TbTh, TbSp
ConnD	Coefficient (95%CI)	p value	Controlling for (confounding variables):
Region	0.046 (-0.950 to 1.042)	0.927	BV/TV, TbTh, TbSp, TbN
DA	Coefficient (95%CI)	p value	Controlling for (confounding variables):
Region	-0.320 (-0.510 to -0.129)	0.001	BV/TV, TbTh, ConnD

Table 9. Effect of region on each architectural measure in the 30% diaphysis location for the sheep calcaneus.

BV/TV	Coefficient (95%CI)	p value	Controlling for (confounding variables):
Region	-0.003 (-0.010 to 0.004)	0.436	TbTh, TbSp, TbN, ConnD
TbTh	Coefficient (95%CI)	p value	Controlling for (confounding variables):
Region	0.001 (-0.005 to 0.006)	0.976	TbSp, BV/TV, TbN, ConnD, DA
TbSp	Coefficient (95%CI)	p value	Controlling for (confounding variables):
Region	0.007 (-0.019 to 0.032)	0.613	BV/TV, DA
TbN	Coefficient (95%CI)	p value	Controlling for (confounding variables):
Region	-0.027 (-0.078 to -0.024)	0.301	BV/TV, TbTh, TbSp
ConnD	Coefficient (95%CI)	p value	Controlling for (confounding variables):
Region	-0.095 (-0.731 to 0.541)	0.770	BV/TV, TbSp, DA
DA	Coefficient (95%CI)	p value	Controlling for (confounding variables):
Region	<0.001 (-0.221 to 0.222)	0.996	TbTh, ConnD

Table 10. Effect of region on each architectural measure in the 40% diaphysis location for the sheep calcaneus.

BV/TV	Coefficient (95%CI)	p value	Controlling for (confounding variables):
Region	0.001 (-0.018 to 0.020)	0.917	TbTh, TbSp, TbN, ConnD, DA
TbTh	Coefficient (95%CI)	p value	Controlling for (confounding variables):
Region	<0.001 (-0.014 to 0.014)	0.992	TbSp, BV/TV, TbN, ConnD, DA
TbSp	Coefficient (95%CI)	p value	Controlling for (confounding variables):
Region	0.094 (0.048 to 0.139)	<0.001	BV/TV, DA
TbN	Coefficient (95%CI)	p value	Controlling for (confounding variables):
Region	-0.035 (-0.077 to -0.007)	0.098	BV/TV, TbTh, TbSp, ConnD
ConnD	Coefficient (95%CI)	p value	Controlling for (confounding variables):
Region	-0.508 (-1.590 to 0.578)	0.359	BV/TV, TbSp, DA
DA	Coefficient (95%CI)	p value	Controlling for (confounding variables):
Region	0.150 (-0.111 to 0.405)	0.264	TbTh, ConnD

Table 11. Effect of region on each architectural measure in the 50% diaphysis location for the sheep calcaneus.

BV/TV	Coefficient (95%CI)	p value	Controlling for (confounding variables):
Region	0.004 (-0.102 to 0.018)	0.599	TbTh, TbSp, TbN, ConnD
TbTh	Coefficient (95%CI)	p value	Controlling for (confounding variables):
Region	0.006 (-0.004 to 0.015)	0.236	TbSp, BV/TV, TbN, ConnD, DA
TbSp	Coefficient (95%CI)	p value	Controlling for (confounding variables):
Region	-0.020 (-0.094 to 0.055)	0.608	BV/TV, TbTh, TbN
TbN	Coefficient (95%CI)	p value	Controlling for (confounding variables):
Region	0.011 (-0.040 to -0.062)	0.668	BV/TV, TbTh, TbSp, ConnD, DA
ConnD	Coefficient (95%CI)	p value	Controlling for (confounding variables):
Region	-0.391 (-1.140 to 0.358)	0.307	BV/TV, TbTh, TbSp
DA	Coefficient (95%CI)	p value	Controlling for (confounding variables):
Region	0.196 (-0.005 to 0.397)	0.056	BVTV, TbTh, ConnD

Table 12. Mean and standard deviation (SD) of the cortical thickness ratio (CTR) at each percent diaphysis location for the sheep calcaneus.

Location	Mean	SD
20%	0.61	0.15
30%	1.01	0.19
40%	1.70	0.43
50%	1.71	0.30

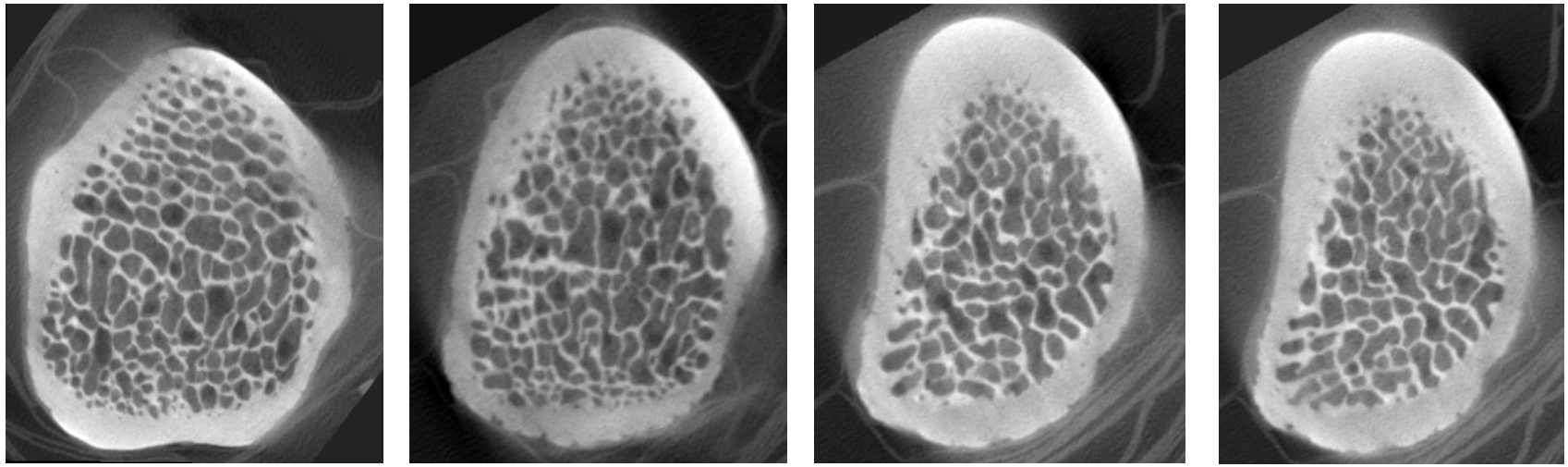

Figure 8. Micro-CT images of cross sections of a sheep calcaneus for each of the percent diaphyseal length location. A) The 20% diaphyseal length location; B) 30% diaphyseal length location; C) 40% diaphyseal length location; D) 50% diaphyseal length location. Images not to scale. Top=dorsal, bottom=plantar.

with percent diaphysis location ($R = 0.87$, $p = < 0.001$).

Correlation analyses for within-subjects variation with repeated measures show that all the trabecular architecture measures are moderately to strongly and statistically significantly correlated with CTR, except for TbN and ConnD in the dorsal region (Table 13).

Each trabecular architectural measure was examined with CTR as the predictor variable and controlling for region and confounding variables (Table 14). Four of the six measures (BV/TV, TbTh, TbN, and ConnD) were found to significantly change with CTR. Bone volume fraction (BV/TV), TbN and ConnD were shown to decrease with increasing CTR, while TbTh increased with increasing CTR. A fifth measure, DA, was shown to be trending toward significantly increasing with CTR, with a $p=0.055$. However, when the analyses were executed with region as the predictor variable and CTR was controlled for along with confounding variables, DA was the only measure found to significantly differ between regions (Table 15). When the dorsal and plantar data were examined separately with CTR as the predictor variable BV/TV and ConnD were shown to significantly decrease with increasing CTR in the dorsal region (Table 16). In the plantar region BV/TV, TbN and ConnD significantly decreased and TbTh and DA significantly increased with increasing CTR (Table 17). Not surprisingly, since CTR is highly correlated with percent location, the results of the analyses with CTR are similar to those with percent diaphysis location. Again the analyses indicate that the most significant changes in trabecular architecture do not occur between the dorsal and plantar regions but across the length of the diaphyses highlighting the important relationship between cortical bone and trabecular bone in the sheep calcaneus.

Table 13. Correlation coefficients (R) of trabecular architectural measures with CTR by region for the sheep calcaneus.

	Dorsal		Plantar	
	R	p value	R	p value
BV/TV	-0.71	<0.001	-0.63	<0.001
TbTh	-0.69	<0.001	0.45	0.007
TbSp	0.41	0.014	0.68	<0.001
TbN	-0.24	0.169	-0.77	<0.001
ConnD	0.03	0.851	-0.80	<0.001
DA	-0.54	<0.001	0.65	<0.001

Table 14. Effect of CTR on each architectural parameter controlling for region and confounding variables for the sheep calcaneus.

BV/TV	Coefficient (95%CI)	p value	Controlling for (confounding variables):
CTR	-0.019 (-0.026 to -0.013)	<0.001	Region, TbTh, TbSp, TbN, ConnD
TbTh	Coefficient (95%CI)	p value	Controlling for (confounding variables):
CTR	0.010 (0.005 to 0.015)	<0.001	Region, BV/TV, TbSp, TbN, ConnD
TbSp	Coefficient (95%CI)	p value	Controlling for (confounding variables):
CTR	0.001 (-0.022to 0.024)	0.927	Region, BV/TV, TbTh, TbN, ConnD, DA
TbN	Coefficient (95%CI)	p value	Controlling for (confounding variables):
CTR	-0.046 (-0.025 to -0.066)	<0.001	Region, BV/TV, TbTh, TbSp, ConnD
ConnD	Coefficient (95%CI)	p value	Controlling for (confounding variables):
CTR	-0.791 (-1.138 to -0.445)	<0.001	Region, BV/TV, TbTh, TbSp, TbN, DA
DA	Coefficient (95%CI)	p value	Controlling for (confounding variables):
CTR	0.117 (-0.002 to 0.235)	0.055	Region, BV/TV, TbTh, TbN ConnD

Table 15. Effect of region on each architectural parameter controlling for CTR and confounding variables for the sheep calcaneus.

BV/TV	Coefficient (95%CI)	p value	Controlling for (confounding variables):
Region	<0.001 (-0.006 to 0.006)	0.992	CTR, TbTh, TbSp, TbN, ConnD, DA
TbTh	Coefficient (95%CI)	p value	Controlling for (confounding variables):
Region	0.002 (-0.003 to 0.007)	0.365	CTR, TbSp, BV/TV, TbN, ConnD, DA
TbSp	Coefficient (95%CI)	p value	Controlling for (confounding variables):
Region	0.012 (-0.007 to 0.031)	0.205	CTR, BV/TV, TbTh, TbN, DA
TbN	Coefficient (95%CI)	p value	Controlling for (confounding variables):
Region	0.002 (-0.017 to 0.021)	0.832	CTR, BV/TV, TbTh, TbSp, ConnD
ConnD	Coefficient (95%CI)	p value	Controlling for (confounding variables):
Region	0.202 (-0.236 to 0.642)	0.3365	CTR, TbTh, TbSp, TbN, DA
DA	Coefficient (95%CI)	p value	Controlling for (confounding variables):
Region	-0.061 (-0.169 to 0.046)	<0.001	CTR, TbTh, ConnD

Table 16. Effect of CTR on each architectural measure in the dorsal region for the sheep calcaneus.

BV/TV	Coefficient (95%CI)	p value	Controlling for (confounding variables):
CTR	-0.059 (-0.079 to -0.040)	<0.001	TbTh, TbSp, ConnD
TbTh	Coefficient (95%CI)	p value	Controlling for (confounding variables):
CTR	-0.003 (-0.012 to 0.006)	0.580	BV/TV, TbSp, TbN, ConnD
TbSp	Coefficient (95%CI)	p value	Controlling for (confounding variables):
CTR	0.029 (-0.036 to 0.094)	0.379	BV/TV, TbTh, TbN, ConnD, DA
TbN	Coefficient (95%CI)	p value	Controlling for (confounding variables):
CTR	0.006 (-0.054 to 0.065)	0.858	BV/TV, TbTh, TbSp
ConnD	Coefficient (95%CI)	p value	Controlling for (confounding variables):
CTR	-0.985 (-1.705 to -0.264)	0.007	BV/TV, TbTh, TbSp, TbN, DA
DA	Coefficient (95%CI)	p value	Controlling for (confounding variables):
CTR	-0.065 (-0.228 to 0.099)	0.439	BV/TV, TbTh, TbSp

Table 17. Effect of CTR on each architectural measure in the plantar region for the sheep calcaneus.

BV/TV	Coefficient (95%CI)	p value	Controlling for (confounding variables):
CTR	-0.017 (-0.033to -0.002)	0.030	TbTh, TbSp, ConnD
TbTh	Coefficient (95%CI)	p value	Controlling for (confounding variables):
CTR	0.009 (0.001 to 0.018)	0.026	BV/TV, TbSp, TbN, ConnD
TbSp	Coefficient (95%CI)	p value	Controlling for (confounding variables):
CTR	0.004 (-0.027 to 0.035)	0.808	BV/TV, TbTh, TbN, ConnD, DA
TbN	Coefficient (95%CI)	p value	Controlling for (confounding variables):
CTR	-0.052 (-0.098 to -0.005)	0.029	BV/TV, TbTh, TbSp
ConnD	Coefficient (95%CI)	p value	Controlling for (confounding variables):
CTR	-0.448 (-0.899 to 0.002)	0.050	BV/TV, TbTh, TbSp, TbN, DA
DA	Coefficient (95%CI)	p value	Controlling for (confounding variables):
CTR	0.267 (0.114 to 0.421)	0.001	BV/TV, TbTh, TbSp

Question 4: Architectural Variation with Imax/Imin

Cross-sectional geometric properties were obtained and the Imax/Imin ratio was calculated for each percent diaphysis location. Mean and standard deviations for each percent diaphysis location of the sheep calcaneus are presented in Table 18. The Imax/Imin measure increases between the 20% and 50% locations indicating a greater departure from circularity and a more strongly defined direction of greatest bending rigidity. A within-subjects correlation for repeated measures indicates that Imax/Imin is strongly and significantly correlated with percent diaphysis location ($R = 0.90$, $p = <0.001$). Correlation analyses of each trabecular architectural measure with Imax/Imin (Table 19) reveal moderate to strong and statistically significant correlation between the measure and Iman/Imin in both the dorsal and plantar regions. The only architectural measure not significantly correlated with Imax/Imin is connectivity density (ConnD) in the dorsal region.

Each trabecular architectural measure was examined with Imax/Imin as the predictor variable and controlling for other confounding variables (Table 20). Four of the six measures were found to significantly change with Imax/Imin (BVTV, TbTh, TbN, and ConnD). BV/TV, TbN and ConnD were found to significantly decrease while TbTh increased with increasing Imax/Imin. When region was the predictor variable controlling for Imax/Imin and confounders (Table 21) none of the trabecular architectural measures varied significantly between regions. The analysis of the dorsal region data with Imax/Imin as the predictor and controlling for confounders showed BV/TV and ConnD were the only measures to significantly change with Imax/Imin (Table 22). Both measures decreased with increasing Imax/Imin. In the plantar region, TbTh, ConnD and DA were shown to significantly change with Imax/Imin (Table 23). TbTh and DA

Table 18. Mean and standard deviation (SD) of the Imax/Imin at each percent diaphysis location for the sheep calcaneus.

Location	Mean	SD
20%	1.23	0.16
30%	1.51	0.27
40%	1.87	0.30
50%	2.24	0.45

Table 19. Correlation coefficient (R) of trabecular architectural measures with Imax/Imin by region for the sheep calcaneus.

	Dorsal		Plantar	
	R	p value	R	p value
BV/TV	-0.73	<0.001	-0.64	<0.001
TbTh	-0.54	0.001	0.42	0.011
TbSp	0.53	0.001	0.65	<0.001
TbN	-0.42	0.011	-0.74	<0.001
ConnD	-0.28	0.110	-0.80	<0.001
DA	-0.41	0.014	0.65	<0.001

Table 20. Effect of Imax/Imin on each architectural parameter controlling for region and confounding variables for the sheep calcaneus.

BV/TV	Coefficient (95%CI)	p value	Controlling for (confounding variables):
Imin/Imax	-0.019 (-0.027 to 0.011)	<0.001	Region, TbTh, TbSp, TbN, ConnD
TbTh	Coefficient (95%CI)	p value	Controlling for (confounding variables):
Imin/Imax	0.009 (0.002 to 0.015)	0.006	Region, BV/TV, TbSp, TbN, ConnD
TbSp	Coefficient (95%CI)	p value	Controlling for (confounding variables):
Imin/Imax	<0.001 (-0.025 to 0.025)	0.996	Region, BV/TV, TbTh, TbN, ConnD, DA
TbN	Coefficient (95%CI)	p value	Controlling for (confounding variables):
Imin/Imax	-0.042 (0.019 to 0.065)	<0.001	Region, BV/TV, TbTh, TbSp, ConnD
ConnD	Coefficient (95%CI)	p value	Controlling for (confounding variables):
Imin/Imax	-0.857 (-1.220 to -0.450)	<0.001	Region, BV/TV, TbTh, TbSp, TbN, DA
DA	Coefficient (95%CI)	p value	Controlling for (confounding variables):
CTR	-0.083(-0.216 to 0.051)	0.224	Region, BV/TV, TbTh, TbSp, TbN, ConnD

Table 21. Effect of region on each architectural parameter controlling for Imax/Imin and confounding variables for the sheep calcaneus.

BV/TV	Coefficient (95%CI)	p value	Controlling for (confounding variables):
Region	<0.001 (-0.006 to 0.007)	0.873	Imin/Imax, TbTh, TbSp, TbN, ConnD, DA
TbTh	Coefficient (95%CI)	p value	Controlling for (confounding variables):
Region	0.002 (-0.003 to 0.006)	0.431	Imin/Imax, TbSp, BV/TV, TbN, ConnD, DA
TbSp	Coefficient (95%CI)	p value	Controlling for (confounding variables):
Region	0.012 (-0.006 to 0.031)	0.208	Imin/Imax, BV/TV, TbTh, TbN, DA
TbN	Coefficient (95%CI)	p value	Controlling for (confounding variables):
Region	0.001 (-0.018 to 0.020)	0.910	Imin/Imax, BV/TV, TbTh, TbSp, ConnD
ConnD	Coefficient (95%CI)	p value	Controlling for (confounding variables):
Region	0.116 (-0.200 to 0.433)	0.471	Imin/Imax, TbTh, TbSp, TbN, DA
DA	Coefficient (95%CI)	p value	Controlling for (confounding variables):
Region	-0.056 (-0.162 to 0.050)	0.298	Imin/Imax, TbTh, ConnD

Table 22. Effect of Imax/Imin on each architectural measure in the dorsal region for the sheep calcaneus.

BV/TV	Coefficient (95%CI)	p value	Controlling for (confounding variables):
Imin/Imax	-0.062 (-0.086 to -0.038)	<0.001	TbTh, TbSp, ConnD
TbTh	Coefficient (95%CI)	p value	Controlling for (confounding variables):
Imin/Imax	-0.007 (-0.016 to 0.002)	0.135	BV/TV, TbSp, TbN, ConnD
TbSp	Coefficient (95%CI)	p value	Controlling for (confounding variables):
Imin/Imax	0.011 (-0.060 to 0.080)	0.768	BV/TV, TbTh, TbN, ConnD, DA
TbN	Coefficient (95%CI)	p value	Controlling for (confounding variables):
Imin/Imax	-0.016 (-0.074 to 0.042)	0.597	BV/TV, TbTh, TbSp
ConnD	Coefficient (95%CI)	p value	Controlling for (confounding variables):
Imin/Imax	-0.944 (-1.641 to -0.247)	0.008	BV/TV, TbTh, TbSp, TbN, DA
DA	Coefficient (95%CI)	p value	Controlling for (confounding variables):
Imin/Imax	0.015 (-0.153 to 0.184)	0.858	BV/TV, TbTh, TbSp

Table 23. Effect of Imax/Imin on each architectural measure in the plantar region for the sheep calcaneus.

BV/TV	Coefficient (95%CI)	p value	Controlling for (confounding variables):
Imin/Imax	-0.016 (-0.034 to -0.001)	0.058	TbTh, TbSp, ConnD
TbTh	Coefficient (95%CI)	p value	Controlling for (confounding variables):
Imin/Imax	0.011 (0.021 to 0.019)	0.015	BV/TV, TbSp, TbN, ConnD
TbSp	Coefficient (95%CI)	p value	Controlling for (confounding variables):
Imin/Imax	0.007 (-0.026 to 0.040)	0.694	BV/TV, TbTh, TbN, ConnD, DA
TbN	Coefficient (95%CI)	p value	Controlling for (confounding variables):
Imin/Imax	-0.040 (-0.094 to -0.015)	0.153	BV/TV, TbTh, TbSp
ConnD	Coefficient (95%CI)	p value	Controlling for (confounding variables):
Imin/Imax	-0.705 (-1.138 to -0.272)	0.001	BV/TV, TbTh, TbSp, TbN, DA
DA	Coefficient (95%CI)	p value	Controlling for (confounding variables):
Imin/Imax	0.246 (0.062 to 0.430)	0.009	BV/TV, TbTh, TbSp

increased with increasing Imax/Imin while ConnD decreased.

Deer Calcaneus

The mean and standard deviation of each trabecular architectural measure by region and diaphysis location are presented in Table 24. The statistical analyses of the deer data mirrored those of the sheep, but provided some interestingly different results.

Question 1: Architectural Variation over Diaphyseal Length

Correlation analyses for within-subjects variation with repeated measures show that all the trabecular architecture measures are moderately to strongly and statistically significantly correlated with the percent diaphysis location in both the dorsal and plantar regions (Table 25).

To assess if the trabecular architecture measures differ over the length of the deer calcaneus diaphysis, multiple regression analyses for repeated measures were again employed. First the analyses examined all the deer data together using diaphysis location and region as predictor variables. The results examining the effect of percent diaphysis location (as the predictor variable) on each measure when controlling for region and confounding variables are presented in Table 26. Five of the six measures were shown to significantly change with diaphysis location. Bone volume fraction (BV/TV) and ConnD were shown to significantly decrease with increasing percent diaphysis location, while TbTh, TbSp, and DA significantly increased with percent diaphysis location. Trabecular number (TbN) was the only measure that did not significantly change with percent diaphysis location.

The deer calcaneus data from the dorsal and plantar regions and each percent

Table 24. Summary statistics, mean (SD), for each trabecular architectural parameter from the deer calcaneus.

		20%	30%	40%	50%
Dorsal	BV/TV	0.550 (0.035)	0.486 (0.045)	0.416 (0.049)	0.279 (0.080)
	TbTh	0.170 (0.017)	0.166 (0.012)	0.195 (0.033)	0.193 (0.027)
	TbSp	0.203 (0.037)	0.271 (0.055)	0.396 (0.089)	0.743 (0.381)
	TbN	2.511 (0.192)	2.317 (0.175)	1.931 (0.205)	1.477 (0.429)
	ConnD	6.485 (2.450)	5.719 (1.952)	4.097 (1.927)	3.192 (1.869)
	DA	2.595 (0.213)	2.555 (0.159)	2.326 (0.262)	2.206 (0.175)
Plantar	BV/TV	0.517 (0.047)	0.497 (0.026)	0.477 (0.038)	0.451 (0.057)
	TbTh	0.148 (0.025)	0.177 (0.026)	0.234 (0.032)	0.253 (0.033)
	TbSp	0.201 (0.044)	0.254 (0.028)	0.373 (0.057)	0.485 (0.077)
	TbN	2.706 (0.270)	2.305 (0.170)	1.893 (0.159)	1.677 (0.130)
	ConnD	11.061 (3.488)	6.206 (2.465)	3.585 (1.633)	2.350 (0.949)
	DA	2.04 (0.292)	2.216 (0.293)	2.313 (0.161)	2.389 (0.114)

BV/TV: bone volume fraction; TbTh: trabecular thickness (mm); TbSp: trabecular separation (mm); TbN: trabecular number (mm^{-1}); ConnD: connectivity density (number per mm^3); DA: degree of anisotropy.

Table 25. Correlation coefficients (R) of trabecular architectural measures with percent diaphysis location by region for the deer calcaneus.

	Dorsal		Plantar	
	R	p value	R	p value
BV/TV	-0.94	<0.001	-0.66	<0.001
TbTh	0.49	0.007	0.90	<0.001
TbSp	0.77	<0.001	0.94	<0.001
TbN	-0.92	<0.001	-0.96	<0.001
ConnD	-0.81	<0.001	-0.86	<0.001
DA	-0.70	<0.001	0.70	<0.001

Table 26. Effect of location on each architectural parameter controlling for region and confounding variables for the deer calcaneus.

BV/TV	Coefficient (95%CI)	p value	Controlling for (confounding variables):
Location	-0.016 (-0.03 to -0.01)	<0.001	Region, TbTh, TbSp, TbN, ConnD
TbTh	Coefficient (95%CI)	p value	Controlling for (confounding variables):
Location	0.007 (0.001 to 0.012)	0.015	Region, TbSp, BV/TV, TbN, ConnD
TbSp	Coefficient (95%CI)	p value	Controlling for (confounding variables):
Location	0.120 (0.078 to 0.163)	<0.001	Region, TbTh, ConnD, DA
TbN	Coefficient (95%CI)	p value	Controlling for (confounding variables):
Location	-0.017 (-0.043 to 0.01)	0.189	Region, TbTh, TbSp, BV/TV, ConnD, DA
ConnD	Coefficient (95%CI)	p value	Controlling for (confounding variables):
Location	-1.753 (-2.74 to -0.77)	<0.001	Region, TbTh, TbSp, BV/TV
DA	Coefficient (95%CI)	p value	Controlling for (confounding variables):
Location	0.266 (0.151 to 0.380)	<0.001	Region, TbTh, TbSp, BV/TV, TbN, ConnD

location were next examined separately. The results of the analyses for dorsal and plantar data individually and examining the effect of location (as predictor variable) while controlling for confounding variables are presented in Tables 27 and 28. In the dorsal region BV/TV and ConnD were shown to significantly decrease and TbSp to significantly increase with percent diaphysis location. In the plantar region ConnD significantly decreased while TbTh, TbSp, and DA significantly increased with present diaphysis location.

Question 2: Architectural Variation by Region

Correlation analyses show that there are only weak correlations between the measures and region, with BV/TV, TbTh, and DA having significant weak correlations with region (Table 29).

The results of the analyses conducted with region as the predictor variable and controlling for location and confounding variables are presented in Table 30. Only DA was found to significantly differ between regions, decreasing between the dorsal and plantar region. Trabecular separation (TbSp) can be considered trending toward significantly differing between dorsal and plantar regions, with a $p=0.055$.

The deer data were next examined by each percent location (20%, 30%, 40%, 50%) with region (dorsal/plantar) as the predictor variable. In the 20% location, ConnD was significantly lower and DA was shown to be significantly higher in the dorsal region compared to the plantar region (Table 31). Trabecular separation (TbSp) and DA were shown to significantly higher in the dorsal region at the 30% diaphysis length location (Table 32). None of the architectural measures were significantly different between regions at the 40% diaphysis location (Table 33). In the 50% location all the trabecular

Table 27. Effect of location on each architectural measure in the dorsal region for the deer calcaneus.

BV/TV	Coefficient (95%CI)	p value	Controlling for (confounding variables):
Location	-0.018 (-0.033 to -0.004)	0.014	TbTh, TbSp, TbN, ConnD
TbTh	Coefficient (95%CI)	p value	Controlling for (confounding variables):
Location	0.010 (-0.004 to 0.024)	0.151	BV/TV, TbSp, TbN, ConnD
TbSp	Coefficient (95%CI)	p value	Controlling for (confounding variables):
Location	0.089 (0.008 to 0.169)	0.030	TbTh, ConnD, DA
TbN	Coefficient (95%CI)	p value	Controlling for (confounding variables):
Location	-0.028 (-0.681 to 0.013)	0.178	BV/TV, TbTh, TbSp, ConnD, DA
ConnD	Coefficient (95%CI)	p value	Controlling for (confounding variables):
Location	-1.549 (-2.89 to -0.211)	0.023	BV/TV, TbTh, TbSp
DA	Coefficient (95%CI)	p value	Controlling for (confounding variables):
Location	-0.002 (-0.160 to 0.157)	0.984	BV/TV, TbTh, TbSp, TbN, ConnD

Table 28. Effect of location on each architectural measure in the plantar region for the deer calcaneus.

BV/TV	Coefficient (95%CI)	p value	Controlling for (confounding variables):
Location	-0.006 (-0.022 to 0.009)	0.419	TbTh, TbSp, TbN, ConnD
TbTh	Coefficient (95%CI)	p value	Controlling for (confounding variables):
Location	0.021 (0.006 to 0.036)	0.006	BV/TV, TbSp, ConnD
TbSp	Coefficient (95%CI)	p value	Controlling for (confounding variables):
Location	0.114 (0.080 to 0.148)	<0.001	TbTh, ConnD, DA
TbN	Coefficient (95%CI)	p value	Controlling for (confounding variables):
Location	-0.024 (-0.069 to 0.021)	0.294	BV/TV, TbTh, TbSp, ConnD, DA
ConnD	Coefficient (95%CI)	p value	Controlling for (confounding variables):
Location	-1.656 (-3.148 to -0.163)	0.030	BV/TV, TbTh
DA	Coefficient (95%CI)	p value	Controlling for (confounding variables):
Location	0.356 (0.220 to 0.491)	<0.001	BV/TV, TbTh, TbSp, TbN, ConnD

Table 29. Correlation Coefficients (R) of trabecular architectural measures with region for the deer calcaneus.

	R	p value
BV/TV	0.31	0.012
TbTh	0.28	0.025
TbSp	-0.18	0.149
TbN	0.11	0.369
ConnD	0.16	0.220
DA	-0.39	0.002

Table 30. Effect of region on each architectural parameter controlling for location and confounding variables for the deer calcaneus.

BV/TV	Coefficient (95%CI)	p value	Controlling for (confounding variables):
Region	0.006 (-0.005 to 0.016)	0.274	Location, TbTh, TbSp, TbN, ConnD
TbTh	Coefficient (95%CI)	p value	Controlling for (confounding variables):
Region	0.002 (-0.005 to 0.009)	0.566	Location, BV/TV, TbN, ConnD, DA
TbSp	Coefficient (95%CI)	p value	Controlling for (confounding variables):
Region	0.036 (-0.001 to 0.073)	0.055	Location, TbTh, BV/TV, TbN, ConnD, DA
TbN	Coefficient (95%CI)	p value	Controlling for (confounding variables):
Region	0.014 (-0.014 to 0.043)	0.328	Location, TbTh, TbSp, BV/TV, ConnD, DA
ConnD	Coefficient (95%CI)	p value	Controlling for (confounding variables):
Region	0.090 (-0.792 to 0.972)	0.841	Location, TbTh, TbN, DA
DA	Coefficient (95%CI)	p value	Controlling for (confounding variables):
Region	-0.241 (-0.34 to -0.14)	<0.001	Location, TbTh, TbSp, BV/TV, TbN, ConnD

Table 31. Effect of region on each architectural measure in the 20% diaphysis location for the deer calcaneus.

BV/TV	Coefficient (95%CI)	p value	Controlling for (confounding variables):
Region	-0.007 (-0.029 to 0.014)	0.502	TbTh, TbSp, TbN, ConnD, DA
TbTh	Coefficient (95%CI)	p value	Controlling for (confounding variables):
Region	< -0.001 (-0.013 to 0.013)	0.982	TbSp, BV/TV, TbN, ConnD, DA
TbSp	Coefficient (95%CI)	p value	Controlling for (confounding variables):
Region	-0.007 (-0.022 to 0.007)	0.308	BV/TV, TbTh, TbN, ConnD, DA
TbN	Coefficient (95%CI)	p value	Controlling for (confounding variables):
Region	0.056 (-0.027 to 0.139)	0.184	TbTh, TbSp, ConnD, DA
ConnD	Coefficient (95%CI)	p value	Controlling for (confounding variables):
Region	2.770 (0.509 to 5.033)	0.016	TbTh, TbN
DA	Coefficient (95%CI)	p value	Controlling for (confounding variables):
Region	-0.440 (-0.603 to -0.280)	< 0.001	BV/TV, TbTh, TbN, ConnD

Table 32. Effect of region on each architectural measure in the 30% diaphysis location for the deer calcaneus.

BV/TV	Coefficient (95%CI)	p value	Controlling for (confounding variables):
Region	0.002 (-0.017 to 0.021)	0.853	TbSp, ConnD
TbTh	Coefficient (95%CI)	p value	Controlling for (confounding variables):
Region	0.001 (-0.005 to 0.006)	0.730	TbSp, BV/TV, TbN, ConnD, DA
TbSp	Coefficient (95%CI)	p value	Controlling for (confounding variables):
Region	-0.016 (-0.029 to -0.003)	0.017	BV/TV, TbTh, TbN, ConnD, DA
TbN	Coefficient (95%CI)	p value	Controlling for (confounding variables):
Region	-0.015 (-0.049 to 0.017)	0.360	BV/TV, TbTh, TbSp, ConnD, DA
ConnD	Coefficient (95%CI)	p value	Controlling for (confounding variables):
Region	1.680 (-0.166 to 3.53)	0.074	TbTh, TbSp, TbN, DA
DA	Coefficient (95%CI)	p value	Controlling for (confounding variables):
Region	-0.366 (-0.628 to -0.105)	0.006	BV/TV, TbTh, TbSp, TbN

Table 33. Effect of region on each architectural measure in the 40% diaphysis location for the deer calcaneus.

BV/TV	Coefficient (95%CI)	p value	Controlling for (confounding variables):
Region	0.016 (-0.004 to 0.035)	0.119	TbTh, TbSp, TbN, ConnD
TbTh	Coefficient (95%CI)	p value	Controlling for (confounding variables):
Region	0.003 (-0.010 to 0.016)	0.619	TbSp, BV/TV, TbN, ConnD, DA
TbSp	Coefficient (95%CI)	p value	Controlling for (confounding variables):
Region	< -0.001 (-0.018 to 0.017)	0.983	TbTh, TbN, ConnD
TbN	Coefficient (95%CI)	p value	Controlling for (confounding variables):
Region	-0.010 (-0.072 to 0.053)	0.766	BV/TV, TbSp, ConnD
ConnD	Coefficient (95%CI)	p value	Controlling for (confounding variables):
Region	-0.249 (-1.46 to 0.96)	0.685	TbTh, TbSp, TbN, DA
DA	Coefficient (95%CI)	p value	Controlling for (confounding variables):
Region	-0.009 (-0.167 to 0.148)	0.910	TbTh, ConnD

architecture measures except for ConnD were significantly different between the dorsal and plantar regions (Table 34). Bone volume fraction (BV/TV), TbTh, TbN and DA were all significantly lower while TbSp was significantly higher in the dorsal region compared to the plantar region.

The results of the primary analysis of the deer data indicate that, similar to the sheep, the most significant changes in trabecular architectural measures were found across the length of the diaphysis and not between the dorsal and plantar regions. However, unlike in the sheep, the deer did have a significant difference in DA and a trend toward significant difference in TbSp between dorsal and plantar regions and several more significant differences between dorsal and plantar regions in the individual percent locations.

Question 3: Architectural Variation with Cortical Thickness Ratio

The CTR mean and standard deviation for each percent diaphysis location is presented in Table 35. Cortical thickness ratio (CTR) increases greatly with percent diaphysis location in the deer calcaneus (also see Figure 9). A within-subjects variation correlation analysis for repeated measures indicates that CTR is significantly and strongly correlated with percent diaphysis location ($R = 0.90$, $p = < 0.001$). Correlation analyses for within-subjects variation with repeated measures show that all the trabecular architecture measures are moderately to strongly and statistically significantly correlated with CTR, except for TbTh in the dorsal region (Table 36).

Each trabecular architectural measure was examined with CTR as the predictor variable and controlling for region and confounding variables (Table 37). Four (TbSp, TbN, ConnD, and DA) of the six measures were found to significantly differ with CTR.

Table 34. Effect of region on each architectural measure in the 50% diaphysis location for the deer calcaneus.

BV/TV	Coefficient (95%CI)	p value	Controlling for (confounding variables):
Region	0.057 (0.018 to 0.095)	0.004	TbTh, TbSp, TbN
TbTh	Coefficient (95%CI)	p value	Controlling for (confounding variables):
Region	0.028 (0.009 to 0.047)	0.003	TbSp, BV/TV, TbN, ConnD, DA
TbSp	Coefficient (95%CI)	p value	Controlling for (confounding variables):
Region	-0.288 (-0.494 to -0.082)	0.006	TbTh, ConnD
TbN	Coefficient (95%CI)	p value	Controlling for (confounding variables):
Region	0.183 (0.094 to 0.271)	<0.001	TbTh, TbSp, ConnD, DA
ConnD	Coefficient (95%CI)	p value	Controlling for (confounding variables):
Region	-1.184 (-2.88 to 0.514)	0.172	TbTh, TbSp, TbN, DA
DA	Coefficient (95%CI)	p value	Controlling for (confounding variables):
Region	0.307 (0.093 to 0.520)	0.005	BV/TV, TbTh, TbSp, TbN, ConnD

Table 35. Mean and standard deviation (SD) of the cortical thickness ratio (CTR) at each percent diaphysis location for the deer calcaneus.

Location	Mean	SD
20%	0.76	0.08
30%	2.45	0.23
40%	2.79	0.46
50%	3.11	0.44

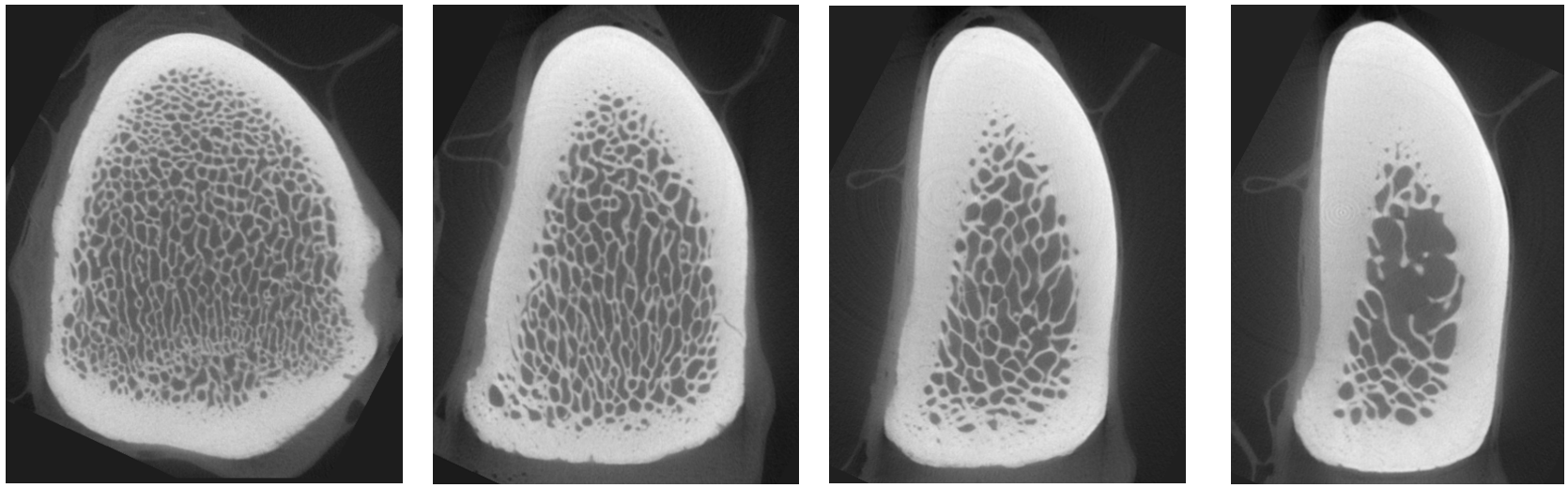

A **B** **C** **D**

Figure 9. Micro-CT images of cross sections of a deer calcaneus for each of the percent diaphyseal length location. A) The 20% diaphyseal length location; B) 30% diaphyseal length location; C) 40% diaphyseal length location; D) 50% diaphyseal length location. Images not to scale. Top=dorsal, bottom=plantar.

Table 36. Correlation coefficients (R) of trabecular architectural measures with CTR by region for the deer calcaneus.

	Dorsal		Plantar	
	R	p value	R	p value
BV/TV	-0.79	<0.001	-0.48	0.009
TbTh	0.31	0.106	0.88	<0.001
TbSp	0.60	<0.001	0.80	<0.001
TbN	-0.76	<0.001	-0.92	<0.001
ConnD	-0.73	<0.001	-0.89	<0.001
DA	-0.54	0.003	0.64	<0.001

Table 37. Effect of CTR on each architectural parameter controlling for region and confounding variables for the deer calcaneus.

BV/TV	Coefficient (95%CI)	p value	Controlling for (confounding variables):
CTR	-0.005 (-0.014 to 0.003)	0.243	Region, TbTh, TbSp, TbN, ConnD, DA
TbTh	Coefficient (95%CI)	p value	Controlling for (confounding variables):
CTR	<0.001 (-0.005 to 0.005)	0.964	Region, BV/TV, TbSp, TbN, ConnD, DA
TbSp	Coefficient (95%CI)	p value	Controlling for (confounding variables):
CTR	0.068(0.013to 0.124)	0.015	Region, BV/TV, TbTh, TbN, ConnD, DA
TbN	Coefficient (95%CI)	p value	Controlling for (confounding variables):
CTR	-0.023 (-0.044 to -0.003)	0.026	Region, BV/TV, TbTh, TbSp, ConnD, DA
ConnD	Coefficient (95%CI)	p value	Controlling for (confounding variables):
CTR	-1.557 (-2.256 to -0.858)	0.001	Region, Bv/TV, TbTh, TbSp, TbN, DA
DA	Coefficient (95%CI)	p value	Controlling for (confounding variables):
CTR	0.113 (0.016 to 0.210)	0.022	Region, BV/TV, TbTh, TbN ConnD

Trabecular number (TbN) and ConnD were shown to decrease with increasing CTR, while TbSp and DA increase with CTR. When the analyses were executed with region as the predictor variable and CTR was controlled for along with confounding variables, DA was the only measure found to significantly differ between regions (Table 38). The dorsal and plantar data were also examined separately with CTR as the predictor variable. In the dorsal region, BV/TV, TbN, and ConnD were shown to significantly decrease and TbSp to increase with increasing CTR (Table 39). In the plantar region, TbN and ConnD significantly decrease while TbTh, TbSp, and DA significantly increase with increasing CTR (Table 40).

Question 4: Architectural Variation with Imax/Imin

The mean values for Imax/Imin by percent location for the deer calcaneus are presented in Table 41. The deer Imax/Imin values are much greater than 1 for all diaphyseal locations and greatly increase between the 20% and 50% diaphysis locations from a mean of 2.38 at 20% to 5.44 at 50%. Thus the deer calcaneus has a much more strongly defined direction of greatest bending rigidity compared to the sheep calcaneus. The correlation analysis with Imax/Imin and percent diaphysis location indicates a very strong and statistically significant correlation between the two ($R = 0.97$, $p = <0.001$). Correlation analyses between each architectural measure and Imax/Imin by region indicate significant moderate to high correlations between all measures and Imax/Imin (Table 42).

The analyses of each architectural measure with Imax/Imin as the predictor variable while controlling for region and other confounders showed only two of the six measures varying significantly with Imax/Imin: TbSp significantly increases and DA

Table 38. Effect of region on each architectural parameter controlling for CTR and confounding variables for the deer calcaneus.

BV/TV	Coefficient (95%CI)	p value	Controlling for (confounding variables):
Region	0.004 (-0.007 to 0.015)	0.463	CTR, TbTh, TbSp, TbN, ConnD
TbTh	Coefficient (95%CI)	p value	Controlling for (confounding variables):
Region	0.005 (-0.001 to 0.013)	0.090	CTR, BV/TV, TbSp, TbN, ConnD, DA
TbSp	Coefficient (95%CI)	p value	Controlling for (confounding variables):
Region	0.028 (-0.008 to 0.063)	0.125	CTR, BV/TV, TbTh, TbN, ConnD, DA
TbN	Coefficient (95%CI)	p value	Controlling for (confounding variables):
Region	0.015(-0.012 to 0.043)	0.275	CTR, BV/TV, TbTh, TbSp, ConnD, DA
ConnD	Coefficient (95%CI)	p value	Controlling for (confounding variables):
Region	0.036 (-0.53 to 0.604)	0.901	CTR, BV/TV, TbTh, TbSp, TbN, DA
DA	Coefficient (95%CI)	p value	Controlling for (confounding variables):
Region	-0.200 (-0.310 to 0.090)	<0.001	CTR, BV/TV, TbTh, TbSp, TbN, ConnD

Table 39. Effect of CTR on each architectural measure in the dorsal region for the deer calcaneus.

BV/TV	Coefficient (95%CI)	p value	Controlling for (confounding variables):
CTR	-0.042 (-0.057 to -0.026)	<0.001	TbTh, TbSp, TbN
TbTh	Coefficient (95%CI)	p value	Controlling for (confounding variables):
CTR	0.005 (-0.008 to 0.018)	0.456	BV/TV, TbSp, TbN, ConnD
TbSp	Coefficient (95%CI)	p value	Controlling for (confounding variables):
CTR	0.133 (0.055 to 0.217)	0.001	BV/TV, TbTh, TbN, ConnD, DA
TbN	Coefficient (95%CI)	p value	Controlling for (confounding variables):
CTR	-0.059 (-0.010 to -0.018)	0.005	BV/TV, TbTh, TbSp, ConnD
ConnD	Coefficient (95%CI)	p value	Controlling for (confounding variables):
CTR	-0.752 (-1.431 to -0.074)	0.030	BV/TV, TbTh, TbSp
DA	Coefficient (95%CI)	p value	Controlling for (confounding variables):
CTR	-0.015 (-0.103 to 0.073)	0.732	BV/TV, TbTh, TbSp, TbN, ConnD

Table 40. Effect of CTR on each architectural measure in the plantar region for the deer calcaneus.

BV/TV	Coefficient (95%CI)	p value	Controlling for (confounding variables):
CTR	-0.006 (-0.020 to 0.007)	0.366	TbTh, TbSp, TbN, ConnD
TbTh	Coefficient (95%CI)	p value	Controlling for (confounding variables):
CTR	0.020 (0.008 to 0.033)	0.002	BV/TV, TbSp, TbN, ConnD
TbSp	Coefficient (95%CI)	p value	Controlling for (confounding variables):
CTR	0.045 (0.002 to 0.089)	0.042	BV/TV, TbTh, TbN, ConnD, DA
TbN	Coefficient (95%CI)	p value	Controlling for (confounding variables):
CTR	-0.072 (-0.130 to -0.013)	0.017	BV/TV, TbTh, TbSp
ConnD	Coefficient (95%CI)	p value	Controlling for (confounding variables):
CTR	-1.893 (-3.285 to -0.502)	0.008	BV/TV, TbTh, TbSp
DA	Coefficient (95%CI)	p value	Controlling for (confounding variables):
CTR	0.195 (0.052 to 0.338)	0.008	BV/TV, TbTh, TbSp, TbN, ConnD

Table 41. Mean and standard deviation (SD) of Imax/Imin at each percent diaphysis location for the deer calcaneus.

Location	Mean	SD
20%	2.38	0.42
30%	3.09	0.68
40%	4.39	0.81
50%	5.44	0.73

Table 42. Correlation coefficient (R) of trabecular architectural measures with Imax/Imin by region for the deer calcaneus.

	Dorsal		Plantar	
	R	p value	R	p value
BV/TV	-0.94	<0.001	-0.64	<0.001
TbTh	0.47	0.011	0.88	<0.001
TbSp	0.78	<0.001	0.93	<0.001
TbN	-0.91	<0.001	-0.92	<0.001
ConnD	-0.79	<0.001	-0.79	<0.001
DA	-0.67	<0.001	0.64	<0.001

increases with increasing Imax/Imin (Table 43). When region was used as the predictor variable while controlling for Imax/Imin and confounders only DA was found to significantly change with Imax/Imin (Table 44). Dorsal and plantar sections were assessed separately with Imax/Imin as the predictor variable (Tables 45 and 46). BV/TV, TbTh, and TbSp were found to significantly vary with Imax/Imin in the dorsal region. In the plantar region, only TbSp was shown to significantly vary with Imax/Imin.

The deer data, similar to the sheep data, indicate that trabecular architecture differs more significantly across the length of the diaphysis and with increasing Imax/Imin than between the dorsal and plantar regions within the bone.

Both Species

Question 5: Trabecular Architecture by Species

Analyses with species as the predictor variable while controlling for percent diaphysis location and confounding variables indicated that TbSp and DA were the only measures to significantly differ by species (Table 47). TbSp was shown to be higher in the sheep and DA higher in the deer. Similarly, when species is used as predictor variable while controlling for region and cofounding variables, only TbSp and DA were found to significantly differ between the sheep and deer; again with TbSp found to be higher in the sheep than in the deer and DA to be higher in the deer than in the sheep (Table 48).

The dorsal and plantar data were also examined separately with species as the predictor variable. In the dorsal region TbSp, TbN, and DA were all shown to be significantly higher in the deer than in the sheep (Table 49). In the plantar region BV/TV and DA were shown to be significantly higher in the deer and TbSp significantly lower in

Table 43. Effect of Imax/Imin on each architectural parameter controlling for region and confounding variables for the deer calcaneus.

BV/TV	Coefficient (95%CI)	p value	Controlling for (confounding variables):
Imin/Imax	-0.003 (-0.008 to 0.003)	0.416	Region, TbTh, TbSp, TbN, ConnD, DA
TbTh	Coefficient (95%CI)	p value	Controlling for (confounding variables):
Imin/Imax	<0.001 (-0.003 to 0.004)	0.653	Region, BV/TV, TbSp, TbN, ConnD, DA
TbSp	Coefficient (95%CI)	p value	Controlling for (confounding variables):
Imin/Imax	0.030 (-0.052to -0.008)	0.008	Region, BV/TV, TbTh, TbN, ConnD, DA
TbN	Coefficient (95%CI)	p value	Controlling for (confounding variables):
Imin/Imax	-0.012 (-0.026 to 0.002)	0.100	Region, BV/TV, TbTh, TbSp, ConnD, DA
ConnD	Coefficient (95%CI)	p value	Controlling for (confounding variables):
Imin/Imax	-0.307 (-0.951 to 0.337)	0.350	Region, Bv/TV, TbTh, TbSp, DA
DA	Coefficient (95%CI)	p value	Controlling for (confounding variables):
Imin/Imax	0.122 (0.038 to 0.205)	0.004	Region, BV/TV, TbTh, TbSp, TbN ConnD

Table 44. Effect of region on each architectural parameter controlling for Imax/Imin and confounding variables for the deer calcaneus.

BV/TV	Coefficient (95%CI)	p value	Controlling for (confounding variables):
Region	0.003 (-0.008 to 0.015)	0.562	Imin/Imax, TbTh, TbSp, TbN, ConnD
TbTh	Coefficient (95%CI)	p value	Controlling for (confounding variables):
Region	0.006 (-0.001 to 0.012)	0.092	Imin/Imax, BV/TV, TbSp, TbN, ConnD, DA
TbSp	Coefficient (95%CI)	p value	Controlling for (confounding variables):
Region	0.016 (-0.022 to 0.054)	0.414	Imin/Imax, BV/TV, TbTh, TbN, ConnD, DA
TbN	Coefficient (95%CI)	p value	Controlling for (confounding variables):
Region	0.011(-0.017 to 0.038)	0.446	Imin/Imax, BV/TV, TbTh, TbSp, ConnD, DA
ConnD	Coefficient (95%CI)	p value	Controlling for (confounding variables):
Region	0.060 (-0.494 to 0.614)	0.831	Imin/Imax, BV/TV, TbTh, TbSp, TbN, DA
DA	Coefficient (95%CI)	p value	Controlling for (confounding variables):
Region	-0.199 (-0.304 to -0.094)	<0.001	Imin/Imax, BV/TV, TbTh, TbSp, TbN, ConnD

Table 45. Effect of Imax/Imin on each architectural measure in the dorsal region for the deer calcaneus.

BV/TV	Coefficient (95%CI)	p value	Controlling for (confounding variables):
Imin/Imax	-0.037 (-0.048 to -0.026)	<0.001	TbTh, TbSp, TbN, ConnD
TbTh	Coefficient (95%CI)	p value	Controlling for (confounding variables):
Imin/Imax	0.0123 (0.037 to 0.0210)	0.005	BV/TV, TbSp, TbN, ConnD
TbSp	Coefficient (95%CI)	p value	Controlling for (confounding variables):
Imin/Imax	0.059 (-0.086 to- 0.032)	<0.001	BV/TV, TbTh, TbN, ConnD
TbN	Coefficient (95%CI)	p value	Controlling for (confounding variables):
Imin/Imax	-0.044 (-0.096 to -0.008)	0.095	BV/TV, TbTh, TbSp
ConnD	Coefficient (95%CI)	p value	Controlling for (confounding variables):
Imin/Imax	-0.334 (-1.212 to 0.543)	0.455	BV/TV, TbTh, TbSp
DA	Coefficient (95%CI)	p value	Controlling for (confounding variables):
Imin/Imax	-0.016 (-0.114 to 0.082)	0.745	BV/TV, TbTh, TbSp, TbN, ConnD

Table 46. Effect of Imax/Imin on each architectural measure in the plantar region for the deer calcaneus.

BV/TV	Coefficient (95%CI)	p value	Controlling for (confounding variables):
Imin/Imax	0.002 (-0.007 to 0.011)	0.667	TbTh, TbSp, TbN, ConnD
TbTh	Coefficient (95%CI)	p value	Controlling for (confounding variables):
Imin/Imax	0.010 (-0.006 to 0.021)	0.065	BV/TV, TbSp, TbN, ConnD
TbSp	Coefficient (95%CI)	p value	Controlling for (confounding variables):
Imin/Imax	0.014 (<0.000 to 0.028)	0.050	BV/TV, TbTh, TbN, ConnD
TbN	Coefficient (95%CI)	p value	Controlling for (confounding variables):
Imin/Imax	-0.010 (-0.053 to 0.032)	0.632	BV/TV, TbTh, TbSp
ConnD	Coefficient (95%CI)	p value	Controlling for (confounding variables):
Imin/Imax	-0.181 (-0.705 to 0.343)	0.499	BV/TV, TbTh, TbSp, TbN
DA	Coefficient (95%CI)	p value	Controlling for (confounding variables):
Imin/Imax	0.109 (-0.004 to 0.223)	0.058	BV/TV, TbTh, TbSp, TbN, ConnD

Table 47. Effect of species on each architectural parameter controlling for location and confounding variables. The coefficient represents the amount of change (difference) in the outcome variable (architectural parameter) for a unit increase in the predictor variable (species, were sheep=0 and deer=1).

BV/TV	Coefficient (95%CI)	p value	Controlling for (confounding variables):
Species	0.005 (-0.002 to 0.014)	0.170	Location, TbTh, TbSp, TbN, ConnD
TbTh	Coefficient (95%CI)	p value	Controlling for (confounding variables):
Species	-0.001 (-0.007 to 0.006)	0.877	Location, TbSp, BV/TV, TbN, ConnD, DA
TbSp	Coefficient (95%CI)	p value	Controlling for (confounding variables):
Species	-0.048 (-0.091 to -0.006)	0.025	Location, TbTh, BV/TV, TbN, ConnD
TbN	Coefficient (95%CI)	p value	Controlling for (confounding variables):
Species	0.005 (-0.020 to 0.030)	0.681	Location, BV/TV, TbTh, TbSp, ConnD, DA
ConnD	Coefficient (95%CI)	p value	Controlling for (confounding variables):
Species	0.364 (-0.060 to 0.788)	0.092	Location, BV/TV, TbTh, TbSp, TbN, DA
DA	Coefficient (95%CI)	p value	Controlling for (confounding variables):
Species	0.490 (0.369 to 0.611)	<0.001	Location, BV/TV, ConnD

Table 48. Effect of species on each architectural parameter controlling for region and confounding variables.

BV/TV	Coefficient (95%CI)	p value	Controlling for (confounding variables):
Species	<0.001 (-0.008 to 0.008)	0.994	Region, TbTh, TbSp, TbN, ConnD
TbTh	Coefficient (95%CI)	p value	Controlling for (confounding variables):
Species	0.001 (-0.005 to 0.008)	0.687	Region, TbSp, BV/TV, TbN, ConnD, DA
TbSp	Coefficient (95%CI)	p value	Controlling for (confounding variables):
Species	-0.044 (-0.087 to -0.001)	0.043	Region, TbTh, BV/TV, ConnD
TbN	Coefficient (95%CI)	p value	Controlling for (confounding variables):
Species	0.011(-0.014 to 0.035)	0.387	Region, BV/TV, TbTh, TbSp, ConnD, DA
ConnD	Coefficient (95%CI)	p value	Controlling for (confounding variables):
Species	0.200 (-0.221 to 0.622)	0.351	Region, BV/TV, TbTh, TbSp, TbN, DA
DA	Coefficient (95%CI)	p value	Controlling for (confounding variables):
Species	0.448 (0.550 to 0.345)	<0.001	Region, BV/TV, TbTh, ConnD

Table 49. Effect of species on each architectural measure in the dorsal region.

BV/TV	Coefficient (95%CI)	p value	Controlling for (confounding variables):
Species	0.012 (-0.002 to 0.0267)	0.097	Location, TbTh, TbSp, TbN
TbTh	Coefficient (95%CI)	p value	Controlling for (confounding variables):
Species	-0.003 (-0.012 to 0.001)	0.441	Location, BV/TV, TbSp, TbN
TbSp	Coefficient (95%CI)	p value	Controlling for (confounding variables):
Species	0.060 (0.026 to 0.094)	<0.001	Location, BV/TV, TbTh, ConnD
TbN	Coefficient (95%CI)	p value	Controlling for (confounding variables):
Species	0.029 (0.003 to 0.055)	0.030	Location, BV/TV, TbTh, TbSp, ConnD
ConnD	Coefficient (95%CI)	p value	Controlling for (confounding variables):
Species	-0.090 (-0.830 to 0.650)	0.812	Location, BV/TV, TbSp, TbN, DA
DA	Coefficient (95%CI)	p value	Controlling for (confounding variables):
Species	0.558 (0.406 to 0.710)	<0.001	Location, BV/TV, ConnD

the deer compared to the sheep (Table 50).

Each measure was also examined at each percent location (20%, 30%, 40%, 50%) with species as the predictor variable and controlling for region and confounding variables. In the 20% location, statistically significant differences were found between the species in TbTh, TbSp, and DA, with TbTh and TbSp being significantly higher in the sheep and DA significantly higher in the deer (Table 51). In the 30% location, TbN and DA were both found to be significantly higher in the deer (Table 52). At the 40% and 50% locations, only DA was shown to be significantly different, with it being higher in the deer at both locations (Tables 53 and 54).

The effect of species was also examined using CTR. As Tables 12 and 35 indicate, the CTR of the sheep and deer follow a similar trend of increasing CTR with percent shaft location, but the deer have a much greater increase in CTR, representing a much greater increase in dorsal cortical thickness. When the effect of species (as predictor variable) is examined while controlling for CTR and confounding variables, significant differences were found in BV/TV, TbSp, and DA (Table 55). Bone volume fraction (BV/TV) and DA were shown to be higher in the deer while TbSp were shown to be higher in the sheep. When the effect of species (predictor variable) was examined while controlling for CTR and region, BV/TV, ConnD, and DA were found to be significantly higher in the deer and TbSp was significantly higher in the sheep (Table 56). The dorsal and plantar region data were also examined separately with species as predictor variable and controlling for CTR and confounding variables. In the dorsal region, BV/TV, TbSp, TbN, and DA were significantly higher in the deer (Table 57). In the plantar region, BV/TV and DA were significantly higher in the deer and TbSp was significantly higher in the sheep (Table 58).

Table 50. Effect of species on each architectural measure in the plantar region.

BV/TV	Coefficient (95%CI)	p value	Controlling for (confounding variables):
Species	0.012 (0.001 to 0.023)	0.036	Location, TbTh, TbSp, TbN, ConnD
TbTh	Coefficient (95%CI)	p value	Controlling for (confounding variables):
Species	-0.004 (-0.132 to 0.006)	0.460	Location, BV/TV, TbSp, TbN, ConnD, DA
TbSp	Coefficient (95%CI)	p value	Controlling for (confounding variables):
Species	-0.103 (-0.146 to- 0.060)	<0.001	Location, TbTh, ConnD
TbN	Coefficient (95%CI)	p value	Controlling for (confounding variables):
Species	0.015 (-0.021 to 0.052)	0.401	Location, BV/TV, TbTh, TbSp, ConnD
ConnD	Coefficient (95%CI)	p value	Controlling for (confounding variables):
Species	0.441 (0.232 to 1.113)	0.199	Location, BV/TV, TbTh, TbSp, TbN, DA
DA	Coefficient (95%CI)	p value	Controlling for (confounding variables):
Species	0.513 (0.310 to 0.720)	<0.001	Location, BV/TV, ConnD

Table 51. Effect of species on each architectural measure in the 20% diaphysis location controlling for region and confounders.

BV/TV	Coefficient (95%CI)	p value	Controlling for (confounding variables):
Species	0.011 (-0.014 to 0.036)	0.387	Region, TbTh, TbSp, TbN, ConnD
TbTh	Coefficient (95%CI)	p value	Controlling for (confounding variables):
Species	-0.012 (-0.025 to 0.010)	0.068	Region, BV/TV, TbN, ConnD
TbSp	Coefficient (95%CI)	p value	Controlling for (confounding variables):
Species	-0.026 (-0.052 to -0.001)	0.044	Region, BV/TV, TbN, ConnD
TbN	Coefficient (95%CI)	p value	Controlling for (confounding variables):
Species	0.047 (-0.035 to 0.147)	0.356	Region, BV/TV, TbSp, ConnD, DA
ConnD	Coefficient (95%CI)	p value	Controlling for (confounding variables):
Species	0.340 (-0.995 to 1.675)	0.618	Region, BV/TV, TbTh, TbN, DA
DA	Coefficient (95%CI)	p value	Controlling for (confounding variables):
Species	0.526 (0.276 to 0.775)	<0.001	Region, BV/TV, ConnD

Table 52. Effect of species on each architectural measure in the 30% diaphysis location controlling for region and confounders.

BV/TV	Coefficient (95%CI)	p value	Controlling for (confounding variables):
Species	0.008 (-0.005 to 0.021)	0.259	Region, TbTh, TbSp, TbN, ConnD
TbTh	Coefficient (95%CI)	p value	Controlling for (confounding variables):
Species	-0.005 (-0.012 to 0.003)	0.206	Region, BV/TV, TbSp, TbN, ConnD
TbSp	Coefficient (95%CI)	p value	Controlling for (confounding variables):
Species	-0.006 (-0.027 to 0.015)	0.586	Region, BV/TV, TbTh, TbN, ConnD
TbN	Coefficient (95%CI)	p value	Controlling for (confounding variables):
Species	0.072 (0.007 to 0.137)	0.030	Region, BV/TV, TbSp, ConnD, DA
ConnD	Coefficient (95%CI)	p value	Controlling for (confounding variables):
Species	-0.621 (-1.928 to 0.688)	0.353	Region, BV/TV, TbSp, DA
DA	Coefficient (95%CI)	p value	Controlling for (confounding variables):
Species	0.649 (0.445 to 0.852)	<0.001	Region, BV/TV, ConnD

Table 53. Effect of species on each architectural measure in the 40% diaphysis location controlling for region and confounders.

BV/TV	Coefficient (95%CI)	p value	Controlling for (confounding variables):
Species	0.003 (-0.130 to 0.194)	0.697	Region, TbTh, TbSp, TbN, ConnD
TbTh	Coefficient (95%CI)	p value	Controlling for (confounding variables):
Species	0.003 (-0.014 to 0.019)	0.744	Region, BV/TV, TbSp, ConnD
TbSp	Coefficient (95%CI)	p value	Controlling for (confounding variables):
Species	-0.148 (-0.32 to 0.003)	0.092	Region, BV/TV, TbTh, TbN, ConnD
TbN	Coefficient (95%CI)	p value	Controlling for (confounding variables):
Species	0.002 (-0.038 to 0.042)	0.924	Region, BV/TV, TbSp, ConnD, DA
ConnD	Coefficient (95%CI)	p value	Controlling for (confounding variables):
Species	-0.506 (-1.450 to 0.442)	0.295	Region, BV/TV, TbTh, TbSp, TbN, DA
DA	Coefficient (95%CI)	p value	Controlling for (confounding variables):
Species	0.523 (0.350 to 0.700)	<0.001	Region, BV/TV, ConnD

Table 54. Effect of species on each architectural measure in the 50% diaphysis location controlling for region and confounders.

BV/TV	Coefficient (95%CI)	p value	Controlling for (confounding variables):
Species	0.007 (-0.005 to 0.019)	0.249	Region, TbTh, TbSp, TbN, ConnD
TbTh	Coefficient (95%CI)	p value	Controlling for (confounding variables):
Species	0.002 (-0.020 to 0.024)	0.858	Region, BV/TV, TbSp, ConnD
TbSp	Coefficient (95%CI)	p value	Controlling for (confounding variables):
Species	0.043 (-0.023 to 0.109)	0.202	Region, BV/TV, TbTh, TbN, ConnD
TbN	Coefficient (95%CI)	p value	Controlling for (confounding variables):
Species	0.018 (-0.036 to 0.071)	0.520	Region, BV/TV, TbSp, ConnD, DA
ConnD	Coefficient (95%CI)	p value	Controlling for (confounding variables):
Species	0.476 (-0.096 to 1.047)	0.103	Region, BV/TV, TbTh, TbSp, TbN, DA
DA	Coefficient (95%CI)	p value	Controlling for (confounding variables):
Species	0.425 (0.290 to 0.560)	<0.001	Region, BV/TV, ConnD

Table 55. Effect of species on each architectural parameter controlling for CTR and confounding variables.

BV/TV	Coefficient (95%CI)	p value	Controlling for (confounding variables):
Species	0.014 (0.003 to 0.026)	0.011	CTR, TbTh, TbSp, TbN, ConnD, DA
TbTh	Coefficient (95%CI)	p value	Controlling for (confounding variables):
Species	-0.002 (-0.010 to 0.005)	0.581	CTR, TbSp, BV/TV, TbN, ConnD, DA
TbSp	Coefficient (95%CI)	p value	Controlling for (confounding variables):
Species	-0.105 (-0.159 to -0.051)	<0.001	CTR, TbTh, BV/TV, ConnD
TbN	Coefficient (95%CI)	p value	Controlling for (confounding variables):
Species	0.011(-0.021 to 0.042)	0.496	CTR, BV/TV, TbTh, TbSp, ConnD, DA
ConnD	Coefficient (95%CI)	p value	Controlling for (confounding variables):
Species	0.300 (-0.479 to 1.081)	0.450	CTR, TbTh, TbSp, TbN, DA
DA	Coefficient (95%CI)	p value	Controlling for (confounding variables):
Species	0.520 (0.372 to 0.669)	<0.001	CTR, BV/TV, TbTh, ConnD

Table 56. Effect of species on each architectural parameter controlling for region, CTR, and confounding variables.

BV/TV	Coefficient (95%CI)	p value	Controlling for (confounding variables):
Species	0.012 (0.003 to 0.023)	0.010	Region, CTR, TbTh, TbSp, TbN, ConnD
TbTh	Coefficient (95%CI)	p value	Controlling for (confounding variables):
Species	-0.002 (-0.010 to 0.005)	0.544	Region, CTR, TbSp, BV/TV, TbN, ConnD, DA
TbSp	Coefficient (95%CI)	p value	Controlling for (confounding variables):
Species	-0.105 (-0.159 to- 0.051)	<0.001	Region, CTR, TbTh, ConnD
TbN	Coefficient (95%CI)	p value	Controlling for (confounding variables):
Species	0.011 (-0.021 to 0.042)	0.512	Region, CTR, BV/TV, TbTh, TbSp, ConnD, DA
ConnD	Coefficient (95%CI)	p value	Controlling for (confounding variables):
Species	0.603 (0.058 to 1.148)	0.030	Region, CTR, BV/TV, TbTh, TbSp, TbN, DA
DA	Coefficient (95%CI)	p value	Controlling for (confounding variables):
Species	0.496 (0.338 to 0.643)	<0.001	Region, CTR, BV/TV, ConnD

Table 57. Effect of species on each architectural parameter controlling for CTR and confounding variables in the dorsal region.

BV/TV	Coefficient (95%CI)	p value	Controlling for (confounding variables):
Species	0.026 (0.007 to 0.044)	0.006	CTR, TbTh, TbSp, TbN
TbTh	Coefficient (95%CI)	p value	Controlling for (confounding variables):
Species	-0.001 (-0.011 to 0.009)	0.848	CTR, BV/TV, TbSp, TbN
TbSp	Coefficient (95%CI)	p value	Controlling for (confounding variables):
Species	0.090 (0.046 to 0.135)	<0.001	CTR, BV/TV, TbTh, TbN, ConnD
TbN	Coefficient (95%CI)	p value	Controlling for (confounding variables):
Species	0.053 (0.008 to 0.098)	0.021	CTR, BV/TV, TbTh, TbSp, ConnD, DA
ConnD	Coefficient (95%CI)	p value	Controlling for (confounding variables):
Species	-0.051 (-0.904 to 0.803)	0.907	CTR, BV/TV, TbTh, TbSp, TbN, DA
DA	Coefficient (95%CI)	p value	Controlling for (confounding variables):
Species	0.593 (0.154 to 0.771)	<0.001	CTR, BV/TV, ConnD

Table 58. Effect of species on each architectural parameter controlling for CTR and confounding variables in the plantar region.

BV/TV	Coefficient (95%CI)	p value	Controlling for (confounding variables):
Species	0.017(0.002 to 0.033)	0.033	CTR, TbTh, TbSp, TbN, ConnD
TbTh	Coefficient (95%CI)	p value	Controlling for (confounding variables):
Species	-0.006 (-0.018 to 0.006)	0.332	CTR, BV/TV, TbSp, TbN, ConnD, DA
TbSp	Coefficient (95%CI)	p value	Controlling for (confounding variables):
Species	-0.121 (-0.181 to -0.062)	<0.001	CTR, BV/TV, TbTh, TbN, ConnD
TbN	Coefficient (95%CI)	p value	Controlling for (confounding variables):
Species	0.017 (-0.034 to 0.069)	0.504	CTR, BV/TV, TbTh, TbSp, ConnD, DA
ConnD	Coefficient (95%CI)	p value	Controlling for (confounding variables):
Species	0.578 (-0.284 to 1.440)	0.189	CTR, BV/TV, TbTh, TbSp, TbN, DA
DA	Coefficient (95%CI)	p value	Controlling for (confounding variables):
Species	0.466 (0.230to 0.704)	<0.001	CTR, BV/TV, ConnD

The effect of species was additionally examined including Imax/Imin. When the effect of species (predictor variable) was examined controlling for Imax/Imin and other confounders, BV/TV, TbSp, and DA were shown to significantly differ between the two species (Table 59). When controlling for region also, BV/TV, TbSp, and DA were also shown to vary significantly with species (Table 60). In the analysis of the dorsal data, BV/TV, TbSp, TbN, and DA all varied significantly with species (Table 61). In the plantar region, TbSp, and DA varied with species (Table 62).

Table 59. Effect of species on each architectural measure controlling for Imax/Imin and confounding variables.

BV/TV	Coefficient (95%CI)	p value	Controlling for (confounding variables):
Species	0.016 (0.001 to 0.031)	0.041	Imax/Imin, TbTh, TbSp, TbN, ConnD, DA
TbTh	Coefficient (95%CI)	p value	Controlling for (confounding variables):
Species	-0.004 (-0.014 to 0.005)	0.429	Imax/Imin, TbSp, BV/TV, TbN, ConnD, DA
TbSp	Coefficient (95%CI)	p value	Controlling for (confounding variables):
Species	-0.079 (0.410 to 0.117)	<0.001	Imax/Imin, TbTh, BV/TV, ConnD
TbN	Coefficient (95%CI)	p value	Controlling for (confounding variables):
Species	0.023(-0.016 to 0.063)	0.249	Imax/Imin, BV/TV, TbTh, TbSp, ConnD, DA
ConnD	Coefficient (95%CI)	p value	Controlling for (confounding variables):
Species	-0.037 (-1.030 to 0.955)	0.941	Imax/Imin, TbTh, TbSp, TbN, DA
DA	Coefficient (95%CI)	p value	Controlling for (confounding variables):
Species	0.641 (0.458 to 0.824)	<0.001	Imax/Imin, BV/TV, TbTh, ConnD

Table 60. Effect of species on each architectural parameter controlling for region, Imax/Imin, and confounding variables.

BV/TV	Coefficient (95%CI)	p value	Controlling for (confounding variables):
Species	0.016 (0.001 to 0.031)	0.041	Region, Imax/Imin, TbTh, TbSp, TbN, ConnD, DA
TbTh	Coefficient (95%CI)	p value	Controlling for (confounding variables):
Species	-0.005 (-0.015 to 0.005)	0.362	Region, Imax/Imin, TbSp, BV/TV, TbN, ConnD, DA
TbSp	Coefficient (95%CI)	p value	Controlling for (confounding variables):
Species	-0.079 (0.041 to 0.117)	<0.001	Region, Imax/Imin, BV/TV, TbTh, TbN, ConnD
TbN	Coefficient (95%CI)	p value	Controlling for (confounding variables):
Species	0.022 (-0.017 to 0.063)	0.265	Region, Imax/Imin, BV/TV, TbTh, TbSp, ConnD, DA
ConnD	Coefficient (95%CI)	p value	Controlling for (confounding variables):
Species	-0.068 (-1.062 to 0.927)	0.894	Region, Imax/Imin, BV/TV, TbTh, TbSp, TbN, DA
DA	Coefficient (95%CI)	p value	Controlling for (confounding variables):
Species	0.602 (0.420 to 0.785)	<0.001	Region, Imax/Imin, BV/TV, ConnD

Table 61. Effect of species on each architectural measure controlling for Imax/Imin and confounding variables in the dorsal region.

BV/TV	Coefficient (95%CI)	p value	Controlling for (confounding variables):
Species	0.039 (0.015 to 0.064)	0.002	Imax/Imin, TbTh, TbSp, TbN
TbTh	Coefficient (95%CI)	p value	Controlling for (confounding variables):
Species	-0.007 (-0.021 to 0.006)	0.292	Imax/Imin, BV/TV, TbSp, TbN
TbSp	Coefficient (95%CI)	p value	Controlling for (confounding variables):
Species	0.108 (0.046 to 0.169)	0.001	Imax/Imin, BV/TV, TbTh, TbN, ConnD
TbN	Coefficient (95%CI)	p value	Controlling for (confounding variables):
Species	0.806 (0.010 to 0.127)	0.022	Imax/Imin, BV/TV, TbTh, TbSp, ConnD, DA
ConnD	Coefficient (95%CI)	p value	Controlling for (confounding variables):
Species	-0.047 (-1.613 to 0.676)	0.422	Imax/Imin, BV/TV, TbTh, TbSp, TbN, DA
DA	Coefficient (95%CI)	p value	Controlling for (confounding variables):
Species	0.724 (0.504 to 0.944)	<0.001	Imax/Imin, BV/TV, ConnD

Table 62. Effect of species on each architectural measure controlling for Imax/Imin and confounding variables in the plantar region.

BV/TV	Coefficient (95%CI)	p value	Controlling for (confounding variables):
Species	0.007 (-0.012 to 0.026)	0.462	Imax/Imin, TbTh, TbSp, TbN, ConnD
TbTh	Coefficient (95%CI)	p value	Controlling for (confounding variables):
Species	-0.003 (-0.017 to 0.011)	0.632	Imax/Imin, BV/TV, TbSp, TbN, ConnD, DA
TbSp	Coefficient (95%CI)	p value	Controlling for (confounding variables):
Species	-0.170 (-0.239 to -0.101)	<0.001	Imax/Imin, BV/TV, TbTh, TbN, ConnD
TbN	Coefficient (95%CI)	p value	Controlling for (confounding variables):
Species	0.027 (-0.033 to 0.086)	0.380	Imax/Imin, BV/TV, TbTh, TbSp, ConnD, DA
ConnD	Coefficient (95%CI)	p value	Controlling for (confounding variables):
Species	0.395 (-0.629 to 1.420)	0.450	Imax/Imin, BV/TV, TbTh, TbSp, TbN, DA
DA	Coefficient (95%CI)	p value	Controlling for (confounding variables):
Species	0.557 (0.274 to 0.840)	<0.001	Imax/Imin, BV/TV, ConnD

DISCUSSION AND CONCLUSIONS

The purpose of this study was to analyze trabecular architecture from the cancellous bone of the artiodactyl calcaneus to examine how trabecular bone architecture varies with respect to habitual loading in compression and tension. The variation in architecture was assessed along the length of the bone, between dorsal and plantar regions, and with variation in cortical bone thickness ratio and Imax/Imin ratio. The artiodactyl calcaneus was chosen because it has been shown to be habitually loaded in bending with compression predominant in the dorsal aspect of the bone and tension predominant in the plantar aspect in separate in vivo and in vitro strain gauge studies (Lanyon, 1973; Su et al., 1999). While these strain gauge studies on the artiodactyl calcaneus reported predominant loading of the cortical bone and not cancellous bone, it was assumed that the cancellous bone in the same regions would be subject to similar load types, although certainly not as great of magnitude.

The research sought to answer five main questions: 1) does trabecular bone architecture vary across the length of the bone, 2) does trabecular architecture differ between regions of cancellous bone under habitual compression and tension, 3) does trabecular architecture vary with cortical bone thickness ratio of the cross section, 4) does trabecular architecture vary with Imax/Imin ratio of the cross section, and 5) does trabecular bone architecture vary between the species. To answer these questions trabecular architectural measures were computed from 3 mm cubic ROIs of cancellous

bone in the dorsal and plantar regions and across the diaphyseal length of each bone from micro-CT scans.

Question 1: Architectural Variation over Diaphyseal Length

The correlation analyses for each trabecular architectural measure and diaphysis location for the dorsal and plantar regions of the sheep and deer indicate that for nearly all the measures there is moderate to high and statistically significant correlation between architectural measure variation and diaphysis location. All but one trabecular architecture measures exhibited similar correlation trends (sign of correlation) in both the sheep and deer. TbTh was negatively correlated with percent diaphysis location in the dorsal region of the sheep but positively correlated with percent location in the same region of the deer.

When the data are separated into dorsal and plantar regions and change over percent diaphysis location is examined, the sheep dorsal region showed only a significant reduction in BV/TV while the deer had significant reduction in BV/TV and ConnD, and an increase in TbSp in the dorsal region. Conversely, the plantar regions of the sheep and deer both had more significant differences in trabecular architecture over the diaphysis lengths. The sheep plantar regions exhibited significant decreases in BV/TV, TbN, and ConnD but increases in TbTh, and DA. The deer plantar regions similarly exhibited significant increases in TbTh and DA and decreases in ConnD, but also had significant increases in TbSp.

The results show that the cancellous bone of the artiodactyl calcaneus becomes less dense and less connected with greater trabecular separation and fewer trabeculae when moving from posterior (i.e., 20% location) to anterior (i.e., 50% location).

Additionally, the cortical bone of both the sheep and deer becomes thicker overall and more asymmetrical in thickness between the dorsal and plantar cortices (see CTR results). The distribution of cortical bone also becomes more asymmetrical in both species; however, it is much more pronounced in the deer than in the sheep (see Imax/Imin). This differential thickening of the cortices and distribution of cortical bone across the length of the diaphysis is shown to be associated with significant variation in trabecular architecture.

Functionally the artiodactyl calcaneus has been and can be best described as a cantilevered beam with habitual prevalent/predominant bending. Beam theory indicates that the bending moments increase toward the middle region of a cantilevered beam. It has been shown that bending (compression and tension) is more effectively countered by cortical bone than cancellous bone (Keaveny et al., 1994b; Bayraktar et al., 2004); thus, it would be expected that there would be an increase in cortical bone and decrease in cancellous bone toward the middle of the artiodactyl calcaneus.

The increase in TbTh and DA seen in both the sheep and deer plantar regions suggest that while the amount of cancellous bone is decreasing with increasing percent diaphyseal length, the trabeculae are becoming thicker and more anisotropic. Increased trabecular thickness has been shown to be highly correlated with maximum compressive stress, ultimate stress, and Young's modulus, higher trabecular bone stiffness, and shear modulus (Follet et al., 2005; Perilli et al., 2008) while lower TbTh values have been associated with lower Young's and shear moduli (Ulrich et al., 1999; Mittra et al., 2005; Diederich et al., 2009; Liu et al., 2010). Increasing DA values have been shown to be associated with increasing values of the mechanical properties (i.e., elastic modulus, yield strength, and ultimate stress) when cancellous bone samples are loaded in the principal

direction of trabecular structure (Follet et al., 2005; Mittra et al., 2008). Accordingly, it can be inferred that the cancellous bone of the plantar region has increased mechanical properties toward the middle of the diaphysis.

The plantar regions of both species are believed to benefit from stress shielding due to the plantar ligaments and other soft tissues attached to and surrounding it. This is associated with and has been used to explain a less significant increase in cortical thickness between 20% and 50% in the plantar region compared to the dorsal region. The cancellous bone of both the sheep and deer plantar regions, however, appear to be altering the architecture in response to increased mechanical loads experienced toward the middle of the bone suggesting that despite the stress shielding effect of the soft tissues, the cancellous bone is experiencing and adapting to the increased loads.

Question 2: Architectural Variation by Region

The correlation analyses of each trabecular architecture measure with region showed mostly weak and not statistically significant correlations for both the sheep and deer. The only significant correlation in the sheep was a weak (R=0.30) correlation between TbTh and region. In the deer, significant weak correlations were found between BV/TV (R=0.31), TbTh (R=0.28) and DA (R= -0.39). The results of the initial analysis with the whole data show that for the sheep calcaneus there were no differences between the dorsal and plantar regions for any of the architectural measures. Similarly, in the deer calcaneus there were also no significant differences found between architectural measures in the dorsal and plantar regions, except in DA. In the deer calcaneus, DA was found to be higher in the dorsal (compression) region than in the plantar (tension) region. This would appear to result in a failure to reject the null hypothesis and indicates that in the

sheep calcaneus, as a whole, trabecular architecture does not vary between the dorsal and plantar regions, and thus does not vary between cancellous bone under habitual compression and tension. However, when each percent diaphysis location was examined separately for differences between the two regions, several significant differences were identified that indicate that the alteration in trabecular architecture between dorsal and plantar occurs on a considerably localized level, especially in the deer calcaneus. The only significant differences in regional trabecular architecture exhibited by the sheep were at the 20% region where DA was found to be significantly higher in the dorsal region, and at the 40% location where TbSp was significantly higher in plantar region. The deer data exhibited slightly more significant differences between dorsal and plantar regions at the individual percent diaphysis locations. In the 20% location, ConnD was significantly higher and DA significantly lower in the plantar region. Trabecular separation and DA both were found to be significantly higher in the dorsal region at the 30% location. In the 50% location, five of the six measures were found to be significantly different between the dorsal and plantar regions. Bone volume fraction (BV/TV), TbTh, TbN, and DA were all higher in the plantar region while TbSp was higher in the dorsal region. In the 50% location, the trabecular architecture of the deer calcaneus is significantly different between the dorsal and plantar regions. The cancellous bone of the plantar region is more dense, with thicker less separated trabeculae, greater number of trabeculae, and more anisotropic arrangement compared to the cancellous bone in the dorsal region. This is the location where the highest bending moments are expected. The thicker cortical bone of the dorsal region is able to effectively counter the increased loads resulting in less magnitude of load reaching the cancellous bone, while the thinner cortical bone of the plantar region may necessitate an

increased role for the cancellous bone in load bearing resulting in the identified differences in trabecular architectural measures. The 40% location of the deer, however, did not have any significant differences between the dorsal and plantar regions. It would be expected that the 40% location would have nearly as great of bending moments and, accordingly, should have similar trabecular architecture, but it does not have any significant differences between the dorsal and plantar regions. These contradictory data require further analysis. One possible explanation is the fact that at the 50% location, in some of the specimens, there is a separation between the dorsal and plantar cancellous bone with sparse trabeculae connecting the two regions. This does not occur in the 40% location or in the sheep (See Figures 8 and 9).

Question 3: Architectural Variation with Cortical Thickness Ratio (CTR)

The CTR was shown to have strong statistically significant correlation with percent diaphysis location in both the sheep and deer. The CTR was also shown to be moderately to strongly and significantly correlated with all trabecular architecture measures except for TbN and ConnD in the sheep in the dorsal region and all but TbTh in the dorsal region of the deer. In the plantar region all trabecular measures were significantly correlated with CTR for both the sheep and deer. Due to the strong correlation with percent diaphysis location, it is not surprising that the results of the analyses with CTR were similar to those with location. When CTR was used as the predictor variable significant differences were found in five of the six architectural measures in the sheep and four of the six measures in the deer. In both species TbN decreased, ConnD decreased, and DA increased with increasing CTR. In the sheep

BV/TV decreased and TbTh increased while in the deer TbSp increased with increasing CTR. Also, similar to the location analyses, when the dorsal and plantar data are separated BV/TV and ConnD showed significant change with CTR in the sheep, decreasing with increasing CTR. In the plantar region all but one measure showed significant difference with CTR (also similar to the location data), BV/TV decreased, TbTh increased, TbN decreased, ConnD decreased, and DA increased with increasing CTR. Thus for the sheep data, as CTR increases (and the dorsal cortical thickness increases relative to the plantar cortical thickness) the cancellous bone becomes less dense and less interconnected, with fewer but thicker trabeculae and more anisotropic in orientation. This is especially seen in the plantar region. These changes occur in conjunction with increased cortical bone thickness across the length of the diaphysis, especially in the dorsal region. In the deer, four of the six measures were found to significantly change with CTR in the dorsal region. BV/TV decreased, TbSp increased, ConnD decreased with increasing CTR. Differing from the location data, TbN was found to significantly decrease with increasing CTR. In the plantar region the deer showed significant differences in TbTh (increasing), TbN (decreasing), ConnD (decreasing), and DA (increasing) with increasing CTR.

Most of the significant differences seen with CTR are associated with an overall decrease in cancellous bone, but the increase in TbTh and DA seen in both the sheep and deer plantar surfaces indicates that while the amount of cancellous bone is decreasing with increasing CTR, the trabeculae are becoming thicker and more anisotropic. As mentioned before, increased trabecular thickness has been shown to be highly correlated with many biomechanical measures of trabecular bone strength (Ulrich et al., 1999; Follet et al., 2005; Mittra et al., 2008; Perilli et al., 2008; Diederich et al., 2009; Liu et al.,

2010). Increasing DA values have been shown to be associated with increasing values of the mechanical properties (i.e., elastic modulus, yield strength, and ultimate stress) when cancellous bone samples are loaded in the principal direction of trabecular structure (Follet et al., 2005; Mittra et al., 2008). The CTR data suggest that plantar regions of both the sheep and deer are altering the trabecular thickness and degree of anisotropy in response to the increased loads experienced toward the middle of the bone, but in the dorsal regions the increased amount of cortical bone effectively counters the increased bending loads.

Analyses with region as the predictor variable and controlling for CTR showed that only DA was significantly different by region for both the sheep and deer data. These results follow the aforementioned results for regional differences indicating that more differences occur in the trabecular architecture in increasing CTR than do between the regions.

Question 4: Architectural Variation with Imax/Imin

Analyses of Imax/Imin ratio revealed that in both the sheep and deer calcaneus Imax/Imin is highly correlated with percent diaphysis location, increasing toward the middle of the bone. The sheep and deer, however, have very different ranges of Imax/Imin values across the calcaneal diaphysis. The sheep values range from a mean of 1.23 at 20% to 2.24 at 50% while the deer have much higher means of 2.38 at 20% and 5.44 at 50%. The higher Imax/Imin values indicated not only a greater departure from circularity but, more importantly, a more defined direction of greatest bending rigidity in the deer than in the sheep across the calcaneal diaphysis. The deer are believed to have more extreme habitual loading (greater magnitudes of load and greater variation in load

modalities experienced) than the domesticated sheep. Relatively, the Imax/Imin data indicate that the cortical bone of the deer calcaneus has much greater bending rigidity through the dorsal and plantar surfaces than the sheep. Correlation analyses of each architectural measure with Imax/Imin ratio by region showed that in the sheep all measures but ConnD in the dorsal region were moderately to highly and significantly correlated with Imax/Imin. In the deer, all trabecular architectural measures were moderately to highly and significantly correlated with Imax/Imin in both the dorsal and plantar regions.

The analyses with region as the predictor variable and controlling for Imax/Imin showed no significant differences in architectural measures between the regions in the sheep and only one (DA) in the deer further confirming that the regional differences in trabecular architecture are not as great or significant as the differences across the diaphysis and with change in cortical bone distribution and geometry.

Results of the analyses with Imax/Imin as the predictor variable for each architectural measure mirrored the results of the same analyses with CTR in the sheep with significant changes in BV/TV, TbTh, TbN and ConnD with increasing Imax/Imin. However, in the deer, the Imax/Imin analyses showed significant change in only two (TbSp and DA) compared to four in the CTR analyses (TbSp, TbN, ConnD, and DA). In the sheep, when the dorsal and plantar regions were individually assessed with Imax/Imin, the results closely mirrored those of the analyses with CTR for both the dorsal and plantar regions. Only TbN fell out of significance in the plantar region with Imax/Imin. For the deer, however, the results with Imax/Imin were quite different from those with CTR especially in the plantar region. Only one of the six measures (TbSp was shown to vary significantly with Imax/Imin in the plantar region versus five of the six

with CTR. Clearly the use of the geometric property to assess trabecular variation is more sensitive than the CTR in the deer.

Question 5: Architectural Variation by Species

Both the sheep and deer calcanei have been shown to be under habitual predominant/prevalent bending with compression dominating the dorsal aspect and tension dominating the plantar aspect (Lanyon, 1974; Su et al., 1999). The deer calcaneus was also shown to have highly consistent dorsal-compression and plantar-tension strains during off-axis loading meant to simulate extreme loading from twisting, running, and jumping (Su et al., 1999). The sheep and deer are species that share a common body plan and general locomotor mode but have altered behavior. The deer is considered to have increased loading due to the natural habitat and habitual activity levels that would subject the deer calcaneus to more extreme loading and thus higher bending loads, as is indicated by the Imax/Imin mean data. This differential loading is expected to produce trabecular architecture more suited to higher stresses and bending loads produced from their habitual activity when compared to the sheep with less extreme habitual loads and activity levels.

The primary whole data analysis showed that the sheep generally have cancellous bone that had greater trabecular separation and less degree of anisotropy. Analyses to compare the effect of species on each trabecular architectural measure, while controlling for region, showed that TbSp and DA differed between the species. The deer were found to have significantly lower TbSp and higher DA compared to the sheep. The analyses by species and controlling for location showed the same pattern of difference. The separated dorsal and plantar data showed that in both regions the sheep have cancellous bone that is

less anisotropically oriented. In the dorsal region, however, the sheep significantly lower TbSp than the deer, and in the planter the sheep had higher TbSp than the deer. The analyses for each percent diaphysis location with species as the predictor variable showed that for all locations the deer had significantly higher DA, at the 20% location sheep had higher TbSp, and at the 30% location the deer had higher TbN.

When the differences between the species are analyzed controlling for CTR, significant differences were shown in BV/TV (higher in deer), TbSp (higher in sheep), and DA (higher in deer). When both CTR and region are controlled for the same pattern is seen except ConnD is also found to be significantly higher in the deer. When dorsal and plantar data are examined separately controlling for CTR, BV/TV and DA were shown to be higher in the deer for both dorsal and plantar regions. Trabecular separation (TbSp) was found to be higher in deer in the dorsal region but lower in the deer in the plantar region.

Analysis of the Imax/Imin ratio with trabecular architectural measures by species showed similar patterns as the CTR analyses for the data as whole and with dorsal and plantar regions separately.

Some clear significant differences between the species exist across all analyses. DA differs significantly between the species, with the deer having higher DA than the sheep. Similarly, the deer exhibit higher BV/TV than the sheep and generally higher TbSp in the dorsal region but lower TbSp in the plantar region. Greater DA is associated with increasing values of the mechanical properties (i.e., elastic modulus, yield strength, and ultimate stress) (Follet et al., 2005; Mittra et al., 2008) as would be expected with more extreme habitual loading seen in the deer. Similarly, lower TbSp has been shown to be associated with increased shear modulus, Young's modulus and stiffness (Follet et

al., 2005; Mittra et al., 2008).

As the deer calcanei are believed to be subjected to more extreme loading conditions and thus higher bending loads, the greater cortical bone asymmetry and cross-sectional distribution along the length of the diaphysis of the deer calcaneus compared to that of the sheep is expected due to the habitual loading conditions. Higher bending loads and greater stresses experienced by the deer would suggest that the cancellous bone of the deer would exhibit trabecular architecture to withstand the high loads compared to the sheep calcaneus. This appears to be the case for the deer calcaneus.

Considerations and Conclusions

There are some technical considerations that also need to be examined as they may have affected the outcome of this research. This research focused only on small 3 mm cubic regions of interest (ROI) taken from the dorsal and plantar portions of the cancellous bone mass. There has been little discussion of appropriate ROI size for micro-CT studies to ensure adequate and meaningful representation of trabecular architectural measures. While not directly associated, van Rietbergen and Hiuskes (2001) state that for cancellous bone mechanical characterization, a volume should be at least five inter-trabecular lengths (or be approximately 3 to 5 mm) to obtain meaningful results. It is possible that there is a similar size threshold for trabecular architectural measures. Increasingly, micro-CT has been used to assess the architecture of much smaller regions of cancellous bone. Most micro-CT studies have used ROI's sized within these parameters. These studies have been based on the hypotheses developed for the whole cancellous bone mass but applied to the smaller regions of interest. Some micro-CT studies have shown statistically significant differences and correlations between

cancellous bone mechanical measures and architectural measures while others have not. It is possible that the focus on such small regions of interest could be too narrow to capture an accurate view of the architecture and trabecular architecture studies should be using the largest possible ROIs.

The ROI's size for this study was dictated by the size and shape of the bones and the research questions. It could be possible that this size of ROI is too small to adequately capture the architecture of the cancellous bone and any variation or differences between the dorsal and plantar aspects of the artiodactyl calcaneus. However, increasing the size of the ROI's would require moving the placement of the regions more toward the middle of the cancellous mass, especially in the dorsal aspect, to ensure exclusion of cortical bone and thus move the ROI away from the bone most likely under compression or tension.

There are some important aspects of cancellous bone adaptation and habitual loading that were not considered in this research and will need to be further examined and addressed in future analyses. It has been suggested that trabecular architecture may develop in a more genetically programmed fashion that is only minimally mechanically influenced by habitual loading (Kriz et al., 2002; Lovejoy et al., 2003). In fetal sheep and deer calcanei arched trabecular tracts similar to those seen in adults of the same species are present (Lanyon, 1973; Skedros et al., 2007) and the orientation of the epiphyseal plate in developing sheep and deer calcanei are described by the same nonlinear equation throughout growth of the bone (Skedros and Brady, 2001). It has been suggested that the trabecular pattern seen in the calcaneus could be the result of genetic positional information, such as the orientation of the growth plate (Kriz et al., 2002; Lovejoy et al., 2003), but also possibly from mechano-biologic stresses present in utero (Lanyon, 1973;

Carter and Beaupre, 2001; Skerry, 2000; Skedros and Baucom 2007). Supporting the latter hypothesis, an unpublished account from Lanyon and Goodship, reported by Skerry (2000), reports that with transection of the Achilles tendon in a living fetal lamb prenatal growth resulted in disorganized trabeculae compared with the contralateral control. Further analyses are required to examine the development of trabecular architecture and influence of positional information and mechano-biological loading.

Similarly, an important variable that needs to be considered is the magnitude of the strains experienced by the bone not just the strain modes, as differences in the organization of bone may be more strongly correlated with the magnitudes of the principal compressive and tensile strains (Su et al., 1999). In vitro functional loading of the deer calcaneus produced near-longitudinal principal compressive strains in the dorsal cortex and near-longitudinal principal tensile strains in the plantar cortex. The magnitude of the compressive strains in the dorsal cortex was shown to be nearly half as great as the magnitude of the tensile strains. However, it was noted that the plantar strains were recorded after separation of the plantar ligament, necessary to attach the strain gauges, and also after transection of the plantar ligament. The authors estimated the plantar tensile strains before the plantar ligament was separated, and indicated that the plantar cortex typically experiences moderately high peak strains, even with the attached tendon and ligament. The magnitude of strains experienced by the cortical shell is logically greater than that experienced by the underlying cancellous bone. Measurement of the magnitude of cancellous bone loads (either through FEA analysis or with an in vitro/in vivo device designed to measure specifically cancellous loads) will be required to examine the effect of magnitude on trabecular architecture.

Mechanical testing of the trabecular bone of the artiodactyl calcaneus from the study locations and regions also needs to be completed to see if the architecture correlates with mechanical properties as studies of other bones have found. Such mechanical testing would be helpful in understanding the significance of the few differences seen between the dorsal and plantar surfaces at the difference percent locations. It may be that the cancellous bone mass in the artiodactyl calcaneus is too small to have significant differences regionally (between dorsal and plantar). Loads engendered on one surface/region may be transferred to the opposite due to the smaller distance between the surfaces. Again, additional studies on how loads are transferred through cancellous bone, and in this instance especially in the artiodactyl calcaneus, are needed to understand how far/deep loads are transferred into a mass of cancellous bone. These future studies need to take into account the magnitude of the loads and geometry of surrounding cortical bone to see how well trabecular architecture is adapted to predominant loads alone or if it is also adapted to loads transferred from opposing surfaces.

The statistical analyses specifically for repeated measures were required for the data in this study to account for the lack of independence among the metrics analyzed. The final multiple regression models for repeated measures that were used in this analysis included all other variables that were found to be confounding variables in the model. The importance of confounding variables due to intercorrelation of the measures has not been included or discussed in most research concerning architectural measures. However, as indicated by this study and the high prevalence of multiple confounding variables for each architectural measurement, this is a consideration that needs to be included in these types of analyses as it could have a significant effect on the outcomes.

It is clear from the results of this study that cancellous bone of the artiodactyl calcaneus cannot be looked at in isolation. In the artiodactyl calcaneus, cortical bone plays a significant role in bearing loads and trabecular architecture appears to be correlated with cortical bone thickness and distribution more than with load type. In the dorsal region, most of the load is likely absorbed (carried) by the thicker cortical bone while in the plantar region the thinner cortical bone may result in more of the load reaching the cancellous bone and therefore the trabecular architecture of this region has to be adapted for the increased loading the bone would experience. The trabecular bone from the plantar region has more significant changes likely due to the inherent properties of trabecular bone under tension and also due to the thinner cortical bone in the area resulting in more of the loads, greater magnitude, being experienced by the trabecular bone. Additionally, the role of soft tissue on the plantar surface needs to be better elucidated. While the area is thought to benefit from stress shielding due to the plantar ligament and superficial digital flexor tendon, the extent of protection provided by these tissues and how that affects the trabecular bone needs to be better understood through additional studies.

Deer appear to have trabecular bone, especially in the plantar region, that is more adapted to more extreme loads compared to the sheep. Deer trabecular bone is more anisotropic and has less trabecular separation in this region. Imax/Imin data show that deer have much higher ratio than the sheep in all diaphyseal locations. This relates to the shape of the cross section of the deer being much more oval/oblong along the dorsal/plantar plane but also the asymmetrical distribution of the cortical bone between dorsal and plantar surfaces as well as a more defined plane of bending. There are also questions related to the magnitude of loading. While both species are loaded similarly,

deer have more extreme habitual loading. The magnitude of the loads as well as the amount of variation in loading pattern is likely very different between the two species. Deer are more likely to have more varied loading regimes at times that produce more varied loads (more twisting, shear, and lateral loads) that result in more "nonnormal" loading of the calcaneus and thus the deer trabecular bone could be more adapted to varied loads as well.

Finally, the use of trabecular bone to identify or distinguish locomotor activity for extant and extinct species may be premature. More work needs to be done with in vivo and in vitro analyses of loading mode and magnitude on the architecture of trabecular bone before it can be applied to unknowns as a diagnostic tool. Similar to cross-sectional data it could be that trabecular architectural variation is best used in a relative sense and that direct behavioral or loading type/magnitude reconstructions using trabecular architecture are not appropriate at this time.

REFERENCES

Barak MM, Lieberman DE, Hublin JJ. 2011. A Wolff in sheep's clothing: Trabecular bone adaptation in response to changes in joint loading orientation. Bone *49*: 1141-1151.

Bayraktar HH, and Keaveny TM. 2004. Mechanisms of uniformity of yield strains for trabecular bone. J Biomech *37:*1671-8.

Biewener AA, and Bertram JEA. 1993. Mechanical loading and bone growth *in vivo*. In BK Hall ed.): Bone. Volume 7: Bone Growth - B. Boca Raton, FL: CRC Press, pp. 1-36.

Biewener AA, Fazzalari NL, Konieczynski DD, and Baudinette RV. 1996. Adaptive changes in trabecular architecture in relation to functional strain patterns and disuse. Bone *19:*1-8.

Black MT. 2004. Correspondence of trabecular and cortical geometries: A natural test of Wolff's Law. American Journal of Physical Anthropology Suppl. *38:*63.

Bland JM, Altman DG. 1994. Correlation, regression, and repeated data. BMJ 308:896.

Bland JM, Altman DG. 1995. Calculating correlation coefficients with repeated observations: Part 1—correlation within-subjects. BMJ 310:446.

Burr DB, and Piotrowski G. 1982. How do trabeculae affect the calculation of structural properties of bone? Am. J. Phys. Anthropol. *57:*341-352.

Burr DB, Ruff CB, and Johnson C. 1989. Structural adaptations of the femur and humerus to arboreal and terrestrial environments in three species of macaque. Am J Phys Anthropol *79:*357-67.

Carter DR, and Beaupre GS. 2001 Skeletal Function and Form. Cambridge, UK: Cambridge University Press.

Carter DR, Orr TE, and Fyhrie DP. 1989. Relationships between loading history and femoral cancellous bone architecture. J. Biomech. *22:*231-244.

Compston JE. 1994. Connectivity of cancellous bone: Assessment and mechanical implications. Bone *15:*463-466.

Cowin SC. 1984. Mechanial modeling of the stress adaptation process in bone. Calcif. Tissue Int. *36:*S98-S103.

Cowin SC. 1985. The relationship between the elasticity tensor and the fabric tensor. J Mech Mat *4:*137.

Cowin SC. 1986. Wolff's law of trabecular architecture at remodeling equilibrium. J. Biomech. Eng. *108:*83-88.

Cowin SC. 2001a. Bone Mechanics Handbook. Boca Raton, FL: CRC Press.

Cowin SC. 2001b. The false premise in Wolff's law. In SC Cowin (ed.): Bone Mechanics Handbook. Boca Raton, FL: CRC Press, pp. 30.1-30.15.

Currey JD. 2002. Bones: Structure and Mechanics. Princeton, UK: Princeton University Press.

Demes B, Jungers WL, and Selpien K. 1991. Body size, locomotion, and long bone cross-sectional geometry in indriid primates. Am J Phys Anthropol *86:*537-47.

Demes B, and Jungers WL. 1993. Long bone cross-sectional dimensions, locomotor adaptations and body size in prosimian primates. J Hum Evol *25:*57-74.

Demes B, Stern JT Jr, Hausman MR, Larson SG, McLeod KJ, Rubin CT. 1998. Patterns of strain in the macaque ulna during functional activity. Am J Phys Anthropol 106:87–100.

Demes B, Qin Y-X, Stern JT Jr, Larson SG, Rubin CT. 2001. Patterns of strain in the macaque tibia during functional activity. Am J Phys Anthropol 116:257–265.

Dendorfer S, Maier H, and Hammer J. 2008. How do anisotropy and age affect fatigue and damage in cancellous bone? Stud Health Technol Inform *133:*68-74.

Diederichs G, Link TM, Kentenich M, Schwieger K, HUber, MB, Burghardt AJ, Majumdar S, Rogalla P, Issever AS. 2009. Assessment of trabecular bone structure of the calcaneus using multi-detector CT: correlation with microCT and biomechanical testing. Bone *44*:976-983.

Ding M, Odgaard A, Danielsen CC, and Hvid I. 2002. Mutual associations among microstructural, physical and mechanical properties of human cancellous bone. J Bone Joint Surg Br *84:*900-7.

Fajardo RJ. 2004. Comparative μCT analysis of anthropoid trabecular architecture. Ph.D. Thesis, Stony Brook University, Southampton, NY.

Fajardo RJ, MacLatchy LM, and Muller R. 2000. Analysis of femoral head trabecular architecture using μCT: evidence from some arthropoids and lorisoids. Am J Phys Anthropol *S30:*147.

Fajardo RJ, and Müller R. 2001. Three-dimensional analysis of nonhuman primate trabecular architecture using microcomputed tomography. American Journal of Physical Anthropology *115:*327-336.

Fajardo RJ, Ryan TM, and Kappelman J. 1999. Quantitative analysis of primate trabecular bone architecture: Comparison of high resolution x-ray computed tomography and histologic sections. Am J Phys Anthropol *S28:*125.

Fajardo RJ, Ryan TM, and Kappelman J. 2002. Assessing the accuracy of high-resolution X-ray computed tomography of primate trabecular bone by comparisons with histological sections. Am J Phys Anthropol *118:*1-10.

Fazzalari NL, Crisp DJ, and Vernon-Roberts B. 1989. Mathematical modeling of trabecular bone structure: The evaluation of analytical and quantified surface to volume relationships in the femoral head and iliac crest. J. Biomech. *22:*901-910.

Fazzalari NL, Darracot J, and Vernon-Roberts B. 1983. A quantitative description of selected stress regions of cancellous bone in the head of the femur using automatic image analysis. Metab. Bone Dis. Rel. Res. *5:*119-125.

Feldkamp LA, Goldstein SA, Parfitt AM, Jesion G, and Kleerekoper M. 1989. The direct examination of three-dimensional bone architecture *in vitro* by computed tomography. J. Bone Miner. Res. *4:*3-11.

Follet H, Bruyere-Garnier K, Peyrin F, Roux JP, Arlot ME, Burt-Pichat B, Rumelhart C, and Meunier PJ. 2005. Relationship between compressive properties of human os calcis cancellous bone and microarchitecture assessed from 2D and 3D synchrotron microtomography. Bone *36:*340-51.

Ford CM, and Keaveny TM. 1996. The dependence of shear failure properties of trabecular bone on apparent density and trabecular orientation. J Biomech *29:*1309-17.

Fox JC, and Keaveny TM. 2001. Trabecular eccentricity and bone adaptation. J Theor Biol *212:*211-21.

Fox JC, and Keaveny TM. 2003. Erratum to "Trabecular eccentricity and bone adaptation." J Theor Biol *223:*267.

Freiberg AH. 1902. Wolff's law and the functional pathogenesis of deformity. Am. J. Med. Sci. *124:*956-972.

Fyhrie D, Fazzalari N, Goulet R, and Goldstein S. 1993. Direct calculation of the surface-to-volume ratio for human cancellous bone. Journal of Biomechanics *26:*955-967.

Fyhrie DP, and Carter DR. 1986. A unifying principle relating stress to trabecular bone morphology. J. Orthop. Res. *4:*304-317.

Fyhrie DP, and Kimura JH. 1999. NACOB presentation Keynote lecture. Cancellous bone biomechanics. North American Congress on Biomechanics. J Biomech *32:*1139-48.

Geraets WG. 1998. Comparison of two methods for measuring orientation. Bone *23:*383-8.

Gibson LJ, and Ashby MF. 1997. Cancellous Bone: Cellular Solids: Structure and Properties. Cambridge, UK: Cambridge University Press, pp. 429-452.

Goldstein SA. 1987. The mechanical properties of trabecular bone: Dependence on anatomic location and function. J. Biomech. *20:*1055-1061.

Goldstein SA, Goulet R, and McCrubbrey D. 1993. Measurement and significance of three-dimensional architecture to the mechanical integrity of trabecular bone. Calcified Tissue International *53:*S127-S133.

Goulet RW, Goldstein SA, Ciarelli MJ, Kuhn JL, Brown MB, and Feldkamp LA. 1994. The relationship between the structural and orthogonal compressive properties of trabecular bone. J. Biomech. *27:*375-389.

Greenland S. 1989. Modeling and variable selection in epidemiologic analysis. Am J Public Health *79(3)*:340-349.

Guo, XE and Goldstein, SA. 2000. Vertebral trabecular bone microscopic tissue elastic modulus and hardness do not change in ovarietomized rats, J. Orthop. Res., *18*(2): 333-336.

Harrigan TP, and Mann RW. 1984. Characterization of microstructural anisotropy in orthoptropic material using a second rank tensor. J. Mater. Science *19:*761-767.

Hayes WC and Snyder B. 1981. Toward a quantitative formulation of Wolff's Law in trabecular bone. In Cowin SC (ed), Mechanical Properties of Bone. The American Society of Mechanical Engineers, New York, pp 43-68.

Hildebrand T, and Ruegsegger P. 1997a. A new method for the model-independent assessment of thickness in three-dimensional images. J Microsc *185:*67-75.

Hildebrand T, and Ruegsegger P. 1997b. Quantification of bone microarchitecture with the structure model index. Comput Methods Biomech Biomed Engin *1:*15-23.

Hodgskinson R, and Currey JD. 1990a. The effect of variation in structure on the Young's modulus of cancellous bone: a comparison of human and nonhuman material. Proc Inst Mech Eng, Part H *204:*115-21.

Hodgskinson R, and Currey JD. 1990b. Effects of structural variation on Young's modulus of nonhuman cancellous bone. Proc Inst Mech Eng, Part H *204:*43-52.

Huiskes R. 2000. If bone is the answer, then what is the question? Journal of Anatomy *197:*145-156.

Kabel J, Odgaard A, van Rietbergen B, and Huiskes R. 1999a. Connectivity and the elastic properties of cancellous bone. Bone *24:*115-120.

Kabel J, van Rietbergen B, Dalstra M, Odgaard A, and Huiskes R. 1999b. The role of an effective isotropic tissue modulus in the elastic properties of cancellous bone. J Biomech *32:*673-80.

Kabel J, van Rietbergen B, Odgaard A, and Huiskes R. 1999c. Constitutive relationships of fabric, density, and elastic properties in cancellous bone architecture. Bone *25:*481-6.

Keaveny TM. 2001. Strength of trabecular bone. In SC Cowin (ed.): Bone Mechanics Handbook. Boca Raton, FL: CRC Press, pp. 16.1-16.42.

Keaveny TM, Guo XE, Wachtel EF, McMahon TA, and Hayes WC. 1994a. Trabecular bone exhibits fully linear elastic behavior and yields at low strains. J. Biomech. *27:*1127-1136.

Keaveny TM, and Hayes WC. 1993a. A 20-year perspective on the mechanical properties of trabecular bone. Transactions of the ASME *115:*534-542.

Keaveny TM, and Hayes WC. 1993b. Mechanical properties of cortical and trabecular bone. In BK Hall (ed.): Bone. Boca Raton, FL: CRC Press, pp. 285-344.

Keaveny TM, Morgan EF, Niebur GL, and Yeh OC. 2001. Biomechanics of trabecular bone. Annu Rev Biomed Eng *3:*307-33.

Keaveny TM, Pinilla TP, Crawford RP, Kopperdahl DL, and Lou A. 1997. Systematic and random errors in compression testing of trabecular bone. J Orthop Res *15:*101-10.

Keaveny TM, Wachtel EF, Ford CM, and Hayes WC. 1994b. Differences between the tensile and compressive strengths of bovine tibial trabecular bone depend on modulus. J. Biomech. *27:*1137-1146.

Keaveny TM, Wachtel EF, and Kopperdahl DL. 1999. Mechanical behavior of human trabecular bone after overloading. J Orthop Res *17:*346-53.

Ketcham RA, and Ryan TM. 2004. Quantification and visualization of anisotropy in trabecular bone. J Microsc *213:*158-71.

Kimura T, and Amtmann E. 1984. Distribution of mechanical robustness in the human femoral shaft. J. Biomech. *17:*41-46.

Kopp DV, and Skedros JG. 2007. A control bone for trabecular architecture variation. Am. J. Phys. Anthrop. Suppl *44*:146.

Kopperdahl DL and Keaveny TM, 1998. Yield strain behavior of trabecular bone. J Biomech *31:*601-8.

Kriz MA. 2002. The surface anatomy, internal structure, and external morphology of the mammalian proximal femure with special regerence to its developmental biology. Thesis, Kent State, Kent, Ohio.

Kriz MA, Reno PL, and Lovejoy CO. 2002. Morphometric variation in proximal femoral development in primates and mammals. Am. J. Phys. Anthrop. Suppl *34:*97.

Kuo AD, and Carter DR. 1991. Computational methods for analyzing the structure of cancellous bone in planar sections. J. Orthop. Res. *9:*918-931.

Lanyon LE. 1973. Analysis of surface bone strain in the calcaneus of sheep during normal locomotion. J. Biomech. *6:*41-49.

Lanyon LE. 1974. Experimental support for the trajectorial theory of bone structure. J. Bone Joint Surg. *56-B:*160-166.

Lanyon LE. 1981. The measurement and biological significance of bone strain *in vivo*. In SC Cowin (ed.): Mechanical Properties of Bone: American Society of Mechanical Engineers Symposium (ASME), pp. 93-106.

Lanyon LE. 1990. Functional load-bearing as a controlling influence on bone modelling/remodelling, and thus a determinant for bone mass and architecture. In HE Takahashi (ed.): Bone Morphometry. Japan: Nishimura Co., Ltd., pp. 128-148.

Lanyon LE. 1992. Control of bone architecture by functional load bearing. J. Bone Miner. Res. *7:*S369-S375.

Liu XS, Zhang XH, Sekhon KK, Adams MF, McMahon DJ, Bilezikian JP, Shane E, Guo XE. 2010. High resolution peripheral quantitative computed tomography can assess microstuctural and mechanical properties of human distal tibial bone. Journal of Bone Mineral Research *25*:746-756.

Lovejoy CO, McCollum MA, Reno PL, Rosenman BA. 2003. Developmental biology and human evolution. Annual Review of Antrhopology *32*:85-109.

Macchiarelli R, Bondioli L, Galichon V, and Tobias PV. 1999. Hip bone trabecular architecture shows uniquely distinctive locomotor behaviour in South African australopithecines. Journal of Human Evolution *36:*211-232.

MacLatchy L, and Muller R. 2002. A comparison of the femoral head and neck trabecular architecture of Galago and Perodicticus using micro-computed tomography (microCT). J Hum Evol *43:*89-105.

Maga M, Kappelman J, Ryan TM, and Ketcham RA. 2006. Preliminary observations on the calcaneal trabecular microarchitecture of extant large-bodied hominoids. Am J Phys Anthropol *129:*410-7.

Martin RB. 1991. Determinants of the mechanical properties of bones. J. Biomech. *24:*79-88.

Martin RD, Burr DB, and Sharkey NA. 1998. Skeletal Tissue Mechanics. New York: Springer.

Martinón-Torres M. 2003. Quantifying trabecular orientation in the pelvic cancellous bone of modern humans, chimpanzees, and the Kebara 2 Neanderthal. American Journal of Human Biology *15:*647-661.

McCalden RW, McGeough JA, and Court-Brown CM. 1997. Age-related changes in the compressive strength of cancellous bone. The relative importance of changes in density and trabecular architecture. J Bone Joint Surg [Am] *79-A:*421-427.

Meyer H. 1867. Die architektur der spongiosa. Arch Anat Physiol *34:*615-628.

Mittra E, Rubin C, Gruber B, and Qin Y. 2008. Evaluation of trabecular mechanical and microstructural properties in human calcaneal bone of advanced age using mechanical testing, μCT, and DXA . Journal of Biomechanics *41:*368 - 375.

Mittra E, Rubin C, and Qin YX. 2005. Interrelationship of trabecular mechanical and microstructural properties in sheep trabecular bone. J Biomech *38:*1229-37.

Morgan EF, Bayraktar HH, and Keaveny TM. 2003. Trabecular bone modulus-density relationships depend on anatomic site. J Biomech *36:*897-904.

Morgan EF, and Keaveny TM. 2001. Dependence of yield strain of human trabecular bone on anatomic site. J. Biomech. *34:*569-577.

Nyman JS, Leng H, Dong XN, Wang X. 2009. Differences in the mechanical behavior of cortical bone between compression and tension when subjected to progressive loading. Journal of Mechanical Behavior of Biomedical Materials. *2*:613-619.

Odgaard A. 1997. Three-dimensional methods for quantification of cancellous bone architecture. Bone *20:*315-28.

Odgaard A. 2001. Quantification of cancellous bone architecture. In SC Cowin (ed.): Bone Mechanics Handbook. Boca Raton, FL: CRC Press, pp. 14.1-14.19.

Odgaard A, and Gundersen HJG. 1993. Quantification of connectivity in cancellous bone, with special emphasis on 3D reconstructions. Bone *14:*173-182.

Odgaard A, Kabel J, van Rietbergen B, Dalstra M, and Huiskes R. 1997. Fabric and elastic principal directions of cancellous bone are closely related. J Biomech *30:*487-95.

Patel V, Issever AS, Burghardt A, Laib A, Ries M, and Majumdar S. 2003. MicroCT evaluation of normal and osteoarthritic bone structure in human knee specimens. J Orthop Res *21:*6-13.

Pauwels F. 1980. On the distribution of the density of cancellous bone in the upper end of the femur and its significance for the theory of the functional structure of bone. In F Pauwels (ed.): Biomechanics of the Locomotor Apparatus. New York: Springer-Verlag, pp. 299-309.

Perilli E, Baleani m, Ohman C, Fognani R, Baruffaldi F, and Viceconti M. 2008. Dependence of mechanical compressive strength on local variations in microarchitecture in cancellous bone of proximal human femur. Journal of Biomechanics *41:*438 - 446.

Pidaparti RMV and Turner CH. 1997. Cancellous bone architecture: advantages of nonorthogonal trabecular alignment under multidirectional loading. Journal of Biomechanics *30*:979-983.

Pontzer H, Leiberman DE, Momin E, Devlin MJ, Polk JD, Hallgrimsson B, Cooper DM. 2006. Trabecular bone in the bird knee responds with high sensitivity to changes in load orientation. Journal of Experimental Biology. *209*:57-65.

Radin, EL, Orr RB, Kelman, JL. 1982.. Effect of prolonged walking on concrete on the knees of sheep. J. Biomech. *15*:487–492.

Rincon-Kohli L and Zysset PK. 2009. Multi-axial mechanical properties of human trabecular bone. Biomechanics and Modeling in Mechanobiology *8*:195-208.

Roesler H. 1981. Some historical remarks on the theory of cancellous bone structure (Wolff's Law). In SC Cowin (ed.): Mechanical Properties of Bone. New York: The American Society of Mechanical Engineers, pp. 27-42.

Ruff CB. 1981. Structural changes in the lower limb bones with aging at Pecos Pueblo. Ph.D. Thesis, University of Pennsylvania, Philadelphia, PA.

Ruff CB. 1983. The contribution of cancellous bone to long bone strength and rigidity. Am J Phys Anthropol *61:*141-143.

Ruff, C.B. 1987. Structural allometry of the femur and tibia in Hominoidea and Macaca. Folia Primatol., 48: 9-49.

Ruff CB. 1989. New approaches to structural evolution of limb bones in primates. Folia Primatol. (Basel) *53:*142-159.

Ruff CB., and Hayes W 1984. Age changes in geometry and mineral content of the lower limb bones. Ann Biomed Eng *12:*573-584.

Ruff CB, and Hayes WC. 1983. Cross-sectional geometry of Pecos Pueblo femora and tibiae -- a biomechanical investigation: I. Method and general patterns of variation. Am. J. Phys. Anthrop. *60:*359-381.

Ruff CB, Holt BH, and Trinkaus E. 2006. Who's afraid of the big bad Wolff? Wolff's Law and bone functional adaptation. Am. J. Phys. Anthrop. *129*:484-498

Ruff CB, McHenry HM, Thackeray F, and Berger LR. 1999a. Femoral neck cross-sectional morphology in South African early hominids. Am. J. Phys. Anthrop. *28:*237.

Ruff CB, McHenry HM, and Thackeray JF. 1999b. Cross-sectional morphology of the SK 82 and 97 proximal femora. Am. J. Phys. Anthrop. *109:*509-21.

Ryan TM. 2000. Quantitative analysis of trabecular bone structure in the femur of lorisoid primates using high resolution x-ray computed tomography. Am. J. Phys. Anthrop. *S30:*266-267.

Ryan TM. 2001. The structure and function of trabecular bone in the femoral head of strepsirhine primates. Doctor of Philosophy, University of Texas at Austin, Austin, TX.

Ryan TM, and Ketcham RA. 2002a. Femoral head trabecular bone structure in two omomyid primates. J. Hum. Evol. *43:*241-63.

Ryan TM, and Ketcham RA 2002b. The three-dimensional structure of trabecular bone in the femoral head of strepsirhine primates. J Hum Evol *43:*1-26.

Ryan TM, and Ketcham RA. 2005. Angular orientation of trabecular bone in the femoral head and its relationship to hip joint loads in leaping primates. Journal of Morphology *265:*249-263.

Sanyal A, Gupta A, Bayraktar HH, Kwon RY, Keaveny TM. 2012. Shear strength behavior of human trabecular bone. In: 58th Annual Meeting of the Orthopaedic Research Society. *37*:125.

Silva MJ, and Gibson LJ. 1997. Modeling the mechanical behavior of vertebral trabecular bone: effects of age-related changes in microstructure. Bone *21:*191-9.

Singh I. 1978. The architecture of cancellous bone. Journal of Anatomy *127:*305-310.

Skedros JG. 1994. Collagen fiber orientation in skeletal tension/compression systems: A potential role of variant strain stimuli in the maintenance of cortical bone organization. J. Bone Miner. Res. *9:*S251.

Skedros JG. 1995. Examination of trabecular bone for material adaptation to habitual differences in physiologic strain modes. J. Biomed. Mater. Res. *10:*5442.

Skedros JG, and Baucom SL. 2007. Mathematical analysis of trabecular 'trajectories' in apparent trajectorial structures: the unfortunate historical emphasis on the human proximal femur. J Theor Biol *244:*15-45.

Skedros JG, and Bloebaum RD. 1991. Geometric analysis of a tension/compression system: Implications for femoral neck modeling. Orthopaedic Research Society 37th Annual Meeting. Trans. Orthopaed. Res. Soc., pp. 421.

Skedros JG and Brady JH. 2001. Ontogeny of cancellous bone anisotropy in a natural trajectorial structure: Genetics or epigenetics? J. Bone Miner. Res., *16 (Suppl. 1)*: S331

Skedros JG, Bloebaum RD, Mason MW, and Bramble DM. 1994a. Analysis of a tension/compression skeletal system: Possible strain-specific differences in the hierarchical organization of bone. The Anatomical Record *239:*396-404.

Skedros JG, Chow F, and Patzakis MJ. 1995. The artiodactyl calcaneus as a model for examining mechanisms governing regional differences in remodeling activities in cortical bone. J. Bone Miner. Res. *10:*5441.

Skedros JG, Dayton MR, and Bachus KN. 2001a. Strain-mode specific loading of cortical bone reveals an important role for collagen fiber orientation in energy absorption. Orthopaedic Research Society 47th Annual Meeting. Trans. Orthopaed. Res. Soc., pp. 0519.

Skedros JG, Dayton MR, Sybrowsky CL, Bloebaum RD, and Bachus KN. 2006. The influence of collagen fiber orientation and other histocompositional characteristics on the mechanical properties of equine cortical bone. J Exp Biol *209:*3025-42.

Skedros JG, and Dirksmeier P. 1995. Evidence of strain-mode-related ultrastructural adaptation in cortical bone -Detected using circularly polarized light in thin sections. 2nd Ann. Meeting of the Trans. Int. Orthop. Res. Soc., pp. 129.

Skedros JG, Hunt KJ, and Bloebaum RD. 2004. Relationships of loading history and structural and material characteristics of bone: Development of the mule deer calcaneus. J Morphol *259:*281-307.

Skedros JG, Hunt K, Dayton M, Bloebaum R, and Bachus K. 2003a. The influence of collagen fiber orientation on mechanical properties of cortical bone of an artiodactyl calcaneus: Implications for broad applications in bone adaptation.

Transactions of the 49th Annual Meeting of the Orthopaedic Reaserch Society, pp. 0411.

Skedros JG, Hunt KJ, Dayton MT, Bloebaum RD, and Bachus KN. 2001b. Relative contributions of material characteristics to failure properties of cortical bone in strain-mode-specific loading: Implications for fragility in osteoporosis & aging. Proceedings of the 25th Annual Meeting of the American Society of Biomechanics, pp. 215-216.

Skedros JG, Knight AN, Farnsworth RW, Bloebaum RD. 2012. Do regional modifications in tissue mineral content and microscopic mineralization heterogeneity adapt trabecular tracts for habitual bending? Analysis in the context of trabecular architecture of deer calcanei. Journal of Anatomy *220*: 242-255.

Skedros JG, Kuo TY, Bloebaum RD, and Bachus KN. 2001c. The role of cross-sectional cortical morphologies in interpreting habitual bending across the anthropoid hip: A comparative analysis. Am J Phys Anthropol *32:*138.

Skedros JG, Mason MW, and Bloebaum RD. 1993a. Evidence of potential strain-mode-specific differences in cortical bone microstructure in a tension/compression system. Orthopaedic Research Society 39th Annual Meeting. Trans. Orthopaed. Res. Soc., pp. 533.

Skedros JG, Mason MW, and Bloebaum RD. 1994b. Differences in osteonal micromorphologies between tensile and compressive cortices of a bending skeletal system: Indications of potential strain-specific differences in bone microstructure. Anat. Rec. *239:*405-413.

Skedros JG, Mason MW, and Bloebaum RD. 2001d. Modeling and remodeling in a developing artiodactyl calcaneus: A model for evaluating Frost's mechanostat hypothesis and its corollaries. Anat. Rec. *263:*167-185.

Skedros JG, Mason MW, Nelson MC, and Bloebaum RD. 1996. Evidence of structural and material adaptation to specific strain features in cortical bone. Anat Rec *246:*47-63.

Skedros JG, Ota D, and Bloebaum RD. 1993b. Mineral content analysis of tension/compression skeletal systems: Indications of potential strain-specific differences. J. Bone Miner. Res. *8:*789.

Skedros JG, Sorenson SM, Hunt KJ, and Holyoak JD. 2007. Ontogenetic structural and material variations in ovine calcanei: a model for interpreting bone adaptation. Anat Rec (Hoboken) *290:*284-300.

Skedros JG, Su SC, and Bloebaum RD. 1997. Biomechanical implications of mineral content and microstructural variations in cortical bone of horse, elk and sheep calcanei. Anat. Rec. *249:*297-316.

Skedros JG, Sybrowsky C, Parry T, and Bloebaum R. 2003b. Regional differences in cortical bone organization and microdamage prevalence in rocky mountain mule deer. Anat. Rec. *274 A:*837-850.

Skedros JG, Sybrowsky CL, Dayton MR, Bloebaum RD, and Bachus KN. 2003c. The role of osteocyte lacuna population density on the mechanical properties of cortical bone. 49th Annual Meeting of the Orthopaedic Research Society, pp. 0414.

Skerry T. 2000. Biomechanical influences on skeletal growth and development. In Development, Growth, and Evolution, ed. O'Higgins P, Cohn MJ, pp29-40. London, UK: Academic Press.

Sinclair KD, Farnsworth RW, Pham TX, Knight AN, Bloebaum RD, Skedros JG. 2013. The artiodactyl calcaneus as a potential 'control bone' cautions against simple interpretations of trabecular bone adaptation in the anthropoid femoral neck. Journal of Human Evolution *64*:366-379.

Su SC. 1998. Microstructure and mineral content correlations to strain parameters in cortical bone of the artiodactyle calcaneus. Master of Science, University of Utah, Salt Lake City, UT.

Su SC, Skedros JG, Bachus KN, and Bloebaum RD. 1999. Loading conditions and cortical bone construction of an artiodactyle calcaneus. J. Exp. Biol. *202:*3239-3254.

Turner CH. 1992. On Wolff's law of trabecular architecture. J. Biomech. *25:*1-9.

Turner CH, Cowin SC, Rho JY, Ashman RB, and Rice JC. 1990. The fabric dependence of the orthotropic elastic constants of cancellous bone. J Biomech *23:*549-61.

Ulrich D, van Rietbergen B, Laib A, and Ruegsegger P. 1999. The ability of three-dimensional structural indices to reflect mechanical aspects of trabecular bone. Bone *25:*55-60.

van der Meulen MC, Morgan TG, Yang X, Baldini TH, Myers ER, Wright TM, Bostrom MP. 2006. Cancellous bone adaptation to in vivo loading in a rabbit model. Bone *38*:871-877

van der Meulen MC, Yang X, Morgan TG, Bostrom MP. 2009. The effects of loading on cancellous bone in the rabbit. Clinical Orthopaedic Related Research *467*:2000-2006.

Van Rietbergen B, and Huiskes R. 2001. Elastic constants of cancellous bone. In SC Cowin (ed.): Bone Mechanics Handook. New York: CRC Press, pp. 15.1-15.24.

Van Rietbergen B, Muller R, Ulrich D, Ruegsegger P, and Huiskes R. 1999. Tissue stresses and strain in trabeculae of a canine proximal femur can be quantified from computer reconstructions. J Biomech *32:*165-73.

Whitehouse WJ. 1974. The quantitative morphology of anisotropic trabecular bone. J. Microsc. *101:*153-168.

Whitehouse WJ. 1975. Scanning electron micrographs of cancellous bone from the human sternum. J Pathol. *116:*213-224.

Whitehouse WJ, and Dyson ED. 1974. Scanning electron microscope studies of trabecular bone in the proximal end of the human femur. J. Anat. *118:*417-444.

Wolff J. 1879. Uber die innere Architektur der Knochen und ihre Bedeutung für die Frame von Knockenwaschstum. Virchows Arch. path. Anat. Physiol. *50:*389-453.

Wolfram U, Wilke HJ, Zysset PK. 2011. Damage accumulation in vertebral trabecular bone depends on loading mode and direction. Journal of Biomechanics *44*:1164-1169.

Wu Z and Neibur GL. 2012. Microdamage in human femoral trabecular bone depends on loading mode and pre-existing damage. In: 58th Annual Meeting of the Orthropeadic Research Society. *37*:1372.

Zylstra M. 2000. Trabecular architecture of metacarpal heads in catarrhines: A preliminary report. American Journal of Physical Anthropology *30:*331.